



Department of Statistics

Diploma Thesis

On the Valuation of Foreign Exchange Options Using Stochastic Volatility Models

Rupert Hughes-Brandl
February 26, 2010

Supervised by:
Prof. Stefan Mittnik, PhD
Dipl. Stat. Sebastian Kaiser, Dr. Ulrich Nögel

Abstract

This research examines the issue of option pricing using stochastic volatility models and compares the results to the Black-Scholes-Merton approach. The analysis of the models and the pricing concepts are focused on the foreign exchange market, however, most of the procedures and techniques proposed in this thesis can be applied to other markets and asset classes. The schema is thus presented with an introduction to the foreign exchange market and to the financial derivatives which are followed by the derivation of the Black-Scholes-Merton framework. After introducing foreign exchange specifics besides expounding the drawbacks of the Black-Scholes-Merton model and presenting more complex option strategies including exotics, stochastic volatility models are developed to provide solutions to the problems of the initial framework. The concept of stochastic volatilities is represented by the Heston and the Heston-Nandi model and enables more sophisticated option pricing as it does not wrongly assume the volatility to be constant. The latter builds on an NGARCH process to describe the variance (i.e. squared volatility) movements and can be fitted to given market data in different ways. Extensions of the stochastic volatility models are shown in order to deliver a complete specification of the foreign exchange market, its derivatives and how to determine the value of these financial instruments with different pricing schemes. Great value has been laid on comparing the different models with empirical results in order to give a distinct insight into the entire theme.

Acknowledgments

First and foremost, I would like to thank my supervisors Sebastian Kaiser and Ulrich Nögel for the huge support and trust given to me. Special thanks goes to my professor Stefan Mittnik for enabling me to write about this remarkable and highly interesting theme and guiding me into the fields of econometrics and finance.

Also, I would like to thank the two companies DEVnet and Assénagon who have provided me with data, material and a tremendous amount of insight and experience including the practical know-how during this research. I would like to emphasise that the empirical work would not have been possible without the contributed data.

Above all, many thanks go to all my family and friends for supporting me throughout this work. Amongst many others I would like to name Carole Hughes, Julia Endlicher, Maximilian Hughes-Brandl and Kirsten Eckel.

In the end, a theory is accepted not because it is confirmed by conventional empirical tests, but because researchers persuade one another that the theory is correct and relevant.

(Fischer Black 1986)

Contents

Abstract	I
Acknowledgments	II
1. Introduction	1
1.1. Motivation	1
1.2. Schema	2
2. The Forex Market and Basic Financial Derivatives	3
2.1. An Introduction to the Forex Market	3
2.2. A Brief Summary of Derivatives	5
2.2.1. Spot Contracts	6
2.2.2. Forward Contracts	6
2.2.3. Futures Contracts	7
2.2.4. Options	8
2.2.5. Swaps	10
2.3. An Introduction to Valuating the Derivatives	11
2.3.1. Valuating Forward Contracts	11
2.3.2. Valuating Futures Contracts	13
2.3.3. Valuating Options	13
2.3.4. Valuating Swaps	15
3. The Black-Scholes-Merton Model	17
3.1. Properties of Stock Prices	17
3.1.1. The Process of Stock Prices	17
3.1.2. The Lognormal Property of Stock Prices	18
3.1.3. Itô's Lemma	19
3.2. Pricing Derivatives Using the BSM Model	20
3.2.1. The Black-Scholes-Merton Differential Equation	20
3.2.2. Black-Scholes-Merton Pricing Formulae for Options	22
3.2.3. Interpretation and Properties of the BSM-Formulae	24
3.3. Implied Volatility	25
3.4. The Greeks	27
4. Distinctive Forex Market Features and Exotic Options	29
4.1. The BSM Model in the Forex Market	29

4.1.1.	The General BSM Model Including Dividends	29
4.1.2.	The Specific Forex BSM Model	30
4.2.	Notations in the Forex Market and the Δ -Quotation	31
4.2.1.	Specifics in the Forex Market	31
4.2.2.	Delta-Quotations	32
4.3.	Volatility Surface	35
4.3.1.	Comparing the Volatility Surfaces	35
4.4.	Further Strategies Containing Vanilla Options	39
4.4.1.	Call and Put Spread	40
4.4.2.	Risk Reversal	40
4.4.3.	Straddle	41
4.4.4.	Strangle	41
4.4.5.	Butterfly	42
4.5.	Describing the Volatility Smile by Decomposition of Options	42
4.6.	Exotics	43
4.6.1.	Barrier Options	43
4.6.2.	Forward Start Options	45
4.6.3.	Cliquet Options	46
4.7.	Motivation for Further Option Pricing Models	47
5.	Heston's Stochastic Volatility Model	51
5.1.	Heston's Stochastic Volatility Process	51
5.2.	Pricing Options Applying Heston's Stochastic Volatility Process	53
5.2.1.	The Partial Differential Equation in the Heston Framework	53
5.2.2.	The Market Price of Volatility Risk	55
5.2.3.	Pricing a European Option with the Heston Model	56
5.3.	Volatility Surface in the Heston Model	59
6.	The GARCH Model	62
6.1.	The General GARCH Process	62
6.1.1.	Definition of the GARCH(p,q) Process	62
6.1.2.	Properties of GARCH(p,q)	64
6.1.3.	Example: GARCH(1,1)	64
6.1.4.	GARCH Extensions	65
6.2.	Valuating Options Applying the GARCH Model	66
6.2.1.	Model Derivation and Specification	66
6.3.	Pricing European Options in the GARCH framework	68
6.4.	Continuous Time Limit of the GARCH(1,1) Process	69
6.5.	Volatility Surfaces Containing NGARCH Processes	72
6.5.1.	Maximum Likelihood Estimation of the NGARCH Process	73
6.5.2.	Applying Implied Volatilities for Fitting the NGARCH Process	73
6.5.3.	Calibration of the Heston-Nandi Model	78
7.	Empirical Analysis	79

7.1.	Description of the Data	79
7.2.	Estimating and Calibrating the Models	81
7.2.1.	Calibrating the BSM Model	81
7.2.2.	Calibrating the Heston Model	84
7.2.3.	Maximum Likelihood Estimation of the NGARCH Process	85
7.2.4.	Fitting the NGARCH Process to an Implied Volatility Index	88
7.2.5.	Calibrating the Heston-Nandi Model	89
8.	Valuations and Comparisons of the Different Models	93
8.1.	Model Valuations	93
8.1.1.	Graphical Comparison	93
8.1.2.	Mean Square Error	94
8.2.	Comparing the Return Densities of the Individual Models	96
9.	Pricing Exotic Options	100
9.1.	Pricing Barrier Options with Stochastic Volatility Models	100
9.2.	Pricing Cliquets with Stochastic Volatility Models	101
10.	Extensions of the Models	102
10.1.	Heston Model Extensions	102
10.1.1.	Adjustment of the Least Squared Error Function	102
10.1.2.	Time Dependant Parameters	103
10.1.3.	Jumps	104
10.1.4.	Further GARCH Models	105
11.	Conclusions and Summary	106
A.	The Statistical Basis	108
A.1.	Stochastic Processes	108
A.1.1.	Theory and Notation	108
A.1.2.	Examples of Stochastic Processes	112
A.2.	Change of the Measure & Numeraire	113
A.2.1.	Measure	113
A.2.2.	A Numéraire	114
A.2.3.	Change of the Numéraire	114
A.3.	Characteristic Functions and Fourier Transformation	115
A.4.	Heston	118
A.4.1.	Boundary Conditions of the Heston Model	118
A.4.2.	Deriving the Call Equation by Changing the Numéraire	118
A.4.3.	Deriving the Pseudo-Probability PDE	119
A.5.	GARCH	119
A.5.1.	Locally Risk-Neutral Valuation Relationship	119
A.5.2.	Derivation of the Correlation	119
B.	Volatility Surfaces	122

B.1. Market Volatility Surfaces	122
B.2. Deviations of the Calibrated BSM Call Prices to the Market Call Prices .	128
B.3. Grafical Results of the Calibrated Heston Model	133
B.3.1. Calibrated Heston Volatility Surfaces	133
B.3.2. Deviations of the Heston Call Prices	138
B.4. Grafical Results of the Heston-Nandi Model with ML Estimated Parameters	143
B.4.1. Heston-Nandi Volatility Surfaces with ML Estimated Parameters	143
B.4.2. Deviations of the Heston-Nandi Call Prices with ML Estimated Parameters	148
B.5. Grafical Results of the Heston-Nandi Model with Calibrated Volatility Index Parameters	153
B.5.1. Heston-Nandi Volatility Surfaces with Calibrated Volatility Index Parameters	153
B.5.2. Deviations of the Heston-Nandi Call Prices with Calibrated Volatil- ity Index Parameters	158
List of Figures	VI
List of Tables	VII
References	XI
Assertion Under Oath	XII

1. Introduction

Option pricing and stochastic volatility models are both extraordinary and remarkably interesting themes which are as boundless as they are important and fascinating. The entire financial industry lives from the accurate pricing of financial instruments and correctly modelling the market behaviours. The knowledge and ability to value complex derivatives and understand the underlying processes is of great interest to the supporting companies DEVnet and Assénagon.

The mathematical and statistical theory which deliver the essential basis of these tools are methods developed in recent years and still provide many problems to be solved. The cornerstone was undoubtedly laid by the Black-Scholes-Merton model in the 1970s. Since then a vast amount of models and concepts have been developed. The two main models presented in this thesis are the Heston and the Heston-Nandi framework which have had another deep impact on pricing options as they deliver closed form solutions for stochastic volatility models. These approaches were produced¹ in the years 1993 and 2000 and have been enlarged upon since then.

1.1. Motivation

One reason for writing this diploma thesis is to give a beneficial and thorough insight into the option pricing theory concentrating on closed form stochastic volatility models and the foreign exchange market. It also summarises approximately the first half of [Hull02] which is one of the absolute standard references on basic option pricing and gives a good understanding of the general theme.

However, the foremost motivation is to challenge the theory of more advanced approaches adding the necessary complexity in order to deliver more sophisticated and accurate pricing schemes. The concepts chosen in this context are two widely used closed form stochastic volatility frameworks provided by the Heston and the Heston-Nandi model. The interesting questions arising from different possible option pricing schemes can be asked in the following way. How well can they determine the market prices of options? What are the empirical and theoretical similarities and differences between the distinctive approaches? How well do the models fit the volatility implied by the market? What

¹Parts of the Heston-Nandi framework were published beforehand.

are the different assumptions underlying the models? How well do the more complicated stochastic volatility models perform especially when comparing the results to the original BSM option pricing concept?

These questions are examined carefully in the subsequent chapters including an intensive empirical analysis as well as some digressions and outlines. The basic schema of this research can be found in the following section. It should be emphasised that all concepts and models presented in this diploma thesis are of equal theoretical and practical value.

1.2. Schema

This diploma thesis can be partitioned into three parts. The first gives an introduction to the basic knowledge of the foreign exchange market, its financial derivatives and the option pricing theory applying the Black-Scholes-Merton model which are presented in Chapters 2 and 3. Moreover, the motivation for using stochastic volatility models, particularly when more complex (foreign exchange) options need to be priced is found in Chapter 4.

The derivation of the Heston and the Heston-Nandi stochastic volatility model is depicted in the second part of this research, i.e. Chapters 5 - 6. The empirical analysis of these models, including a description of the calibration and estimation, the comparison and validation and also option pricing with stochastic volatility processes is treated in Chapters 7 - 9. The last Chapter 10 provides an outline of further concepts and extensions and is seen as a supplementary part. Practically all the statistical and theoretical background is given in Appendix A. As the graphical analysis is quite intensive, most of the figures are also presented in Appendix B.

2. The Forex Market and Basic Financial Derivatives

2.1. An Introduction to the Forex Market

The *foreign exchange (forex, or FX) market* with its financial instruments, or *derivatives*, is of particular interest for investigating the occurrence of stochastic volatility in financial data as there are many exotics and complex derivatives being traded which usually tend to be sensitive to the volatility smile seen in the market. This will be the motivation for using Heston's stochastic volatility model as seen later on.

The forex market is also predetermined to compare different models as it provides sizable amounts of data being the largest and one of the most liquid financial markets in the world. It includes trading between large banks, central banks, currency speculators, corporations, governments, and other financial institutions. Daily turnovers were reported to be over US \$ 3.2 trillion (€ 2.25 trillion) in April 2007 by the Bank for International Settlements ([BIS07] p.1, confer also Figure 2.1). Since then, the market has continued to grow. According to the annual Forex Poll by [Euromoney08], volumes grew a further 41% between 2007 and 2008.

The forex market is not restricted to an actual stock *exchange*, it is, therefore, an *over-the-counter (OTC)* or off-exchange market where market participants¹ trade *directly* with each other. The word “exchange” in foreign exchange is hence somewhat misleading as there is no central exchange or clearing house. OTC markets are in general more flexible than exchange markets as there are hardly any restrictions to what is traded and which parties trade with each other. This differs to exchange trading where parties can only trade with facilities like the New York Stock Exchange (NYSE) or the Chicago Board of Trade (CBOT, established in 1848 to bring farmers and merchants together [Hull02] ch.1) which only offer standardized goods like futures or stocks determined and specified by these facilities.

The actual purpose of the forex market is to facilitate international trading and investing. Any market participant can exchange currencies at a negotiable price, to be able to do business in another country in a different currency (as mentioned, forex is OTC). Currency trading always arises in pairs (e.g. USD-EUR) where one currency is sold, i.e.

¹The main categories of market participants or traders are: hedgers, speculators and arbitrageurs. For more information compare [Hull02] ch.1.

Growth of the Forex Market and the Underlying Contracts



Figure 2.1.: Average daily turnover of global foreign exchange (billions of US dollars, April 2007). *Traditional markets*: spot transactions, outright forwards and forex swaps². *Other forex instruments*: currency swaps and options & exchange traded contracts compare also Section 2.2 and [IFSL07] p.1.

exchanged simultaneously for another and is depicted by EUR/USD or USD/EUR (c.f. Chapter 4). By doing so a foreign currency is valued relative to another currency. This is where speculators try to make a profit by betting on whether a certain currency is going to gain or lose value relative to another in the future. The price of a currency, therefore, obeys the laws of supply and demand. The actual valuation of currencies is another very important purpose of the forex market as it indicates an economy's condition. However, it is to be noted that some, especially emerging markets, prevent their currencies from being freely traded. A brief overview of the forex market is depicted in Table 4.1.

Summarizing, the forex market is unique because of:

- the size of the trading volume
- the large number and variety of traders in the market
- the extreme liquidity of the market
- the variety of factors that affect exchange rates
- its geographical dispersion
- its long trading hours: from 22:00 UTC on Sunday until 22:00 UTC Friday 24 hours a day, inter-bank forex trading continues 5.5 days a week, from Monday to midday on Saturday
- the low margins of profit compared with other markets of fixed income (but profits can be high due to very large trading volumes)

*Outline of the Forex Market:
The Leading Forex Markets, Currency Traders and Currency Pairs*

(a) *Forex Markets:*

position	forex market	overall market share
1.	UK	34.1%
2.	USA	16.6%
3.	Switzerland	6.1%
4.	Japan	6.0%
5.	Singapore	5.8%

(b) *Currency Traders:*

position	trader	overall market share
1.	Deutsche Bank AG	21.70%
2.	UBS AG	15.80%
3.	Barclays Capital	9.12%
4.	Citigroup Inc	7.49%
5.	Royal Bank of Scotland	7.30%

(c) *Currency Pairs:*

position	currency pair	overall market share
1.	USD-EUR	27%
2.	USD-YEN	13%
3.	USD-GBP	12%
4.	USD-AUD	6%
5.	USD-CHF	5%

Table 2.1.: (a) The top 5 foreign exchange markets in 2007, according to [RBA07]
 (b) The leading currency traders in 2008, see [Euromoney08]
 (c) The most traded currency pairs in 2007, compare [BIS07]

Apart from the aspect that forex is a market it is also seen as an *asset class*, just as *fixed incomes* (bonds) and *equities* (stocks) represent a family of asset classes. Moreover, forex has become a very interesting asset class because they are often not correlated to other asset classes and also seem to deliver descent annual excess returns, when comparing to bonds and stocks, as the Deutsche Bank Currency Index suggests [IFSL07].

2.2. A Brief Summary of Derivatives

As seen in Figure 2.1, there are different kinds of derivatives traded on the forex market which also exist in many other markets. The following segmentation has been undertaken in the respective figure: traditional forex instruments which include spot transactions,

outright forwards and forex swaps and describe nearly 90% of the global turnover in April 2007. The rest of the turnover is divided into OTC currency swaps and options². The following sections outline the most important derivatives in analogy to [Hull02] ch.1-7. It is to be noted that transaction costs are neglected which simplifies calculations and the notational burden, c.f. Section 2.3.2.

2.2.1. Spot Contracts

Starting with the simplest derivative, *spot transactions* or *spot deals* simply express a trade being done and confirmed right away, or “on the spot”. During the settlement period, which is usually a few days, money and securities change hands.

2.2.2. Forward Contracts

A *forward contract* is an agreement to buy or sell an asset at a certain future time for a certain price, c.f. [Hull02] ch.1. The difference to spot contracts, therefore, is the time component: Spot contracts are exercised the same day, forwards will be exercised at an arranged future date. As forwards can be traded between any parties and can consist of any kind of assets, forwards are classed as OTC transactions. Forward contracts which only consist of currency assets, are referred to as *currency forwards*, *forex forwards* or *outright forwards*.

The idea of forwards is to fix the future buying or selling price. One can either take a *long position* (buy to the arranged future date) or a *short position* (sell to the arranged future date). At time t_0 the forward price $F_{t_0,T}$ is negotiated (or often just given) for a forward maturing at T . When settling the contract, the *forward price* becomes the *delivery price* to which the forward is exchanged at expiration date T . So, at time t_0 the forward price equals the delivery price. During the time period $\tau := T - t_0$ the delivery price, of course, stays the same until clearance at time T , as it is fixed in the contract. The forward price $F_{t,T}$ at time $t \in [t_0, T]$, however, will almost certainly change during the time period τ . When the spot price of an asset changes, the future price of the asset also shifts consistently. The main reason for this occurrence is the no-arbitrage theorem which implies that the difference in price between a forward and the underlying asset, depending on the contract risk, must be proportional to the risk-free interest rate otherwise there would be an arbitrage possibility (for more details, see Section 2.3).

It can easily be concluded that if the value of the asset rises until maturity the long (short) position gains (loses) as the asset price S_T at time T is worth more than the delivery price (K) which is paid at time T but was contracted at time t_0 , i.e. $S_T > K$.

²A forex swap is the simultaneous purchase and sale of identical amounts of one currency for another with two different value dates (normally spot to forward), [Reuterser]. Where as currency swaps involve two reversed bonds in two different currencies as seen in Section 2.2.5

Payoff Curves of a Forward at Maturity T

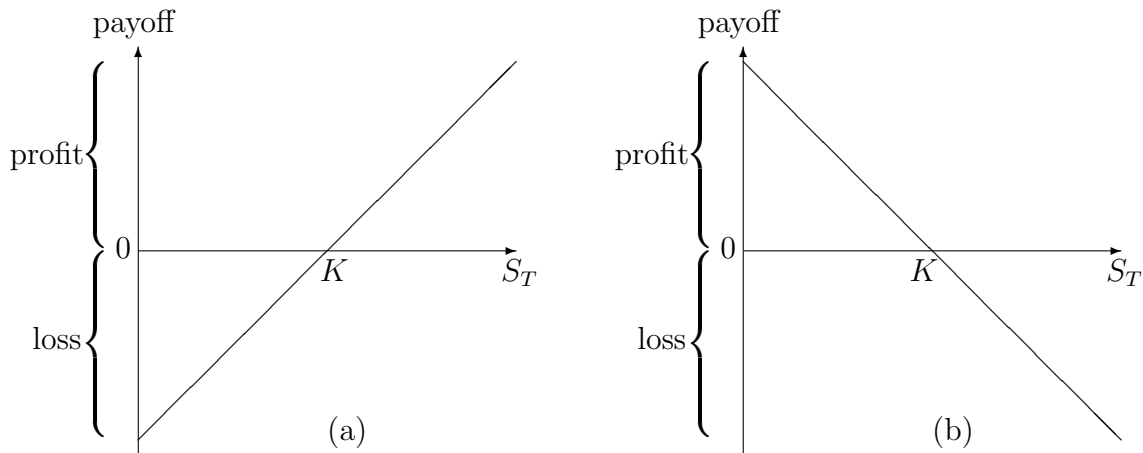


Figure 2.2.: Payoff curves of a forward at maturity T : (a) long position, (b) short position

Equivalently, if the price falls until maturity ($S_T < K$) the long (short) position loses (gains). The payoff from a long position is thus given by

$$S_T - K \quad (2.1)$$

and the payoff from a short position is

$$K - S_T \quad (2.2)$$

which also can be seen in Figure 2.2. Note, that the parties involved are obliged to fulfill their contract at maturity, no matter whether their payoffs are positive or negative.

2.2.3. Futures Contracts

Futures contracts are practically the same as forward contracts except that they are usually traded on an exchange as opposed to OTC markets. This means, as stated in Section 2.1, that futures are standardized and usually only mature to certain dates as opposed to any specified date when dealing with forwards.

The exchange institution also facilitates the actual formal exchange and often maintains the *marketing-to-market* undertakings which have the purpose of checking and balancing the exchange market participants' transactions performed from their *margin account* so that the contract risk is limited. This is clearly one advantage to forwards but with the disadvantage that only standardized assets are offered by the exchange. The latter characteristic, however, insures greater liquidity which is useful for trading and speculating.

Note, when valued on the expiration date T , futures have similar payoff curves to forwards as shown in Figure 2.2. However, due to the marketing-to-market procedure, adjustments are undertaken as seen in Section 2.3.2.

2.2.4. Options

Forwards and futures are binding contracts to exchange assets in the future, whereas *options* only *give the right* to be able to buy or sell assets in the future at an arranged price. The holder of an option, therefore, is not obliged to exercise this right. This has an impact on the payoff curve as seen in Figure 2.3. Options which give the right to buy are referred to as *call options* and options which allow one to sell are cited as *put options*.

To this point only the long position has been regarded where a market participant actually *buys* the right to purchase or sell an asset in the future. The other party of the contract *writes* or *sells* this right, so, it has a short position. As seen in Figure 2.3, the payoffs of the short positions of an option are the reverse of the long positions. The gains of the party with a long position are the losses of the market participant holding the short position and vice versa. The graphs are simply mirrored around the x-axis (asset price axis).

Options exist in both exchange and OTC markets. There are two main subclasses of options: *American options* and *European options*³. European options can only be exercised at maturity whereas American options can be carried out to any arbitrary time between t_0 and T . This is one reason why trading American options is popular. European options, however, are easier to handle and also easier to price, as seen later on.

As mentioned, the writer of an option receives a fixed payment called *premium* at time t_0 from the buyer of this option who, therefore, acquires the option's right. At maturity of a (European) option it is irrelevant how much was paid for the option at time t_0 , as they are sunk costs. Therefore, when working with options' payoffs the initial payment is ignored which also simplifies calculations (dashed lines in Figure 2.3).

When dealing with options the term delivery price is not used as with forwards and futures. Instead K denotes the *strike* or *exercise price*. As depicted earlier, let S_T be the terminal spot price of the underlying asset, the payoff of a long European call option is then given by

$$\max \{S_T - K, 0\} \tag{2.3}$$

which can easily be seen by noting that the call will only be exercised when $S_T > K$. The holder of the long position call can, hence, acquire the asset to the strike K smaller than S_T , instantaneously sell the asset at S_T and, therefore, make a profit of $S_T - K > 0$. Whereas if $S_T < K$, the call option will simply not be exercised, as the asset can be

³The terms "American" and "European" do not refer to the geographical area where these options are traded. Instead they are just named in this way to distinguish between these two options and can generally be traded on all markets.

Payoff Curves of a European Option at Maturity T

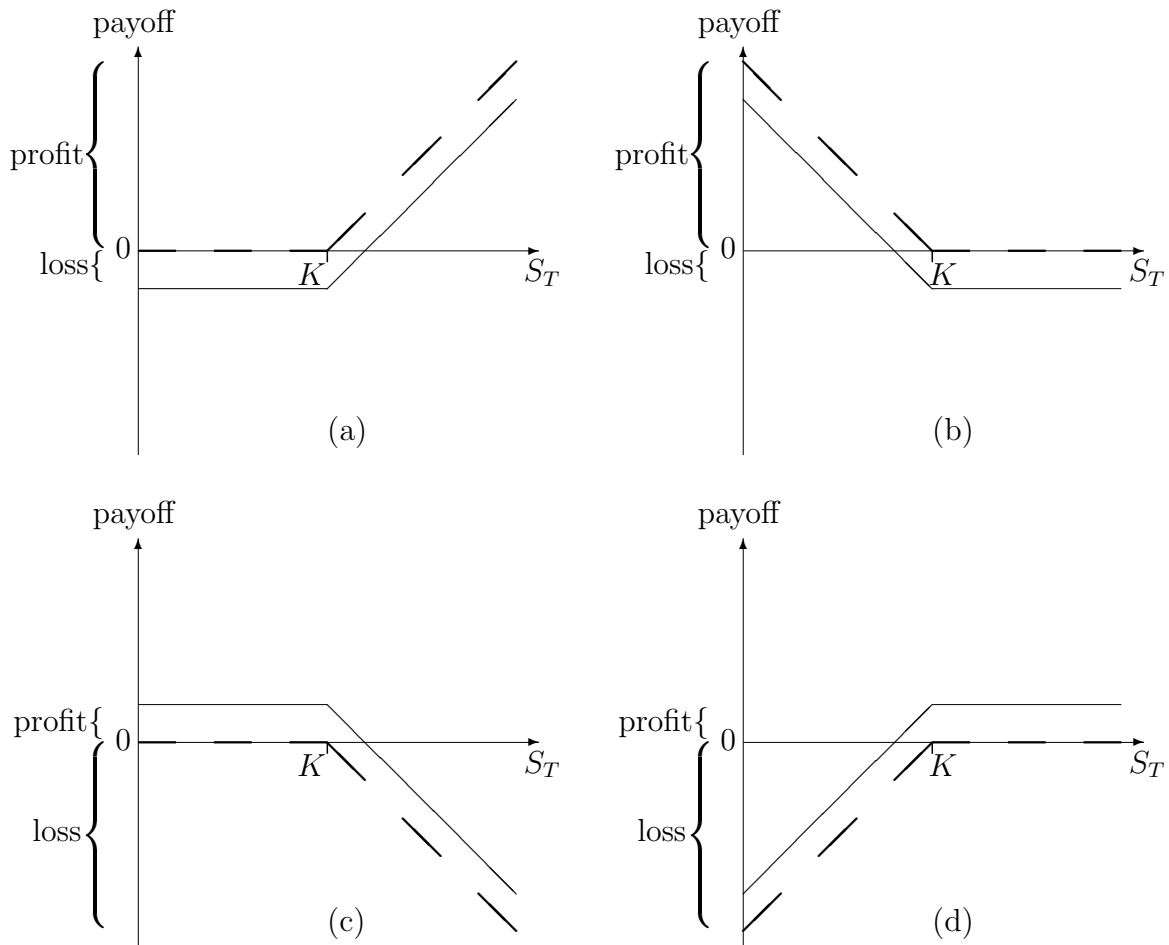


Figure 2.3.: Payoff curves of a European option at maturity T : (a) long position in a call option, (b) long position in a put option, (c) short position in a call option, (d) short position in a put option

bought to the market price S_T (which is less than K), so the payoff is zero. Similarly, the payoff of a long European put option is

$$\max \{K - S_T, 0\}, \tag{2.4}$$

as the holder will only exercise the put option if the strike K is above the terminal spot price S_T , otherwise the asset can be sold to the market price (i.e. spot price) at time T .

The payoffs of the short position are, as stated above, reverted to the long position. By multiplying the negative sign to the payoffs of the long position one obtains the payoff of a short position of a European call option and a short position of a European put

option, i.e.

$$- \max \{S_T - K, 0\} = \min \{K - S_T, 0\}, \quad (2.5)$$

$$- \max \{K - S_T, 0\} = \min \{S_T - K, 0\}. \quad (2.6)$$

The payoff which an option would have at any given time t to maturity, $t_0 \leq t \leq T$, is referred to as the *intrinsic value*. It is to be remembered that American options can be exercised at an arbitrary time before maturity, so they are worth at least as much as the intrinsic value. If American options are worth more, they have an additional *time value* which reflects positive expected price movements. Options, in general, are referred to as being *in-the-money (ITM)* if the holder can sell or exercise the option at a (positive) profit at a certain time. *out-of-the-money (OTM)* means that the holder of an option would, at a set time t , only be able to sell or exercise at a loss. Hence, an option is *at-the-money (ATM)* if the strike is the same as the spot price ($K = S_t$) and would only generate a zero cash flow. The latter descriptions are summarized by the term *moneyness* which is usually defined by the ration of the asset price to the strike, $M_t := \frac{S_t}{K}$. Hence, if the option is ATM, it has a moneyness of $M_t = 1$, if OTM: $M_t < 1$ and if ITM: $M_t > 1$, compare Section 4.2.2.

2.2.5. Swaps

A *swap* is OTC traded and can be seen as a forward contract to exchange cash flows in the future. The emphasis is laid on *cash flows* which stresses the difference to ordinary forwards. The idea of forwards, as stated above, is to lock in the future price of an asset. Swaps are mainly used to fix the future price of interest rates (*plain vanilla⁴ interest rate swaps*) and to fix future cash flows in two different currencies generated from two reversed loans or bonds (*fixed-for-fixed currency swaps*). As solely monetary quantities are involved, only the differences of values (net cash flows) are exchanged and not the total amount of the values⁵. Another related characteristic of swaps in comparison to forwards is the fact that the latter usually refers to only one exchange date in the future (which was depicted above by T) whereas swaps consist of more than one future dates where (monetary) exchanges take place ($t_0, t_1, \dots, t_n = T$).

Swaps, in general, are motivated by comparative advantages. There are often sizable differences between the interest rates offered to individual companies and parties which is due to their credit risk. The comparative advantages arise from the relative prices for long and short term bonds of differently rated companies. These companies can then negotiate with each other to be able to benefit from these discrepancies. Often,

⁴The term *plain vanilla* is often used in the financial language and has the meaning of being 'standard' or 'default'. E.g. a plain vanilla option refers to the standard (or simple) option as opposed to a more complex structured option.

⁵This certainly accounts for plain vanilla interest rate swaps, but not always for fixed-for-fixed currency swaps as the two bonds of the underlying swap are valid in two different currencies.

the parties only negotiate directly with a financial intermediary and do not actually know about each other. The financial institute undertakes the cash flow exchanges and, therefore, charges a fee (but in most cases also takes the risk of one party defaulting).

2.3. An Introduction to Valuating the Derivatives

There are certain restrictions to be considered before being able to price derivatives. At first it is assumed that there are no transaction costs and all trading profits are subject to the same tax rate. These properties enable comparisons between the derivatives and also ease the calculations. Secondly, borrowing and lending is undertaken at the same risk-free interest rate. This is not too unreasonable for big financial institutions. It is also assumed that *any* market participant will undertake the opportunity of *any* arbitrage possibilities. Therefore, these occurrences disappear instantly, and it is assumed they do not exist. The interest rate r is to be seen as a positive value.

2.3.1. Valuating Forward Contracts

The *present value* PV of a *bond* (or in general, *future cash flows*) is generally obtained by discounting the cash flows c_i exchanged in different time periods to the present time t_0 using the continuous or discrete *discount factor* $p_{t_i, t_0}(r_i)$, where r_i denotes the market interest (*LIBOR*⁶) rate during the time period $\delta t_i = t_i - t_0$,

$$\text{PV}_{t_0} = \sum_{i=1}^n c_i p_{t_i, t_0}(r_i). \quad (2.7)$$

For example, when trading with coupon bonds, c_0 usually is the issue price, c_1, \dots, c_{T-1} refer to the coupon payments and c_T depicts the face value including the last coupon payment. Depending on whether one receives or transfers at t_i , the single c_i 's are either positive or negative. This notation has the advantage that one can see the essential dates right away and can discount c_i to the market interest r_i even when the time periods of the cash flows do not overlap. However, for the sake of simplicity, it is assumed that the underlying time intervals fit. Also, continuous compounding is used and, if not stated otherwise, at a constant risk-free interest rate r , so when *discounting* one obtains

$$p_{t_i, t_0}(r_i) = \exp \left\{ - \int_{t_0}^{t_i} r_s ds \right\} \stackrel{!}{=} p_{t_i, t_0}(r) = e^{-r(t_i - t_0)}, \quad (2.8)$$

⁶London Interbank Offer Rate (LIBOR) is the on average offered interest rate (of preselected banks) to which banks lend to other banks. The rate is determined by supply and demand depending on economic conditions and is not risk free.

and, when *compounding* one applies

$$p_{t_0, t_i}(r_i) = \exp \left\{ \int_{t_0}^{t_i} r_s ds \right\} \stackrel{!}{=} p_{t_0, t_i}(r) = e^{r(t_i - t_0)}. \quad (2.9)$$

As indicated earlier, the forward price of an asset is proportional to the spot price, S_{t_0} . It can easily be concluded that the price of the forward $F_{t_0, T}$ is exactly⁷

$$F_{t_0, T} = S_{t_0} e^{r\tau} = S_{t_0} e^{r(T-t_0)}, \quad (2.10)$$

as, on average, the interest earned on a forward has to be the risk-free interest rate r earned during that period of time, τ (in practice, however, the LIBOR rate is often used as a reference rate to reflect the opportunity cost of capital). If this were not so and if $S_{t_0} e^{r\tau} - F_{t_0, T} > 0$, arbitrage profits could be made by selling the underlying asset at time t_0 , investing the proceeds for the time period τ at the interest rate r and by taking a long position forward, $F_{t_0, T}$, with duration T . The reverse is done if $F_{t_0, T} - S_{t_0} e^{r\tau} > 0$, namely: at t_0 borrow S_{t_0} for $\tau = T - t_0$ to instantaneously buy an asset worth S_{t_0} and short a forward $F_{t_0, T}$. The profit is $F_{t_0, T} - S_{t_0} e^{r\tau}$, which is positive, as given above.

If *known* future cash flows are given, e.g. coupon payments from a bond, the present value PV_{t_0} of these cash flows is subtracted from the spot price and then compounded to T in order to obtain the actual value of the forward. The equation (2.12) uses known yields, which is depicted by q , instead of known incomes and, with minor assumptions, it can be transformed to (2.11),

$$F_{t_0, T} = (S_{t_0} - PV_{t_0}) e^{r\tau}, \quad (2.11)$$

$$F_{t_0, T} = S_{t_0} e^{(r-q)\tau}. \quad (2.12)$$

The price of a currency forward can be seen as a special case of (2.12), where r_f is the yield (positive or negative) of a foreign risk-free interest rate and S_{t_0} is the currency spot price valued in the domestic currency per foreign currency unit,

$$F_{t_0, T} = S_{t_0} e^{(r-r_f)\tau}. \quad (2.13)$$

At time t_0 or any other time $t \in [t_0, T]$, the *value* of a long forward $V_{\text{long}(F_{t_0, T})}$ can easily be computed by subtracting the strike K , which will be received at maturity T , from the price of a forward at t_0 , maturing at T . This is then discounted to acquire the value of a long position of a forward at t_0 ,

$$V_{\text{long}(F_{t_0, T})} = (F_{t_0, T} - K) e^{-r\tau}. \quad (2.14)$$

So, as K is constant, the value of the forward changes with $F_{t_0, T}$ which is dependant on the spot price S_{t_0} , as seen in equations (2.10) - (2.13). The value of a short forward contract is obtained by the reverse subtraction, hence, the absolute values are equal,

$$V_{\text{short}(F_{t_0, T})} = (K - F_{t_0, T}) e^{-r\tau}. \quad (2.15)$$

⁷It is often assumed that $t_0 = 0$ but here the general case is regarded: $\tau := T - t_0$. Also, incomes and yields are assumed away and will be considered in the following.

2.3.2. Valuating Futures Contracts

As forwards and futures are very similar the question arises whether the two derivatives (are able to) have a difference in value. It can be concluded, as outlined in [Hull02] ch.3 that if the risk-free interest rate is constant and the maturities are the same (futures normally only have specific duration dates), then the prices of forwards and futures of the same underlying asset are equal. In reality, though, interest rates do change significantly over time, and also price differences between forwards and futures can be observed. This is due to the marketing-to-market procedure, as gains and losses are balanced every day and, therefore, have an impact on the exposure to the interest rate. If, for example, the underlying asset is positively correlated to the interest rate, a holder of a long futures contract will profit from the positive price movement immediately and is able to earn interest on the proceeds, whereas the long forward position will only gain from this movement (if at all) at the end of the derivatives life time.

The price asymmetries usually are not significant in the short term. For long dated contracts, however, a *convexity adjustment* is made. According to [Hull02] p.111, forward interest rates can be converted into future interest rates applying the following approximative formula

$$\text{forward rate} = \text{futures rate} - \frac{1}{2}\sigma^2 t_1 t_2, \quad (2.16)$$

where t_1 is the time to maturity of the futures contract, t_2 is the time to maturity of the rate underlying the futures contract, and σ is the standard deviation of the change in the short-term interest rate in one year (using continuous compounding).

2.3.3. Valuating Options

Price *estimates* for options can be specified with the Black-Scholes-Merton model or related models shown later on. However, certain rules can easily be obtained to specify a *range* in which the price of an option has to lie.

As options consist of altogether four “sub-derivatives”, namely European and American calls and puts, American calls \mathcal{C} and puts \mathcal{P} are denoted in script letters as opposed to the normal font used for European calls C and puts P .

Upper Bounds The (European or American) call price $C_{t,T}$, with $t \in [t_0, T]$, cannot be higher than the underlying asset price itself, otherwise arbitrage can easily be taken by buying the asset and selling the call option. Therefore,

$$C_{t,T} \leq S_{t_0} \quad (2.17)$$

must hold. Equivalently, the price of a put option $P_{t,T}$ cannot be higher than the strike K , or else, a profit $P_{t,T} - K > 0$ would always be possible by shorting the put with strike K , so:

$$P_{t,T} \leq K. \quad (2.18)$$

Put-Call Parity There is an important relationship between the call price and the put price of a European option which *always* holds: the put-call parity,

$$C_{t,T} - P_{t,T} = S_t - Ke^{-r(T-t)}. \quad (2.19)$$

To see why this is so, the values of each side of the equation are observed as individual portfolios. The lhs (left hand side) is, therefore, a portfolio consisting of a long call and a short put. The rhs contains a long position of an asset and a short position of a risk-less zero coupon bond discounted to t_0 with a notional amount of K . At maturity T the following payoffs arise:

- As the call and the put have the same strike K and the same underlying stock which is worth S_T at maturity, only one of the two options will have a positive payoff and be exercised at time T . If $S_T - K > 0$ the call is in-the-money and the payoff for the long position is $S_T - K$, compare (2.3). If $S_T - K < 0$, or equivalently $K - S_T > 0$, the put is in-the-money and will be exercised, so the payoff (i.e. loss) of the short position is, *again*, $-(K - S_T) = S_T - K$, c.f. equation (2.6).
- At time T the rhs is simply $S_T - K$, as the spot price is now S_T and the bond is worth $K = Ke^{-r(T-T)}$.

So, both sides of (2.19) have the same *deterministic* value at maturity T and, as arbitrage is not possible, the equation must hold at any given time $t \in [t_0, T]$.

Lower Bounds The lower bound of a European call can be acquired by adding the put price $P_{t,T}$ on both sides of (2.19) resulting in

$$C_{t,T} = S_{t_0} - Ke^{-r\tau} + P_{t,T}. \quad (2.20)$$

By dropping $P_{t,T}$ one obtains the inequality, $C_{t,T} \geq S_{t_0} - Ke^{-r\tau}$, and as the call is only exercised if greater than zero,

$$C_{t,T} \geq \max \{S_{t_0} - Ke^{-r\tau}, 0\} \quad (2.21)$$

holds and is the t_0 -equivalent to statement (2.3). Note that (2.21) only holds for European call options $C_{t,T}$, and not for American calls which can be exercised early. Similar conclusions can be drawn to be able to receive the following European put price

$$P_{t,T} \geq \max \{Ke^{-r\tau} - S_{t_0}, 0\}. \quad (2.22)$$

Early Exercising: American Calls and Puts American call options⁸ have the same exercising opportunities as the corresponding European calls, so , it can be concluded that American calls are worth at least as much as the European equivalents, $\mathcal{C}_{t,T} \geq C_{t,T}$, and, by using equation (2.21), $\mathcal{C}_{t,T} \geq S_{t_0} - Ke^{-r\tau}$. It can be shown that it is never optimal to exercise early so an American call is practically equal to a European call. If $r > 0$ and, hence, $e^{-r\tau} > 1$, one has

$$\mathcal{C}_{t,T} > S_{t_0} - K. \quad (2.23)$$

At time t_0 , the price of an American call has a time value as it is above its intrinsic value (see Section 2.2.4) and, for this reason, will not be exercised. As time moves on the same arguments hold, as the call option can always be sold at $\mathcal{C}_{t,T} \geq S_t - Ke^{-r\tau}$, and therefore, $\mathcal{C}_{t,T} > S_t - K$, for any $t \in (t_0, T)$.

The European put price has at least to be worth $P_{t,T} \geq Ke^{-r\tau} - S_{t_0}$, compare equation (2.22). the American put, however, has to have the value of

$$\mathcal{P}_{t,T} \geq K - S_{t_0}, \quad (2.24)$$

with $K - S_{t_0} > Ke^{-r\tau} - S_{t_0}$, as the American put can be exercised right after the contract has been settled at t_0 . So, in comparison to (2.23), the American put is only greater than *or equal to* the difference between the strike K and the stock price S_{t_0} , and as soon as the stock price is sufficiently low (the difference or profit due to $K - S_{t_0}$ is then relatively large), the American put option is exercised.

For American options the put-call parity does not hold as in (2.19), however, in agreement [Hull02] p.175, one can derive the following inequalities

$$S_{t_0} - K \leq \mathcal{C}_{t,T} - \mathcal{P}_{t,T} \leq S_{t_0} - Ke^{-r\tau}. \quad (2.25)$$

2.3.4. Valuating Swaps

As stated in Section 2.2.5, swaps, in general, are defined as an exchange of cash flows, compare [Neftci04] ch.5. However, according to [Hull02] ch.6, the difference between the present values PV_{fix,t_0} and PV_{fl,t_0} of the cash flows generated from the swap can also be seen as two reversed bonds with different characteristics,

$$V_{\text{swap},t_0} = PV_{\text{fix},t_0} - PV_{\text{fl},t_0}, \quad (2.26)$$

where PV_{fix,t_0} depicts the present value of a bond with fixed interest rates and PV_{fl,t_0} specifies the present value of a floating-rate bond underlying the swap. The present

⁸Assuming, that there are no dividends paid on the underlying stock.

value of the bond with floating interest rates equals⁹

$$PV_{\text{fl},t_0} = (L + c^*)e^{-r_1(t_1-t_0)}. \quad (2.27)$$

Equation (2.26) then denotes the value of a swap to a party receiving fixed and paying floating interest rates. In the standard case the value of a swap is usually (close to) zero when issued as the bonds normally have the same principal (the exchanged amounts of the first payment date usually also hardly differ), so $PV_{\text{fix},t_0} \approx PV_{\text{fl},t_0}$. This can change over time as the floating-rate becomes larger or smaller than the fixed-rate.

From the view of a party receiving floating and paying fixed rates (the reverse to equation (2.26)), the value at time t_0 is

$$V_{\text{swap},t_0} = PV_{\text{fl},t_0} - PV_{\text{fix},t_0}. \quad (2.28)$$

For the valuation of currency swaps one has two reversed (fixed-rate) bonds where one bond is valued in a foreign currency. So, additionally, the spot exchange rate, S_{t_0} (domestic currency per unit of foreign currency), has to be multiplied to the foreign currency bond. E.g. if a company receives payments from a bond in its domestic currency (PV_{d,t_0}) and has cash outflows from a bond in a foreign currency (PV_{f,t_0}), the value of the swap is

$$V_{\text{FXswap},t_0} = PV_{\text{d},t_0} - S_{t_0}PV_{\text{f},t_0}. \quad (2.29)$$

⁹The value of PV_{fl,t_i} immediately before the next payment date t_i , $t_0 < t_i \leq T$, is (assumed to be) known, $PV_{\text{fl},t_i-dt} = L + c^*$, where L denotes the principal and c^* specifies the realised floating-rate payment. Right after the actual payment, the bond can be viewed at as newly issued, and is worth $PV_{\text{fl},t_1} = L$. Therefore, at time t_0 the present value of the bond is $PV_{\text{fl},t_0} = (L + c^*)e^{-r_1(t_1-t_0)}$, where t_1 refers to the first payment date and r_1 to the LIBOR rate during $t_1 - t_0$, c.f. [Hull02] p. 137.

3. The Black-Scholes-Merton Model

The *Black-Scholes-Merton (BSM) model* was a milestone in the early 1970s for pricing stock options and other derivatives, and was honored by the Nobel prize for economics in 1997. The basic conclusion made in the model is that an option is priced implicitly when its underlying stock is traded.

This chapter introduces the concept of the BSM framework according to [Hull02] ch.11 and ch.12. The assumptions taken in this model are similar to the ones made in Section 2.3: borrowing and lending is possible at the same risk-free interest rate, no risk-free arbitrage possibilities, no credit risk, no transaction costs or taxes, derivatives are perfectly divisible and there are no restrictions on short selling. Originally, stocks were implied to be non-dividend paying but extensions have been developed to deal with this drawback. However, two disadvantages of this model, i.e constant drift and volatility, remain and cannot be ignored which will be reviewed later on.

3.1. Properties of Stock Prices

3.1.1. The Process of Stock Prices

Although the two properties continuous time and continuous price movements are not completely satisfied (e.g. weekend breaks and discrete price movements) the process of a stock price $\{S_t\}_{t>0}$ is often assumed to follow a *generalized Wiener process* or *Itô process* with a *constant* volatility σ and drift rate μ , see Appendix A.1.12 and A.1.13. Therefore, the formula for the relative price movements $\frac{dS_t}{S_t}$, also referred to as *discrete returns*, can be depicted by

$$\frac{dS_t}{S_t} = \mu dt + \underbrace{\sigma dW_t}_{\stackrel{\text{A.1.12}}{=} Z_t \sqrt{dt}}, \quad t > 0, \quad (3.1)$$

where dW is a standard Wiener process, $dW \sim N(0, dt)$. The *expected return* $E[\frac{dS_t}{S_t}] = \mu$ is, as stated above, specified as the *expected drift rate* which is often considered to be the risk-free interest rate r in the risk-neutral world as seen later on. Due to the properties

Simulated Price Process with BSM Price Process

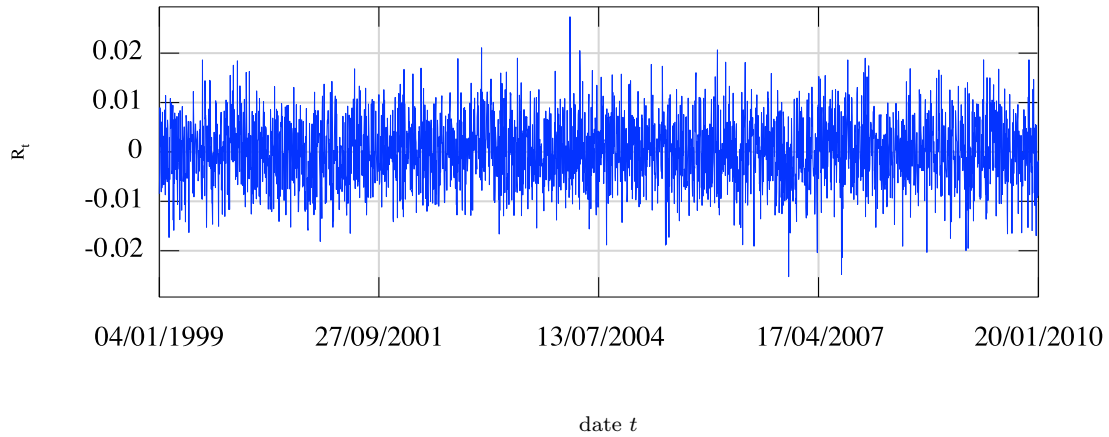


Figure 3.1.: Simulated Price Process with BSM Price Process. Parameters are obtained from Table 7.1. The simulation has the same starting value and time interval as in Figure 4.5

of the normal distribution, the relative price movements are also normally distributed, however, with mean μdt and variance $\sigma^2 dt$,

$$\frac{dS_t}{S_t} \sim N(\mu dt, \sigma^2 dt), \quad t > 0. \quad (3.2)$$

3.1.2. The Lognormal Property of Stock Prices

After assuming that the asset price returns are normally distributed, one can show that the logarithm of the stock price $\ln S_t$, $t > 0$, is lognormally distributed. This property can be derived by applying Itô's Lemma which is depicted in the following section,

$$\ln S_T - \ln S_{t_0} \sim N\left(\left(\mu - \frac{\sigma^2}{2}\right)dt, \sigma^2 dt\right), \quad (3.3)$$

$$\ln S_T \sim N\left(\ln S_{t_0} + \left(\mu - \frac{\sigma^2}{2}\right)dt, \sigma^2 dt\right). \quad (3.4)$$

The preceding statements are the results of setting the general function of the Itô Lemma which is dependent on the stock price, equal to the natural logarithm of the stock price,

$g(S_t, t) \stackrel{!}{=} \ln S_t$. The partial derivatives¹ needed in the formula are

$$\frac{\partial g(S_t, t)}{\partial S_t} = \frac{1}{S_t}, \quad \frac{\partial^2 g(S_t, t)}{\partial S_t^2} = -\frac{1}{S_t^2}, \quad \frac{\partial g(S_t, t)}{\partial t} = 0.$$

Substituting these results into (3.9), one obtains² for $t > 0$

$$dg(S_t, t) = d(\ln S_t) = \left(\mu - \frac{\sigma^2}{2} \right) dt + \sigma dW_t. \quad (3.5)$$

3.1.3. Itô's Lemma

As the Itô Lemma is essential for deriving the price of an option based on the BSM as well as the Heston model, a simple draft of the derivation is outlined in this subsection. For the sake of simplicity, only the stock price S_t and the time t are the dependent variables in this context, c.f. Appendix A.1.13. After employing the Taylor expansion and well known calculus results, the subsequent formula is obtained

$$\begin{aligned} \delta g(S_t, t) &= \frac{\partial g(S_t, t)}{\partial S_t} \delta S_t + \frac{\partial g(S_t, t)}{\partial t} \delta t \\ &\quad + \frac{1}{2} \frac{\partial^2 g(S_t, t)}{\partial S_t^2} \delta S_t^2 + \frac{1}{2} \frac{\partial^2 g(S_t, t)}{\partial t^2} \delta t^2 + \frac{\partial^2 g(S_t, t)}{\partial S_t \partial t} \delta S_t \delta t + \dots \quad (3.6) \end{aligned}$$

When taking the limit $\lim_{\delta t \rightarrow 0}$, the expressions containing higher orders of δt including $\delta S_t \delta t$ become zero. The term holding δS_t^2 , however, is proportional to δt and, therefore, cannot be ignored. This can be seen by exploiting the Itô process as depicted in the equation (A.20) in Appendix A.1.13,

$$\delta S_t = \mu(S_t, t) \delta t + \underbrace{\sigma(S_t, t) Z_t \sqrt{\delta t}}_{= \delta W_t},$$

and by squaring (again, higher orders of δt are neglected) is proportional to

$$\delta S_t^2 \propto \sigma^2(S_t, t) Z_t^2 \delta t.$$

The expected value of the rhs is $\sigma^2(S_t, t) \delta t$, as $E[Z_t] = 0$, so $E[Z_t^2] = \text{Var}[Z_t] = 1$. This remaining expression can also be seen as a constant as opposed to a random variable,

¹Financial derivatives and partial derivatives are *not* to be confused:

- a *financial* derivative, or just derivative is a financial instrument gained or derived from its underlying asset,
- a *partial* derivative and, also a total derivative, belong to the mathematical theory of differential calculus.

²Assuming the drift rate $\mu(S_t, t) = \mu S_t$ and the volatility rate $\sigma(S_t, t) = \sigma S_t$ of the Itô process are constant over any time period $\delta t \stackrel{!}{=} \tau \stackrel{2.3.1}{=} T - t_0$, the equations (3.3) and (3.4) hold.

as the *variance* of $Z_t^2 \delta t$ is of order $(\delta t)^2$, so, in the limit it is zero³. After limiting $\lim_{\delta t \rightarrow 0} \delta t = dt$, the latter equation is given by

$$dS_t^2 = \sigma^2(S_{t,t}) Z_t^2 dt \quad (3.7)$$

and equation (3.6) becomes

$$dg(S_{t,t}) = \frac{\partial g(S_{t,t})}{\partial S_t} \underbrace{dS_t}_{\stackrel{(A.18)}{=} \mu(S_{t,t}) dt + \sigma(S_{t,t}) Z_t \sqrt{dt}} + \frac{\partial g(S_{t,t})}{\partial t} dt + \frac{1}{2} \frac{\partial^2 g(S_{t,t})}{\partial S_t^2} \underbrace{dS_t^2}_{\stackrel{(3.7)}{=} \sigma^2(S_{t,t}) S_t^2 dt}. \quad (3.8)$$

Finally, dS_t and dS_t^2 are replaced by (A.18) and (3.7), respectively, and after assuming a constant drift rate $\mu(S_{t,t}) = \mu S_t$ and volatility rate $\sigma(S_{t,t}) = \sigma S_t$, one obtains

$$dg(S_{t,t}) = \left(\frac{\partial g(S_{t,t})}{\partial S_t} \mu S_t + \frac{\partial g(S_{t,t})}{\partial t} + \frac{1}{2} \frac{\partial^2 g(S_{t,t})}{\partial S_t^2} \sigma^2 S_t^2 \right) dt + \frac{\partial g(S_{t,t})}{\partial S_t} \sigma S_t dW_t. \quad (3.9)$$

3.2. Pricing Derivatives Using the BSM Model

The subsequent section shows that the value of *any* derivative $V(S_{t,t})$ which depends on the price of the underlying stock S_t and the time t can be derived solving a partial differential equation based on Itô's Lemma. For example, the value of a long forward $V_{long}(F_{t_0,T}) = V_{long}(S_{t,t}) = S_t - K e^{-r\tau}$, c.f. equation (2.10) and (2.14), also has to fulfill this partial differential equation (PDE). Therefore, the price of (European) call and put options also can be acquired by applying these calculations.

3.2.1. The Black-Scholes-Merton Differential Equation

By setting $g(S_{t,t}) \stackrel{!}{=} V(S_{t,t})$ into the final equation (3.9) of Itô's Lemma, and omitting the dependency of S_t to ease the complexity, $V(S_{t,t}) = V_t$, one obtains

$$dV_t \stackrel{\text{Itô}}{=} \left(\frac{\partial V_t}{\partial S_t} \mu S_t + \frac{\partial V_t}{\partial t} + \frac{1}{2} \frac{\partial^2 V_t}{\partial S_t^2} \sigma^2 S_t^2 \right) dt + \frac{\partial V_t}{\partial S_t} \sigma S_t dW_t. \quad (3.10)$$

It can easily be seen that the above equation and the contingent stock with a price process as in equation (3.1),

$$dS_t = \mu S_t dt + \sigma S_t dW_t, \quad (3.11)$$

³As Z_t is standard normally distributed, $Z_t \sim N(0,1)$, the square of Z_t is χ^2 -distributed, $Z_t^2 \sim \chi^2(k=1)$, with the expected value being $E[Z_t^2] = k = 1$ and the variance $\text{Var}[Z_t^2] = 2k = 2$. Hence, the variance of $Z_t^2 \delta t$ is

$$\text{Var}[Z_t^2 \delta t] = (\delta t)^2 \text{Var}[Z_t^2] = 2(\delta t)^2.$$

have the *same* underlying Wiener process W which describes the uncertainty of the price changes. By offsetting the two stochastic processes, i.e. taking a long position of $\frac{\partial V_t}{\partial S_t}$ shares⁴ of the underlying asset priced at S_t and shorting *one* derivative with the value V_t , so that $\sigma S_t dW_t$ drops out, a risk-less portfolio for an infinitesimal small time dt is derived

$$\Pi_t = -V_t + \frac{\partial V_t}{\partial S_t} S_t, \quad (3.13)$$

with,

$$d\Pi_t = -dV_t + \frac{\partial V_t}{\partial S_t} dS_t. \quad (3.14)$$

Inserting the corresponding values of (3.10) and (3.11) into equation (3.14),

$$d\Pi_t = - \left[\left(\frac{\partial V_t}{\partial S_t} \mu S_t + \frac{\partial V_t}{\partial t} + \frac{1}{2} \frac{\partial^2 V_t}{\partial S_t^2} \sigma^2 S_t^2 \right) dt + \frac{\partial V_t}{\partial S_t} \sigma S_t dW_t \right] + \frac{\partial V_t}{\partial S_t} (\mu S_t dt + \sigma S_t dW_t), \quad (3.15)$$

and by cancelling out the offsetting terms, the following equality is acquired

$$d\Pi_t = \left(-\frac{\partial V_t}{\partial t} + \frac{1}{2} \frac{\partial^2 V_t}{\partial S_t^2} \sigma^2 S_t^2 \right) dt. \quad (3.16)$$

As mentioned, the value of the portfolio does not change in a(n) (infinitesimal) short period of time and, therefore, has to earn the same amount as when invested at the risk-free rate r , otherwise arbitrage profits could be made. Hence,

$$d\Pi_t = r\Pi_t dt \quad (3.17)$$

must hold. To keep the portfolio risk-less it has to be permanently adjusted by the proportion of the stock price to the derivative. After substituting equations (3.16) and (3.13) into the last expression (3.17), the final BSM partial differential equation (PDE) is given by

$$\frac{\partial V_t}{\partial t} + r S_t \frac{\partial V_t}{\partial S_t} + \frac{1}{2} \sigma^2 S_t^2 \frac{\partial^2 V_t}{\partial S_t^2} = r V_t. \quad (3.18)$$

⁴In finance, the partial derivative of the financial derivative's value with respect to the underlying asset is called '*Delta*' and is denoted in an italicised font, i.e. Δ , confer Section 3.4. This partial derivative reflects the amount which is needed to keep the portfolio risk-less,

$$\Delta = \frac{\partial V_t}{\partial S_t}. \quad (3.12)$$

It is to be noted that the theoretical price of *any* financial derivative depending on its underlying stock price S_t and the time t has to satisfy this equation, so no arbitrage possibilities can arise subject to the assumptions made in this chapter. The example of a forward at the beginning of Section 3.2 therefore also fulfills the BSM differential equation with the partial derivatives $\frac{\partial V_t}{\partial t} = -rKe^{-r\tau}$, $\frac{\partial V_t}{\partial S_t} = 1$ and $\frac{\partial^2 V_t}{\partial S_t^2} = 0$, obtaining $-rKe^{-r\tau} + rS_t$ on the lhs which equals rV_t , compare equation (2.14). In general, the BSM-PDE (3.18) is solved by considering the *boundary conditions* of the respective derivative.

3.2.2. Black-Scholes-Merton Pricing Formulae for Options

Pricing call and put options demand somewhat more technical adjustments to satisfy the BSM differential equation (3.18), as the boundary conditions of the payoff functions contain $\max\{\cdot\}$ or $\min\{\cdot\}$ terms, compare equations (2.3) to (2.6).

The BSM-PDE does not contain the expected return of the stock μ , hence, no risk preferences enter the equation (the higher the risk aversion of investors, the higher μ will be). The reason for this is the “perfect” hedge⁴ $\Delta = \frac{\partial V_t}{\partial S_t}$ used to derive the BSM-PDE in Section 3.2.1, where the terms containing μ offset each other in equation (3.15), and therefore, do not appear in the preceding equation 3.16. This simplifies calculations to a great extent, as without loss of generality (w.l.o.g.), one can assume to be in a risk-neutral world, where $\mu = r$. The expected payoff at time t_0 of a European call using a risk-neutral measure⁵ \mathbb{Q} can then be computed by

$$C_{t_0, T}(S_{t_0}) = e^{-r\tau} \mathbb{E}_{\mathbb{Q}} \left[\underbrace{(S_T - K)^+}_{=\max\{S_T - K, 0\}} \right]. \quad (3.19)$$

The stock price follows the process as stated in (3.5), however, it is assumed that the drift rate and the volatility rate stay constant² over τ . So, by replacing dt by $\delta t = T - t_0 = \tau$, exponentiating the remaining equation and substituting the result into S_T , one obtains

$$\begin{aligned} C_{t_0, T}(S_{t_0}) &= e^{-r\tau} \mathbb{E}_{\mathbb{Q}} \left[\left(S_{t_0} e^{(r - \frac{1}{2}\sigma^2)\tau + \sigma Z_t \sqrt{\tau}} - K \right)^+ \right] \\ &= e^{-r\tau} \int_{-\infty}^{\infty} \underbrace{\left(S_{t_0} e^{(r - \frac{1}{2}\sigma^2)\tau + z\sigma\sqrt{\tau}} - K \right)^+}_{\geq 0} \cdot \frac{1}{\sqrt{2\pi}} e^{-\frac{1}{2}z^2} dz. \end{aligned} \quad (3.20)$$

⁵In the BSM framework this means the μ 's get cancelled out when deriving the BSM-PDE and the value of an option equals the expected present value of the payoff (under a risk neutral random walk). Hence, it is irrelevant what the option's rate of return actually is, as one can “perfectly” hedge (at least in the theory) the option with its underlying asset, so any exposure to the asset's performance is eliminated. Generally, one applies Girsanov's theorem which is the formal concept to change the measure from the real world to the risk-neutral world, compare Appendix A.2, [Wilmott07a] p.107 et seq and [Grimmett01] p.549 et seq for more details.

The only stochastic term is the normally distributed random variable z in the stock price process. Therefore, to ensure non-negative values from the difference between the stock price process and the strike K , it only has to be derived from which point onwards one has to integrate, so

$$\begin{aligned} 0 &\leq S_{t_0} e^{(r-\frac{1}{2}\sigma^2)\tau+z\sigma\sqrt{\tau}} - K && \Leftrightarrow \\ z &\geq \frac{\ln\left(\frac{K}{S_{t_0}}\right) - \left(r - \frac{\sigma^2}{2}\right)\tau}{\sigma\sqrt{\tau}}, \end{aligned}$$

denoting,

$$z^* := \frac{\ln\left(\frac{K}{S_{t_0}}\right) - \left(r - \frac{1}{2}\sigma^2\right)\tau}{\sigma\sqrt{\tau}}. \quad (3.21)$$

By inserting this result into (3.20),

$$\begin{aligned} C_{t_0,T}(S_{t_0}) &= e^{-r\tau} \int_{z^*}^{\infty} \left(S_{t_0} e^{r\tau - \frac{1}{2}\sigma^2\tau + z\sigma\sqrt{\tau}} - K \right) \cdot \frac{1}{\sqrt{2\pi}} e^{-\frac{1}{2}z^2} dz \\ &= S_{t_0} \int_{z^*}^{\infty} \underbrace{\frac{1}{\sqrt{2\pi}} e^{-\frac{1}{2}z^2 + z\sigma\sqrt{\tau} - \frac{1}{2}\sigma^2\tau}}_{= e^{-\frac{1}{2}(z-\sigma\sqrt{\tau})^2}} dz - K e^{-r\tau} \underbrace{\int_{z^*}^{\infty} \frac{1}{\sqrt{2\pi}} e^{-\frac{1}{2}z^2} dz}_{\stackrel{6}{=} 1 - \Phi(z^*)}, \end{aligned}$$

and by substituting $\xi = z - \sigma\sqrt{\tau}$, one obtains

$$\begin{aligned} &= S_{t_0} \cdot \underbrace{\int_{z^* - \sigma\sqrt{\tau}}^{\infty} \frac{1}{\sqrt{2\pi}} e^{-\frac{1}{2}\xi^2} d\xi}_{\stackrel{6}{=} 1 - \Phi(z^* - \sigma\sqrt{\tau})} - K e^{-r\tau} (1 - \Phi(z^*)) \\ &= S_{t_0} (1 - \Phi(z^* - \sigma\sqrt{\tau})) - K e^{-r\tau} (1 - \Phi(z^*)). \end{aligned} \quad (3.22)$$

From the properties of the normal distribution it can be concluded that $1 - \Phi(x) = \Phi(-x)$, so equation (3.22) results in

$$1 - \Phi(z^* - \sigma\sqrt{\tau}) = \Phi(\underbrace{-(z^* - \sigma\sqrt{\tau})}_{= -z^* + \sigma\sqrt{\tau}}),$$

⁶As $Z_t \sim N(0,1)$ and $\Phi(x) = \int_{-\infty}^x \frac{1}{\sqrt{2\pi}} e^{-\frac{1}{2}z^2} dz$, with $\lim_{x \rightarrow \infty} \Phi(x) = \int_{-\infty}^{\infty} \frac{1}{\sqrt{2\pi}} e^{-\frac{1}{2}z^2} dz = 1$,

$$1 - \Phi(x) = \int_{-\infty}^{\infty} \frac{1}{\sqrt{2\pi}} e^{-\frac{1}{2}z^2} dz - \int_{-\infty}^x \frac{1}{\sqrt{2\pi}} e^{-\frac{1}{2}z^2} dz = \int_x^{\infty} \frac{1}{\sqrt{2\pi}} e^{-\frac{1}{2}z^2} dz,$$

where $\Phi(\cdot)$ denotes the standard normal cumulative distribution function (cdf).

with,

$$\begin{aligned} -z^* + \sigma\sqrt{\tau} &= -\frac{\ln\left(\frac{K}{S_{t_0}}\right) - \left(r - \frac{\sigma^2}{2}\right)\tau}{\sigma\sqrt{\tau}} + \sigma\sqrt{\tau} \\ &= \frac{\ln\left(\frac{S_{t_0}}{K}\right) + \left(r + \frac{\sigma^2}{2}\right)\tau}{\sigma\sqrt{\tau}} =: d_1, \end{aligned}$$

and analogously,

$$1 - \Phi(z^*) = \Phi(-z^*) = \Phi(\underbrace{d_1 - \sigma\sqrt{\tau}}_{=: d_2}).$$

Applying the latter conclusions, the BSM formula for the value of a European call option is finally acquired by

$$C_{t_0, T}(S_{t_0}) = S_{t_0}\Phi(d_1) - Ke^{-r\tau}\Phi(d_2).$$

The Price of a European put option can easily be computed by employing the put-call parity from equation (2.19),

$$\begin{aligned} P_{t_0, T}(S_{t_0}) &= C_{t_0, T}(S_{t_0}) + Ke^{-r\tau} - S_{t_0} \\ &= S_{t_0}\Phi(d_1) - Ke^{-r\tau}\Phi(d_2) + Ke^{-r\tau} - S_{t_0} \\ &= Ke^{-r\tau}(1 - \Phi(d_2)) - S_{t_0}(1 - \Phi(d_1)) \\ &= Ke^{-r\tau}\Phi(-d_2) - S_{t_0}\Phi(-d_1). \end{aligned}$$

Summarising, the two BSM formulae for the price of European call and put options are given by

$$\begin{aligned} C_{t_0, T}(S_{t_0}) &= S_{t_0}\Phi(d_1) - Ke^{-r\tau}\Phi(d_2), \\ P_{t_0, T}(S_{t_0}) &= Ke^{-r\tau}\Phi(-d_2) - S_{t_0}\Phi(-d_1), \end{aligned} \tag{3.23}$$

with

$$\begin{aligned} d_1 &= \frac{\ln\left(\frac{S_{t_0}}{K}\right) + \left(r + \frac{\sigma^2}{2}\right)\tau}{\sigma\sqrt{\tau}}, \\ d_2 &= d_1 - \sigma\sqrt{\tau}. \end{aligned} \tag{3.24}$$

3.2.3. Interpretation and Properties of the BSM-Formulae

Using the risk-neutral measure \mathbb{Q} and equations (3.19) and (3.20), the term $Ke^{-r\tau}\Phi(d_2)$ in (3.23) can be interpreted as the discounted strike to time t_0 multiplied with the probability of exercising the option in a risk-neutral world. $S_{t_0}\Phi(d_1)$ denotes the expected

value (with respect to \mathbb{Q}) of the stock price S_T if $S_T > K$ at maturity and is zero otherwise, c.f. [Hull02] p.247.

When assuming that there are no dividends, the price of an American call is equal to that of a European call (see Section 2.3.3), so the call equation in (3.23) can also be applied to the American equivalent. For the value of an American put, however, there is no analytical solution known and can only be approximated by numerical procedures.

From the equations in (3.23) and (3.24) one can see that the price of a call and a put are dependent on the spot price S_{t_0} , the strike K , the interest rate r , the maturity T (as $\tau = T - t_0$), the initial time t_0 and the volatility σ . All except the latter are known and given. A simple way to estimate the (historical) volatility σ of a stock would be to calculate the *standard error* ($\hat{\sigma}$) of the returns ($R_t = \frac{S_t - S_{t-1}}{S_{t-1}} \approx \ln \frac{S_t}{S_{t-1}}$, $t = t_0, \dots, T$) for T discrete points of time (e.g. T daily returns), as seen in the formula below. However, this is usually not practised, as shown in Section 3.3,

$$\hat{\sigma} = \sqrt{\frac{1}{T-1} \sum_{t=t_0}^T (R_t - \bar{R})^2}, \quad \text{with} \quad \bar{R} = \frac{1}{T} \sum_{t=t_0}^T R_t. \quad (3.25)$$

3.3. Implied Volatility

An effective way to get an idea of what the volatility looks like which is anticipated by the market is the following: by observing the call and put prices being traded, one can calculate what volatility is *assumed* or *implied* by the market participants to receive these prices. This is referred to as the *implied volatility*.

The function of the BSM call price depending on the implied volatility is monotone which is shown in Figure 3.2 as an example and is also stated in [Wilmott07a] p.151 and in [Wystup07] p.19. This is why it is *equivalent* to express the value of an option as actual call prices or as the respective implied volatilities. Similarly, the BSM put price can be seen as a function of the implied volatility.

Unfortunately, the BSM-formulae (3.23) cannot be inverted analytically to obtain the implied volatility as a function of the remaining variables. Instead, iterative methods such as the Newton-Raphson algorithm are adopted to obtain a solution to any degree of accuracy, see [Wilmott07b], p.192.

The concept of the implied volatility is widely used in finance and has the advantage of reflecting the “*real*” or “*felt*” volatility of the (future) market at any given time t , respectively, at least gives the direction of the volatility as stated in [Wilmott07a], p.153. In contrast, the *historical* volatility measures the volatility of the *past time period* until time t .

Monotone Function: BSM Call Price $C(\sigma_{\text{impl}})$

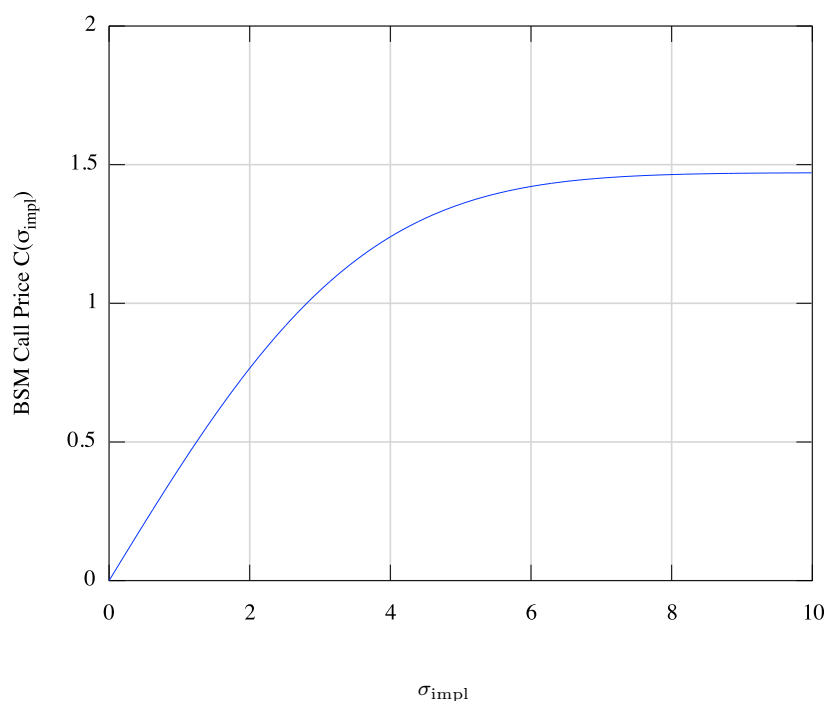


Figure 3.2.: BSM Call Price is a monotone function of the implied volatility, $C(\sigma_{\text{impl}})$. As stated in Section 2.3.3, the call price cannot be larger than the price of the underlying asset. $C(\sigma_{\text{impl}})$ converges to S_t for (unreasonably) high implied volatility σ_{impl} ; usual range for implied volatility of an exchange rate in the forex market: $0 < \sigma_{\text{impl}} < 0.3$. Chosen parameters are arbitrary (spot exchange rate for $\frac{USD}{EUR}$ at $t_0 = 18/09/2009$): $S_{t_0} = 1.4712$, $K = 1.4712$, $r = 0$, $T = 0.5$ years.

3.4. The Greeks

From a mathematical point of view the so called *greeks*⁷ are simply the partial derivatives of a financial derivative's value function. However, in finance each greek measures a different dimension of the risk given by an option and the aim of a trader is to manage the greeks so that all risks are acceptable, compare [Hull02] p.299. They, therefore, estimate the sensitivity of the derivatives price with respect to the time, the underlying asset or other values. Also, these figures lay the bases for hedging.

In Section 3.2.1, a risk-less portfolio was derived, using the partial differential equation (3.14). As mentioned, the partial derivative $\frac{\partial V_t}{\partial S_t}$ describes the amount needed from the underlying stock in order to keep the portfolio risk-free. This is the definition of the Δ -hedge, where $\Delta := \frac{\partial V_t}{\partial S_t}$. In theory, the exposure of the option to the underlying asset is hedged away for an infinitesimal short time. Therefore, this is often referred to as the “*perfect*” hedge but, also due to not being able to continuously readjust (or re hedge) the necessary amount of the underlying, it is not perfect in the real world.

The respective greeks are given in the following, compare [Hull02] ch.14, [Wilmott07a] p.110 et seq and [Wystup07] ch.1:

- $\Delta := \frac{\partial V_t}{\partial S_t}$ is defined as the (infinitesimal small) rate of change in the value of an option (or portfolio of options) when the price of the underlying asset undertakes an infinitesimal small shift. In other words, it is the sensitivity of the option's value (or value of the portfolio of options) to the underlying asset. As mentioned, Δ changes with stock price S_t and with time t . In order to lock-in a *delta-neutral* position, continual *rebalancing* or *rehedging* is required.
- $\Gamma := \frac{\partial^2 V_t}{\partial S_t^2}$ is the second derivative of the value of an option (or portfolio of options) with respect to the underlying asset. It reflects the sensitivity of Δ to the underlying and is a measure of how often reheding needs to be undertaken in order to keep a Δ -neutral position.
- $\Theta := \frac{\partial V_t}{\partial t}$ is the partial derivative of the position with respect to time and measures the exposure to t the value of an option (or portfolio of options) has.
- $\varrho := \frac{\partial V_t}{\partial r}$ is a measure for the sensitivity of the option price to the interest rate r . However, one often applies a time-dependent rate, e.g. LIBOR rate, or an foreign interest rate e.g. for forex options.
- $\mathfrak{V} := \frac{\partial V_t}{\partial \sigma_t}$ measures the exposure to the volatility σ the value of an option (or portfolio of options) has. By measuring this value one assumes the volatility is *not* constant might be inconsistent with the BSM model.

⁷In financial literature the partial derivatives are denoted in certain capitalized Greek letters, i.e. Δ , Γ , Θ , ϱ and \mathfrak{V} which is why they are referred to as the “greeks”. In order to differentiate between Greek letters used elsewhere, the greeks Δ (‘delta’), Γ (‘gamma’) and Θ (‘theta’) are depicted in the italicised Latex font. As the capitalized Greek ‘rho’ is practically identical to the Latin ‘P’, the Latex-style ‘varrho’, ϱ , is used in this context. ‘Vega’ does not exist in the Greek alphabet and will be symbolized by \mathfrak{V} .

The exact formulae of the specific greeks outlined above as well as various other greeks which also measure the sensitivity of options with respect to changes in S_t , r , t or σ are depicted in [Hull02] ch.14, [Wilmott07a] p.110 et seq, [Wilmott07b] p.182 et seq and [Wystup07] ch.1.

4. Distinctive Forex Market Features and Exotic Options

In the preceding chapters a basic understanding of the forex market, financial derivatives and the Black-Scholes-Merton model has been acquired. This unit concentrates on the specific forex characteristics of the experienced tools and also introduces further strategies containing vanilla options as well as more complex derivatives on the basis of exotics. It is also shown that the BSM framework has drawbacks when comparing the results of the model to the real market prices which give the motivation for examining further models in the subsequent chapters.

4.1. The BSM Model in the Forex Market

4.1.1. The General BSM Model Including Dividends

As mentioned in Chapter 3, the BSM model can be extended to be able to account for dividends paid on stocks during the option's lifetime. Similar to equations (2.11) and (2.12) in Section 2.3.1, the dividends can be expressed in terms of *yields* q on the respective stocks during the time period τ which is depicted by

$$S_{t_0} e^{-q\tau}. \quad (4.1)$$

It is to be noted that dividends reduce the value of the underlying stock and thus the yield q is multiplied with a negative sign in the exponent. Hereby, it is assumed that the amount and the timing of the dividends during the options lifetime can be predicted with certainty, c.f. [Hull02] p.252. For short-life options this approximation is very accurate whereas the estimation for long-term options can differ to a notable extent making the pricing of options very challenging.

In order to employ dividend payments of stocks into the BSM framework, only the factor $e^{-q\tau}$ has to be multiplied to the stock price S_{t_0} , given the above assumption. Hence, the options' call and put prices are given by

$$C_{t_0,T}(S_{t_0}) = S_{t_0} e^{-q\tau} \Phi(d_1) - K e^{-r\tau} \Phi(d_2), \quad (4.2a)$$

$$P_{t_0,T}(S_{t_0}) = K e^{-r\tau} \Phi(-d_2) - S_{t_0} e^{-q\tau} \Phi(-d_1), \quad (4.2b)$$

respectively, with

$$d_1 = \frac{\ln\left(\frac{S_{t_0}}{K}\right) + \left(r - q + \frac{\sigma^2}{2}\right)\tau}{\sigma\sqrt{\tau}},$$

$$d_2 = d_1 - \sigma\sqrt{\tau}.$$

Similarly the price process is adjusted to

$$dS_t = \underbrace{(r - q)}_{=\mu} S_t dt + \sigma S_t d\tilde{W}_t, \quad t > 0. \quad (4.3)$$

The put-call parity introduced in Section 2.3.2 also needs to be adjusted to account for the dividend yields of the stock. Again only the discount factor $e^{-q\tau}$ is multiplied to the stock price and equation (2.19) becomes

$$C_{t,T} - P_{t,T} = S_t e^{-q\tau} - K e^{-r(T-t)}. \quad (4.4)$$

4.1.2. The Specific Forex BSM Model

In the above sections, it has been mentioned that in order to adapt formulae to the forex market one simply needs to replace the dividend yield q by the respective foreign interest rate r_f which equivalently has a decreasing effect on the assets' performance. In the forex market the asset is the currency exchange rate S_t , c.f. Section 4.2.1, and the 'yield' on the asset is the foreign interest rate r_f , as seen in Section 2.3. Thus, the specific forex BSM model is given by

$$C_{t_0,T(S_{t_0})} = S_{t_0} e^{-r_f \tau} \Phi(d_1) - K e^{-r\tau} \Phi(d_2), \quad (4.5a)$$

$$P_{t_0,T(S_{t_0})} = K e^{-r\tau} \Phi(-d_2) - S_{t_0} e^{-r_f \tau} \Phi(-d_1), \quad (4.5b)$$

with

$$d_1 = \frac{\ln\left(\frac{S_{t_0}}{K}\right) + \left(r - r_f + \frac{\sigma^2}{2}\right)\tau}{\sigma\sqrt{\tau}}, \quad (4.6a)$$

$$d_2 = d_1 - \sigma\sqrt{\tau}. \quad (4.6b)$$

Again, the price process is modified to

$$dS_t = \underbrace{(r - r_f)}_{=\mu} S_t dt + \sigma S_t d\tilde{W}_t, \quad t > 0 \quad (4.7)$$

and the put-call parity is given by

$$C_{t,T} - P_{t,T} = S_t e^{-r_f \tau} - K e^{-r(T-t)}. \quad (4.8)$$

4.2. Notations in the Forex Market and the Δ -Quotation

The 'delta', i.e. Δ , does not just represent the amount of the underlying stock needed or the partial derivative of the options value, it also has an interesting connection to the moneyness and indicates the likeliness of the option expiring in-the-money. This conclusion and other features of the forex market are examined in this section.

4.2.1. Specifics in the Forex Market

In the forex market one is not confronted with stocks and dividends. Instead, the underlying assets are the exchange rates of currency pairs (c.f. Table 4.1 in Section 2.1) and the foreign interest rates r_f correspond to the dividend yields q , c.f. Section 2.3.1.

The spot price at time t of a foreign currency is also depicted by S_t , as buying one unit of a foreign currency is no different from buying one unit of any other asset. However, in the forex market currency *pairs* can be traded either by

$$\frac{\text{foreign currency}}{\text{domestic currency}} \quad \text{or} \quad \frac{\text{domestic currency}}{\text{foreign currency}}, \quad (4.9)$$

depending on what currency is defined as the numéraire, c.f. Appendix A.2.2. For example, the currency pair USD-EUR can be denoted by USD per EUR, i.e. $\frac{\text{USD}}{\text{EUR}}$, or vice versa by $\frac{\text{EUR}}{\text{USD}}$. It should be registered that the domestic currency in general does *not* have to refer to the location. It is more a convention of expressing the numéraire. In practise, *numéraire*, *domestic currency* and *base currency* are synonyms, as well as *foreign currency* and *underlying*, c.f. [Wystup07] p.8.

A forex option can also be expressed in either of a pair's currencies, so if the domestic currency is for example EUR, the value of a call option at time $t \in [t_0, T]$ is, c.f. Section 4.1.2,

$$C_{t,T}(S_t, K), \quad (4.10)$$

with the payoff at time T of the long position (equivalent to equation 2.3) being

$$\max \{S_T - K, 0\}. \quad (4.11)$$

The value of the same option denoted in a different currency, e.g. USD, is simply given by dividing the call price $C_{t,T}(S_t, K)$ by the current spot exchange rate S_t , e.g. $\frac{\text{USD}}{\text{EUR}}$,

$$\frac{1}{S_t} C_{t,T}(S_t, K). \quad (4.12)$$

The payoff of a long EUR-*call* option is consequently given by

$$\frac{1}{S_T} \cdot \max \{S_T - K, 0\} = \max \left\{ 1 - \frac{K}{S_T}, 0 \right\} \quad (4.13)$$

which can also be seen as a long USD-*put* option. By multiplying $\frac{1}{S_t}$ to equations (3.23) or, equivalently, (4.5), it can easily be verified that the subsequent relations hold

$$\frac{1}{S_t} C_{t,T}(S_t, K) = C_{t,T}\left(1, \frac{K}{S_t}\right), \quad (4.14)$$

$$\frac{1}{S_t} P_{t,T}(S_t, K) = P_{t,T}\left(1, \frac{K}{S_t}\right) \quad (4.15)$$

which is also stated in [Wystup07] p.7-p.8.

4.2.2. Delta-Quotations

The last section describes how to value forex call and put prices in the respective currencies. Especially in the forex market this is an inadequate way to denote the value of an option. This is why BSM implied volatilities are used instead which are independent of currency burdens. By applying this notation, the implied volatilities are assumed to be *random* and *time varying*, as a different volatility is *implied* for each option price with respect to the individual strikes and maturities, c.f. [Neftci04] p.443. In the following two sections one is interested in describing the implied volatilities depending on different strikes K , maturities τ and other variables for a given asset price S_{t_0} at $t_0 > 0$.

However, the figure of interest is not so much the *level* of K . Instead, one would like to examine the *relation* between the strike and the spot price of the underlying asset, as these two values determine whether the option matures in- or out-of the money at expiry T . A figure which measures the difference between the two values is, as stated in Section 2.2.4, the moneyness which is defined¹ by the ratio of the asset price S_t , $t > 0$, to the strike K , c.f. [Wilmott07b] p.242,

$$M_t := \frac{S_t}{K}. \quad (4.16)$$

It can easily be seen that this notation is not dependent on any currency, as the latter gets cancelled out (strike and spot are usually exchanged in the same currency). This also holds when the *log-moneyness* is regarded,

$$m_t := \ln \left(\frac{S_t}{K} \right). \quad (4.17)$$

¹It is to be noted that there are various different definitions of moneyness, c.f. [Neftci04] p.443, [Wikipediaerb] and [IVolatility.com09].

Nevertheless, in finance and especially in the forex market, it is common to use Δ s ('deltas') which are related to the (log-) moneyness as can be seen by the subsequent context, c.f. [Wystup07] p.5 and p.10-p.11 as well as [Neftci04] p.443,

$$\Delta_{C,t} := e^{-r_f(T-t)}\Phi(d_1), \quad (4.18a)$$

$$\Delta_{P,t} := -e^{-r_f(T-t)}\Phi(-d_1), \quad (4.18b)$$

where

$$\Delta_{C,t} = -\Delta_{P,t} \quad (4.19)$$

and

$$d_1 = \frac{m_t + \left(r - r_f + \frac{\sigma_{\text{impl}}^2}{2}\right)(T-t)}{\sigma_{\text{impl}}\sqrt{T-t}} = \frac{\ln\left(\frac{S_t}{K}\right) + \left(r - r_f + \frac{\sigma_{\text{impl}}^2}{2}\right)(T-t)}{\sigma_{\text{impl}}\sqrt{T-t}}. \quad (4.20)$$

The parameter d_1 is equivalent to equation (4.6a) and similar to (3.24a) in the original BSM formula after replacing σ by σ_{impl} . This notation also has the advantage that $\Delta_{\text{Call},t}$ approximates² the probability of the option maturing in the money and at the same time it specifies the amount of the underlying asset needed to hedge the option, c.f. Section 3.4.

Equation (4.19) shows the relation (and symmetry) between the call delta $\Delta_{C,t}$ and the put delta $\Delta_{P,t}$. However, in most financial literature, the sign is omitted, especially when plotting volatility surfaces as in Section 4.3. In order to make the delta notation more symmetric for both parties in the forex market, i.e. the delta has to be the same³ in both currencies, the drift $e^{-r_f(T-t)}$ is also dropped in the following notation and is, therefore, referred to as the *driftless delta* $\Delta_{\text{dl},t}$. To distinguish between the actual greek delta Δ_t and the simple delta notation which is the driftless delta $\Delta_{\text{dl},t}$, the latter is denoted as $\%C-\Delta_{\text{dl},t}$ for the call delta and $\%P-\Delta_{\text{dl},t}$ for the put delta and is defined by

$$C-\Delta_{\text{dl},t} := \Phi(d_1) \cdot 100[\%], \quad (4.21a)$$

$$P-\Delta_{\text{dl},t} := \Phi(-d_1) \cdot 100[\%], \quad (4.21b)$$

and

$$d_1 = \frac{m_t + \left(r - r_f + \frac{\sigma_{\text{impl}}^2}{2}\right)(T-t)}{\sigma_{\text{impl}}\sqrt{T-t}} = \frac{\ln\left(\frac{S_t}{K}\right) + \left(r - r_f + \frac{\sigma_{\text{impl}}^2}{2}\right)(T-t)}{\sigma_{\text{impl}}\sqrt{T-t}}. \quad (4.22)$$

²As stated in Section 3.2.3, the exact probability is $\Phi(d_2)$ which is approximately $\Phi(d_1)$ if $T-t$ and/or σ are not too large ($d_2 = d_1 - \sigma\sqrt{T-t}$).

³this is not exactly true as one still has the difference between the domestic interest rate r and foreign interest rate r_f in d_1 . This difference is, however, comparatively small, apart from the fact that currency pairs have default traded quotations, e.g. $\frac{USD}{EUR}$, c.f. [Wystup07] p.8 et seq. This simplification is also necessary to ease the difficulty of being able to quote prices properly in the forex market which is described by [Wystup07] as: "The entire forex quotation story becomes generally a mess...".

Also, the subsequent relations hold

$$50C_{-\Delta_{dl,t}} = 50P_{-\Delta_{dl,t}} = \text{ATM}, \quad (4.23a)$$

$$90C_{-\Delta_{dl,t}} = 10P_{-\Delta_{dl,t}}. \quad (4.23b)$$

It is also common to only depict the options which are OTM, as they usually have a higher liquidity, c.f. [Wystup07] p.26. For example, a series of options reaching from far OTM put options (far ITM call options) to far OTM call options (far ITM put options) is thus given by

$$\left[5P_{-\Delta_{dl,t}} \quad 25P_{-\Delta_{dl,t}} \quad \text{ATM} \quad 25C_{-\Delta_{dl,t}} \quad 5C_{-\Delta_{dl,t}} \right]. \quad (4.24)$$

It can be seen from the formula in (4.21) and (4.22) that the driftless delta $\Delta_{dl,t}$ is not only dependent on the log-moneyness itself but also the interest rates r and r_f , the time period $T - t$ and the instantaneous implied volatility σ_{impl} . The latter is due to the fact that the probability of an option expiring in ITM at T when being OTM at time $t < T$, has to be dependent on the implied volatility: the higher volatility, the higher the probability, thus the driftless delta has to be dependent on this parameter. For a similar reason, the time interval $[t, T]$ is a relevant factor in the formula: if an option is OTM, then the driftless delta, or probability, has to increase with the size of the interval $[t, T]$, c.f [Neftci04] p.443 and p.449.

Not only does the driftless delta quotation have significant advantages over the simple call-price equivalent, but it also seems to be the more “natural” notation as it indicates how far the option is in- or out-of-the-money, c.f. [IVolatility.com09]. As the example in Table 4.1 illustrates, the driftless delta changes abruptly when the maturity is only seven days ahead, whereas, for the *same* strike and moneyness values, the alterations in the driftless deltas maturing in 180 days are somewhat smaller. This is also the reason why automatically the relevant area is examined in more detail when applying the driftless delta notation.

Given the individual (driftless) deltas Δ_{dl,t_0} , the respective strikes K can be retrieved by inverting the respective equation in (4.18), c.f. [Wystup07] p.10. Let $\omega \in \{-1, +1\}$ be a dummy variable which takes on -1 for a put and $+1$ for a call, then the strike is obtained by

$$K = S_{t_0} \exp \left\{ -\omega \Phi^{-1}(\omega \Delta_{dl,t_0}) \sigma_{\text{impl}} \sqrt{\tau} + \left(r_d - r_f + \frac{\sigma_{\text{impl}}^2}{2} \right) \tau \right\}. \quad (4.25)$$

It is to be noted that if the original greek delta Δ_{t_0} is given in the latter formula, then the driftless delta $\Delta_{dl,t}$ is replaced by $\Delta_{t_0} e^{r_f \tau}$ including the drift.

*Driftless Delta Quotation Example:
Comparing C- $\Delta_{dl,t}$ -Quotes to Moneyness M_t and Strikes K with Different Maturities τ*

Days to Maturity $T - t = 7$			Days to Maturity $T - t = 180$		
strike K	moneyness M_t	C- $\Delta_{dl,t}$	strike K	moneyness M_t	C- $\Delta_{dl,t}$
1.7487	0.839	0 %	1.7487	0.839	1 %
1.6236	0.904	0 %	1.6236	0.904	9 %
1.5635	0.939	0 %	1.5635	0.939	20 %
1.5222	0.964	1 %	1.5222	0.964	32 %
1.4885	0.986	17 %	1.4885	0.986	43 %
1.4576	1.007	69 %	1.4576	1.007	55 %
1.4261	1.029	98 %	1.4261	1.029	67 %
1.3904	1.056	100 %	1.3904	1.056	78 %
1.3427	1.093	100 %	1.3427	1.093	89 %
1.2535	1.171	100 %	1.2535	1.171	99 %

Table 4.1.: Fictive example based on the BSM model with the EUR-USD exchange rate data from $t = 09/18/2009$. However, for the sake of simplicity, the interest rates are set to be $r = r_f = 0$ in this illustration. The remaining parameters are: $S_{t_0} = 1.4678$, $\sigma_{impl} = 0.10522$. The example shows that the C- $\Delta_{dl,t}$ -quotation is in comparison a somewhat more “natural” notation as it indicates how far the option is ITM or OTM, c.f. [IVolatility.com09].

4.3. Volatility Surface

4.3.1. Comparing the Volatility Surfaces

In this section the market volatility surface is introduced and compared to the surface generated by the BSM model. At first the former is analysed which applies the quotations as seen in the preceding section, i.e. the implied volatility depending on $\Delta_{dl,t}$ and τ . As can be seen from Figure 4.1, the market volatility is far from being constant and varies considerably with respect to the dependent variables.

Figure 4.2 shows a selection of volatility smiles in a two-dimensional plot where the individual lines represent the different maturities. The shape of the volatility curve very much depends on the factors specific derivative and distinctive market. It can have the form of a *smile*, e.g. options in the forex market, as well as a *slope* or *skew*. The general interpretation of the shape is that it represents the market’s view of future volatility in some complex way, c.f. [Wilmott07b], p.194.

It is often concluded that when upside movements are as equally large and likely as the downside shifts, the shape of the volatility typically has a smile rather than a slope. Usually, options of indices such as the S&P 500, tend to have a volatility slope as the downside risk is comparatively large. Smiles also implicate that out-of-the-money puts

Market Volatility Surface: EUR-USD, $t_0 = 23/09/2009$

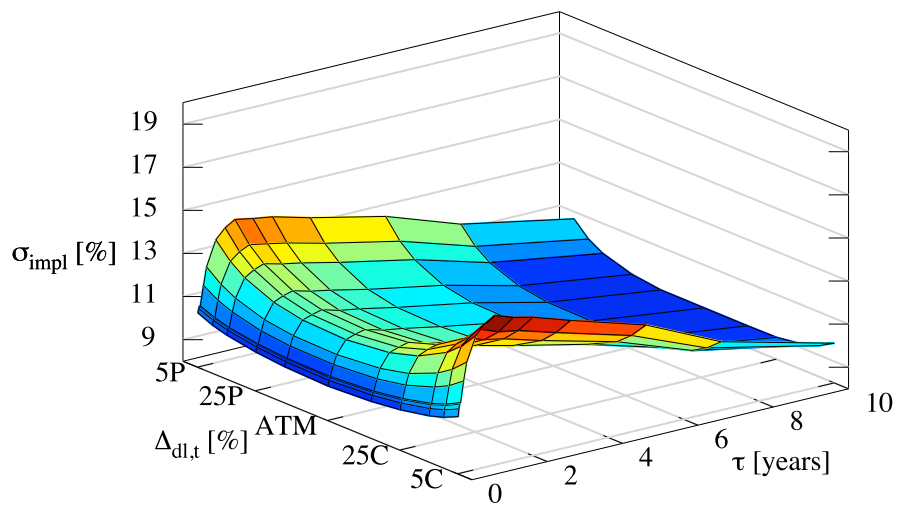


Figure 4.1.: Market Volatility Surface of EUR-USD for $t_0 = 23/09/2009$. Implied volatility σ_{impl} denoted in %, depending on the driftless deltas $\Delta_{\text{dl},t}$ in % of the OTM option and maturity τ in years, c.f. Section 4.2.2.

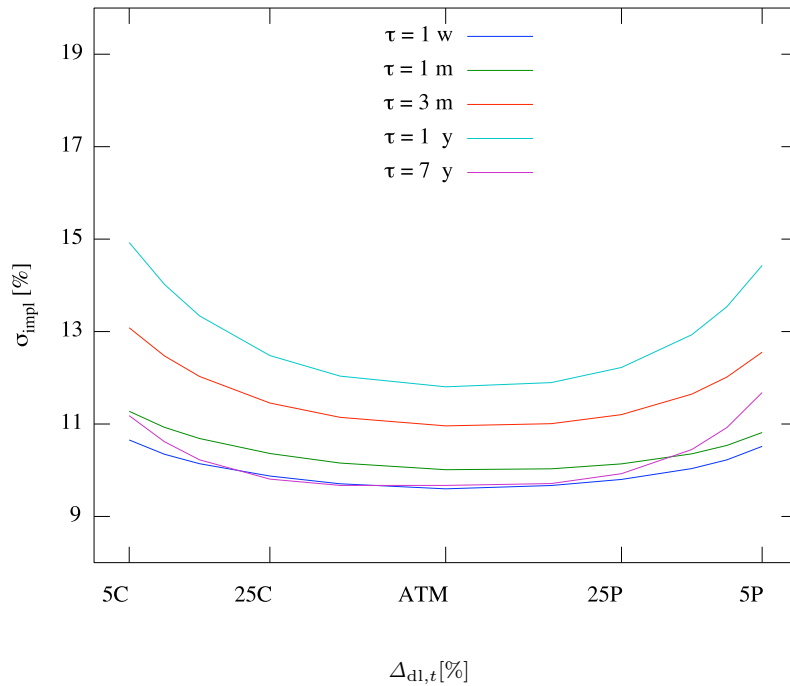


Figure 4.2.: Market Volatility Smile of Individual Maturities: EUR-USD, $t_0 = 23/09/2009$. Implied volatility σ_{impl} denoted in %, depending on the driftless deltas $\Delta_{\text{dl},t}$ in % of the OTM option, as stated in Section 4.2.2. The selected expiries τ are 1 week (w), 1 month (m), 3 months (m), 1 year (y), 7 years (y).

(in-the-money calls) and out-of-the-money calls (in-the-money puts) have higher implied volatilities than at-the-money options.

In order to compare the given market data with the volatility implied by the BSM model, it is necessary to *calibrate* the model. Calibration in this sense means that the sum of the squared differences between the real market data and the respective values from the model is minimised. More details about calibrating models to the market prices are found in Chapter 7. It is to be remembered that the BSM framework assumes constant volatility. Hence, only one value for the volatility is given to model the surface. The results of fitting the model to the data can be viewed in Figure 4.3.

It can be clearly seen that the implied volatility of the BSM model in Figure 4.3 fails to model the given market volatility in Figure 4.3 which is why one needs to derive a more sophisticated model. The differences of the call prices C_t relative to the underlying S_t in percent, i.e. $\frac{C_t}{S_t}[\%]$, of the model in comparison to the market data can also be viewed in Figure 4.4. Nevertheless, due to the fact that the BSM model is easy to employ, the BSM formulae are still widely used. Also, fairly decent results for call and

Volatility of Calibrated BSM Model for EUR-USD, $t_0 = 23/09/2009$

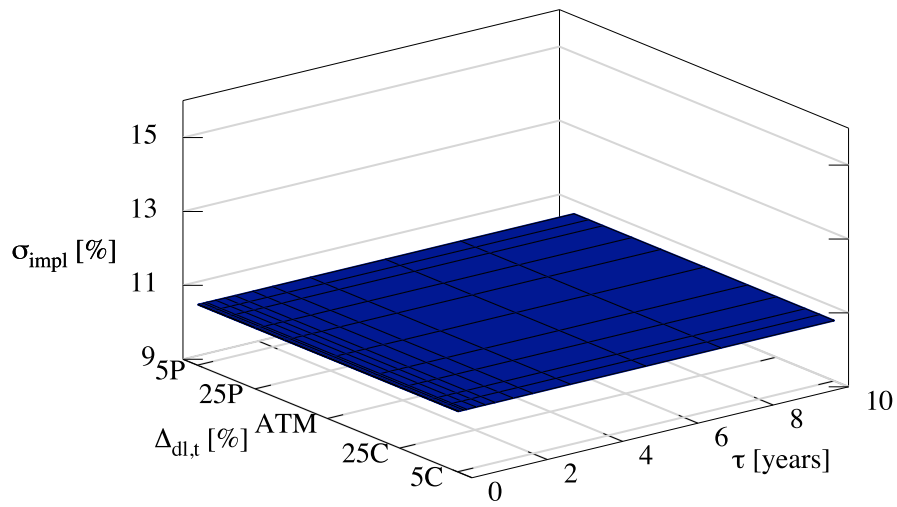


Figure 4.3.: Calibrated BSM model to call prices of EUR-USD, $t_0 = 23/09/2009$. Resulting implied volatility σ_{impl} denoted in % depending on the driftless delta $\Delta_{\text{dl},t}$ in % of the OTM option and maturity τ in years, c.f. Section 4.2.2

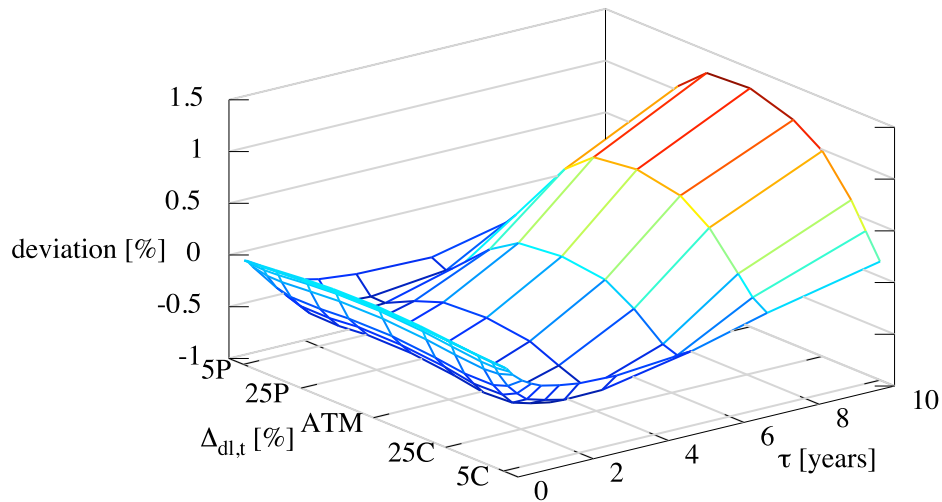


Figure 4.4.: Deviation of BSM to Market Call Prices for EUR-USD, $t_0 = 18/09/2009$. Deviation of BSM call prices to the market call prices relative to the stock price in percent, i.e. $\frac{C_{BSM} - C_{Market}}{S_t} [\%]$, depending on the driftless delta $\Delta_{dl,t}$ in % of the OTM option and maturity τ in years, c.f. Section 4.2.2.

put prices can be accomplished by pricing plain vanilla options which is due to the fact that implied volatility of the BSM model is “*the wrong number in the wrong formula to get the right price*” as stated in [Rebonato99] p.78. However, as soon as non-vanilla options are priced, the discrepancies between the proposed BSM prices and the real market prices as well as the prices one would assume under rational aspects become too large, c.f Chapter 9.

4.4. Further Strategies Containing Vanilla Options

In the preceding chapters options have been introduced as well as techniques to be able to value and price these derivatives. In finance there are many strategies based on linear combinations of options which have the purpose of widening the possibilities of hedging, investing and financing. A selection of the most popular amplifications of plain

vanilla options are outlined in the succeeding sections. These can also be used to describe the volatility smile.

All pursuing approaches are obtained by simply adding and subtracting calls and puts. Hereby, the short positions will not be examined as they are straightforwardly the reverse of the long positions. Figure 2.3 in Section 2.2.4 helps to visualize the combinations of options. Many of the definitions are conform with those in [Wystup07], p.29 - p.37.

4.4.1. Call and Put Spread

Call spreads are defined by adding a long and a short call option with different strikes K_1 and K_2 . This strategy is often chosen if a plain vanilla option is too expensive for protection against a rising asset. E.g. if a company wants to secure its risk arising from a stronger EUR in comparison to the USD (equivalently, weaker USD relative to the EUR) but the long position call has a very high premium (the fixed payment the writer of an option receives, c.f. Section 2.2.4), the firm can sell a call with a higher strike K_2 for the same time period. Hereby the company anticipates that the EUR will rise relative to the USD in a range between $K_1 < S_T < K_2$ which would result in a profit (while neglecting the premiums paid). However, the protection is only limited if the exchange rate rises to $S_T > K$, but at least only the rate $S_T - (K_2 - K_1) < S_t$ has to be paid. Recapitulating, the advantages and disadvantages are:

Pros

- protection against rising assets, e.g. exchange rates
- comparatively low premiums, as the receiving decreases the bearing premium
- maximum loss is the (low) premium

Cons

- protection is limited if $S_T > K$

4.4.2. Risk Reversal

Similarly to the call spread, the motivation of the *risk reversal* (abbrev. *RR*) is to be secured against a rising asset at minimum costs. In the case of the RR it is even “free” in monetary terms. However, the risk of the upside is financed by the *reverse risk* on the downside which gives the derivative its name. Thus, the premium paid for the long call with strike K_1 to protect the risk of a rising asset is equal to the premium received for the short put which is the second option needed in order to obtain a RR and accounts for the downside risk at strike K_2 . Between K_1 and K_2 the holder of a long RR will not make any profit or loss. The distinctive properties are:

Pros

- *full* protection against rising assets, e.g. exchange rates
- *no* monetary costs involved

Cons

- risk of a loss is equivalently high, whereas the holder also usually profits from a weak domestic currency, e.g. when exporting

4.4.3. Straddle

A very simple strategy is the *straddle* consisting of a long call and a long put with the same strike $K_1 = K_2$. The holder of a long straddle profits from an upside as well as a downside movement of the underlying asset. However, the premium is comparatively large which is due to buying two long options. Summarizing:

Pros

- *full* protection against asset movements and also rising volatility
- maximum loss is the premium paid

Cons

- comparatively expensive derivative
- not always suitable for (delta-) hedging, as often only one risk direction is given

4.4.4. Strangle

The *strangle* is identical to the straddle, except for the put strike K_2 being smaller than the call strike K_1 , i.e. $K_2 < K_1$. This is usually done by an out-of-the-money put. In this case, the holder of a long strangle profits from an upside movement of the asset as much as with a long straddle but normally has a lower premium to forfeit and only profits from larger downside movements. The characteristics are:

Pros

- *full* protection against a rising asset as well as *large* movements in either direction
- protection against volatility
- maximum loss is the premium paid
- normally cheaper than a respective straddle

Cons

- still relatively expensive
- not always suitable for (delta-) hedging, as often only one risk direction is given

4.4.5. Butterfly

A long position of a *butterfly* (abbrev. *BF*) is a combination of a long strangle and a short straddle. The BF provides limited protection against a rising or falling asset, i.e. the volatility of an asset. It is also significantly cheaper than a strangle or a straddle as it depicts the difference between the two. This is also the reason for the limited profit made by a butterfly. Summing up, one has

Pros

- limited protection against the asset's movement or increasing volatility
- maximum loss is the (relatively low) premium
- normally cheaper than a respective strangle (and therefore, also straddle)

Cons

- limited profit, respectively limited protection
- not always suitable for (delta-) hedging, as often only one risk direction is given

4.5. Describing the Volatility Smile by Decomposition of Options

The RR and the BF have an interesting relationship to the volatility which can be decomposed into the two derivatives at the 25P- Δ_t and 25C- Δ_t points. The reason for this is that the RR and the BF reflect the level of skew and convexity of the smile. Thus, three points can be given to describe the volatility smile. As stated in [Wystup07] p.22-p.24, the relations between the above values are given by

$$\sigma_{25C-\Delta_t} = \sigma_{ATM} + BF + \frac{1}{2}RR, \quad (4.26)$$

$$\sigma_{25P-\Delta_t} = \sigma_{ATM} + BF - \frac{1}{2}RR, \quad (4.27)$$

$$RR = \sigma_{25C-\Delta_t} - \sigma_{25P-\Delta_t}, \quad (4.28)$$

$$BF = \frac{\sigma_{25C-\Delta_t} + \sigma_{25P-\Delta_t}}{2} - \sigma_{ATM}. \quad (4.29)$$

4.6. Exotics

The so called (first generation) *exotics* are options which in comparison to plain vanilla options have an additional barrier or a touch-level. For example, the *one-touch (no-touch) option* pays a fixed amount if the underlying asset ever (never) trades at or beyond the touch-level and is otherwise zero, c.f. [Wystup07] p.39-p.40. Also *double one-touch* and *no-touch options* with two touch-levels exist.

The following sections, however, concentrate on an assortment of specific exotics consisting of *barrier*, *forward start* and *cliquet* options which give good examples of extensions to the plain vanilla options and also reveal drawbacks of the BSM model. Again, only the long positions are analysed, as the short positions are simply the reverse of the former.

4.6.1. Barrier Options

Instead of paying a fixed amount as with touch options, *barriers* have payoffs like plain vanilla options as seen in Section 2.2.4, *if* they do (not) hit a barrier. An *out option* becomes worthless once the corresponding barrier is reached and is said to be *knocked out*, c.f. [Wilmott07b] p.288. On the other hand an *in option* only pays out as soon as the respective barrier has been hit. This is why barrier options have the characteristic of being path dependant. As with touch options, variations with one upper, one lower or two barriers exist which are referred to as *up*, *down* or *double barrier options*.

To be exact, the above definition of barrier options only refers to *American* barrier options where the barrier option is knocked in or out if the barrier is touched or exceeded at *any* date $t \in [t_0, T]$ before maturity. Additionally, *European* barrier options exist, where only the maturity date T is relevant. However, only the former is regarded in the successive sections.

In general, exotics are usually cheaper than the corresponding plain vanilla options which is one of the main reasons for being popular. Also, the purchaser usually has very precise views about the direction of assets and markets or might want to hedge very specific cashflows with similar properties, c.f. [Wilmott07b] p.288. So, for example, if somebody wants to profit from the payoff of a call but reckons the underlying asset will not rise beyond a certain level S_u , the purchaser can save a certain amount on the premium when acquiring an up-and-out call. The characteristics of barrier options can be summarised by, c.f. [Wystup07] p.41,

Pros

- cheaper than the respective plain vanilla options
- conditional protections against a rising asset, e.g. exchange rate
- full participation in a falling asset

Cons

- option may be knocked out
- premium has to be paid

Let the barrier be denoted by B , and $q \in \{-1, +1\}$ be a dummy variable which takes on the value -1 for an *upper* bound and $+1$ for a *lower* bound. Furthermore, let $\mathbf{1}_{\{\cdot\}}$ be an indicator function which is 1 if the conditions in parentheses are fulfilled and 0 otherwise. The payoff which is also the value $V_{\text{out}, T}(S_T)$ of a standard knock-out barrier call at time T can then be depicted by

$$\mathbf{1}_{\{qS_t > qB, t \in [t_0, T]\}} \max \{S_T - K, 0\}, \quad (4.30)$$

and, hence, the payoff of a knock-out put is given by

$$\mathbf{1}_{\{qS_t > qB, t \in [t_0, T]\}} \min \{S_T - K, 0\}. \quad (4.31)$$

The relation between the value of a knock-in and a knock-out option at time T , subject to the same barrier level and payoff, can easily be given by

$$V_{\text{in}, T}(S_T) + V_{\text{out}, T}(S_T) = V_{\text{vanilla}, T}(S_T) \quad (4.32)$$

which is due to the fact that the in option is triggered at the same level as the out option, c.f. [Wilmott07b] p.294. The latter equation also holds for any given time $t \in [t_0, T]$

$$V_{\text{in}, t}(S_t) + V_{\text{out}, t}(S_t) = V_{\text{vanilla}, t}(S_t). \quad (4.33)$$

In general, the value of a barrier option at any time t can be derived from the BSM-PDE 3.18 with respect to the corresponding boundary conditions, as stated in Section 3.2.2 and [Wilmott07b] p.290. After solving these partial differential equations, the down-and-in call $C_{\text{d-i}}$ which is a call option knocked in at a barrier S_t lower than the initial spot price S_{t_0} and the strike K , is given by

$$C_{\text{d-i}}(s_{t_0}) = S_{t_0} e^{-r_f \tau} \left(\frac{B}{S_{t_0}} \right)^{2\nu} \Phi(d_{B_1}) - K e^{-r \tau} \left(\frac{B}{S_{t_0}} \right)^{2\nu-2} \Phi(d_{B_1} - \sigma \sqrt{\tau}), \quad (4.34)$$

c.f. [Hull02] p.439, where

$$\nu = \frac{r - r_f + \frac{\sigma^2}{2}}{\sigma^2}, \quad (4.35)$$

$$d_{B_1} = \frac{\ln \left(\frac{B^2}{S_{t_0} K} \right)}{\sigma \sqrt{\tau}} + \nu \sigma \sqrt{\tau}. \quad (4.36)$$

It can be seen that equation (4.34) is very similar to (4.5) except for the additional $\frac{B}{S_t}$ and ν terms and also by replacing d_{B_1} for d_1 and d_2 . From the formula (4.33) the respective down-and-out call $C_{\text{d-o}}$ can be acquired,

$$C_{\text{d-o}}(s_{t_0}) = C_{\text{vanilla}}(s_{t_0}) - C_{\text{d-i}}(s_{t_0}). \quad (4.37)$$

An up-and-in call option C_{u-i} is depicted by, c.f. [Hull02] p.440,

$$\begin{aligned}
C_{u-i}(S_{t_0}) = & S_{t_0} e^{-rf\tau} \Phi(d_{B_3}) - K e^{-r\tau} \Phi(d_{B_3} - \sigma\sqrt{\tau}) - \\
& S_{t_0} e^{-rf\tau} \left(\frac{B}{S_{t_0}} \right)^{2\nu} [\Phi(-d_{B_1}) - \Phi(-d_{B_2})] + \\
& K e^{-r\tau} \left(\frac{B}{S_{t_0}} \right)^{2\nu-2} [\Phi(-d_{B_1} + \sigma\sqrt{\tau}) - \Phi(-d_{B_2} + \sigma\sqrt{\tau})] , \quad (4.38)
\end{aligned}$$

with

$$d_{B_2} = \frac{\ln\left(\frac{B}{S_{t_0}}\right)}{\sigma\sqrt{\tau}} + \nu\sigma\sqrt{\tau} \quad d_{B_3} = \frac{\ln\left(\frac{S_{t_0}}{B}\right)}{\sigma\sqrt{\tau}} + \nu\sigma\sqrt{\tau} . \quad (4.39)$$

Although the last call price equation has a more complex form, the original structure of (4.5) can be identified. The up-and-in, up-and-out, down-and-in and down-and-out put prices are denoted by

$$P_{u-i}(S_{t_0}) = K e^{-r\tau} \left(\frac{B}{S_{t_0}} \right)^{2\nu-2} \Phi(-d_{B_1} + \sigma\sqrt{\tau}) - S_{t_0} e^{-rf\tau} \left(\frac{B}{S_{t_0}} \right)^{2\nu} \Phi(-d_{B_1}) , \quad (4.40)$$

$$P_{u-o}(S_{t_0}) = P_{\text{vanilla}}(S_{t_0}) - P_{u-i}(S_{t_0}) , \quad (4.41)$$

$$\begin{aligned}
P_{d-i}(S_{t_0}) = & K e^{-r\tau} \Phi(-d_{B_3} + \sigma\sqrt{\tau}) - S_{t_0} e^{-rf\tau} \Phi(-d_{B_3}) - \\
& K e^{-r\tau} \left(\frac{B}{S_{t_0}} \right)^{2\nu-2} [\Phi(d_{B_1} - \sigma\sqrt{\tau}) - \Phi(d_{B_2} - \sigma\sqrt{\tau})] + \\
& S_{t_0} e^{-rf\tau} \left(\frac{B}{S_{t_0}} \right)^{2\nu} [\Phi(d_{B_1}) - \Phi(d_{B_2})] , \quad (4.42)
\end{aligned}$$

$$P_{d-o}(S_{t_0}) = P_{\text{vanilla}}(S_{t_0}) - P_{d-i}(S_{t_0}) , \quad (4.43)$$

respectively. The parameters ν , d_{B_1} , d_{B_2} and d_{B_3} are as stated in (4.35), (4.36) and (4.39). More details can be found in [Hull02] p.439-p.441 and [Wilmott07b] p.307 et seq.

4.6.2. Forward Start Options

Forward start options are similar to plain vanilla options except for the strike K not being known at the options' initiation at time t_0 . Instead, the strike is set to be $K := \nu S_t$ at time t_0 , with $\nu > 0$ and is realised at some future date $t \in (t_0, T)$, c.f. [Wystup07] p.84. Thus, the payoffs at time T are equivalent to those of (2.3) - (2.6) in Section 2.2.4, as the strike is given as from $t < T$.

Often ν is set to be unity, so at time t the forward start option is exactly ATM. If, however, ν is less than unity, the call (put) is $1 - \nu$ percent ITM (OTM), and if $\nu > 1$, the call (put) is $\nu - 1$ percent OTM (ITM) at time t , c.f. [Haug98] p.36. The corresponding formulae are depicted by

$$C_{\text{fs}} = S_{t_0} e^{-r_f(t-t_0)} \left(e^{-r_f(T-t)} \Phi(d_1) - \nu e^{-r(T-t)} \Phi(d_2) \right), \quad (4.44a)$$

$$P_{\text{fs}} = S_{t_0} e^{-r_f(t-t_0)} \left(\nu e^{-r(T-t)} \Phi(-d_2) - e^{-r_f(T-t)} \Phi(-d_1) \right), \quad (4.44b)$$

where

$$d_1 = \frac{\ln\left(\frac{1}{\nu}\right) + \left(r - r_f + \frac{\sigma^2}{2}\right)(T-t)}{\sigma\sqrt{T-t}}, \quad d_2 = d_1 - \sigma\sqrt{T-t}. \quad (4.45)$$

It is to be noted that d_1 and d_2 in (4.45) are equivalent to the equations (4.6a) and (4.6b) after replacing τ by $T - t$ and K by νS_t . The call and put prices in 4.44 are also similar to those in 4.5, except for the respective time intervals and setting the strike K to νS_t .

The advantages and disadvantages of forward start options, which also hold for cliquet options in the subsequent section, can be summarised by, c.f. [Wystup07] p.84:

Pros

- protection against spot market movements as well as generally increasing volatility
- purchaser can lock in the current volatility level
- spot risk is easy to hedge

Cons

- protection level is not known in advance

4.6.3. Cliquet Options

Cliquet options, also often referred to as ratchet or moving strike options, are defined as a *series* of forward start options where the strike K_i , $i = 2, \dots, n$ of the next forward start option is set to the spot at maturity of the previous, c.f. [Haug98] p.37 and [Wystup07] p.86. The strike of the first period is usually set to be the asset price at t_0 . The option price of a cliquet is, therefore, the sum of all n forward start options, i.e.

$$C_{\text{cliqu}} = \sum_{i=1}^n S_{t_0} e^{-r_f(t_i-t_0)} \left(e^{-r_f(T_i-t_i)} \Phi(d_1) - \nu e^{-r(T_i-t_i)} \Phi(d_2) \right), \quad (4.46)$$

$$P_{\text{cliqu}} = \sum_{i=1}^n S_{t_0} e^{-r_f(t_i-t_0)} \left(\nu e^{-r(T_i-t_i)} \Phi(-d_2) - e^{-r_f(T_i-t_i)} \Phi(-d_1) \right), \quad (4.47)$$

where d_1 and d_2 are equal to the corresponding parameters in (4.45). The payoff of a cliquet call at time T_n when the last forward start option matures is given by, c.f. [Henry-Labordère08] p.63,

$$\sum_{i=1}^n \max \{ (S_{T_i} - \nu S_{T_{i-1}}), 0 \} , \quad (4.48)$$

and the payoff of the corresponding put is calculated by

$$\sum_{i=1}^n \max \{ (\nu S_{T_{i-1}} - S_{T_i}), 0 \} . \quad (4.49)$$

As mentioned in the last section, forward start options are used to lock in the current volatility level. As cliquets are a strip of forward start options at future dates, they also represent a classic group of “volatility products”, c.f. [Overhaus07] p.49. Various extensions of the vanilla cliquets exist, including combinations of locally and globally capped and floored cliquets, multiplicative cliquets and reverse cliquets, c.f. [Overhaus07] p.50 and [Gatheral06] ch. 10. Also, the definitions in the mentioned sources are not always consistent. One main difference between the notations is that some authors such as [Gatheral06] assume ν to always be set to unity and discrete returns $R_i = \frac{S_{T_{i-1}} - S_{T_i}}{S_{T_i}}$ are applied instead of the simple differences $S_{T_{i-1}} - S_{T_i}$.

4.7. Motivation for Further Option Pricing Models

The last sections show how to price some more complex options other than plain vanilla options within the Black-Scholes-Merton framework. However, it is to be recalled that the BSM model assumes constant volatility and the exotic options introduced in the last sections very much depend on the forward volatility. As can be seen for example in Figure 4.5, the volatility of the returns is *not* constant and similarly applies for forward volatilities. This clearly contradicts the assumption made by the BSM price process in equation (3.2). Also cliquets depend on the forward skew, whereas the BSM model does not deliver any skew, as it only depends on the normal distribution, c.f. [Nögel03] p.3. The issue of being able to price exotics consistently is reviewed in Chapter 9.

Even though the BSM formulae deliver reasonably good prices for plain vanilla options, it is not very convincing to depend on a wrong number in forms of the implied volatility which gets inserted into the wrong formulae to produce the right price. Also, another unsatisfying property of the BSM model is the assumption that the returns of the underlying stock are normally distributed (again with constant volatility). It can be seen from Figure 4.6 that this is not reasonable.

As the drawbacks of the model are too great to be ignored, further models of pricing options are examined in the following chapters. The focus is laid on stochastic volatility

Return Time Series of $\frac{USD}{EUR}$ during 04/01/1999 – 20/01/2010

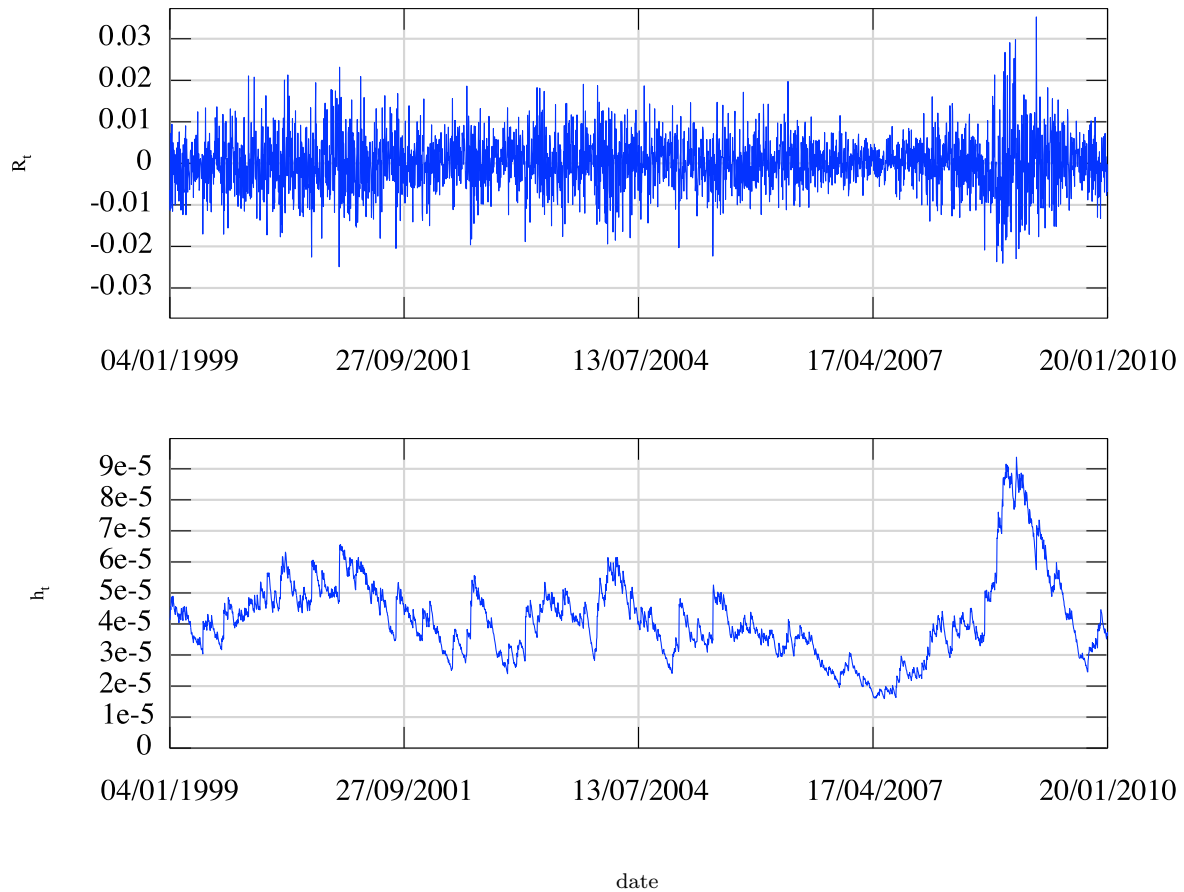


Figure 4.5.: Time series of discrete returns R_t from the underlying asset S_t . Time series ranges from 04/01/1999 to 20/01/2010. Estimated variance h_t by NGARCH model with parameters $\alpha_0 = 1.0e^{-08}$, $\alpha_1 = 9.49e^{-07}$, $\beta = 0.972$, $\gamma = 73.046$ and $\lambda = 0.257$, c.f. Chapter 6. It is shown that the variance of the returns is *not* constant throughout the time series.

Return Histogram of Returns from $\frac{USD}{EUR}$ during 04/01/1999 – 20/01/2010

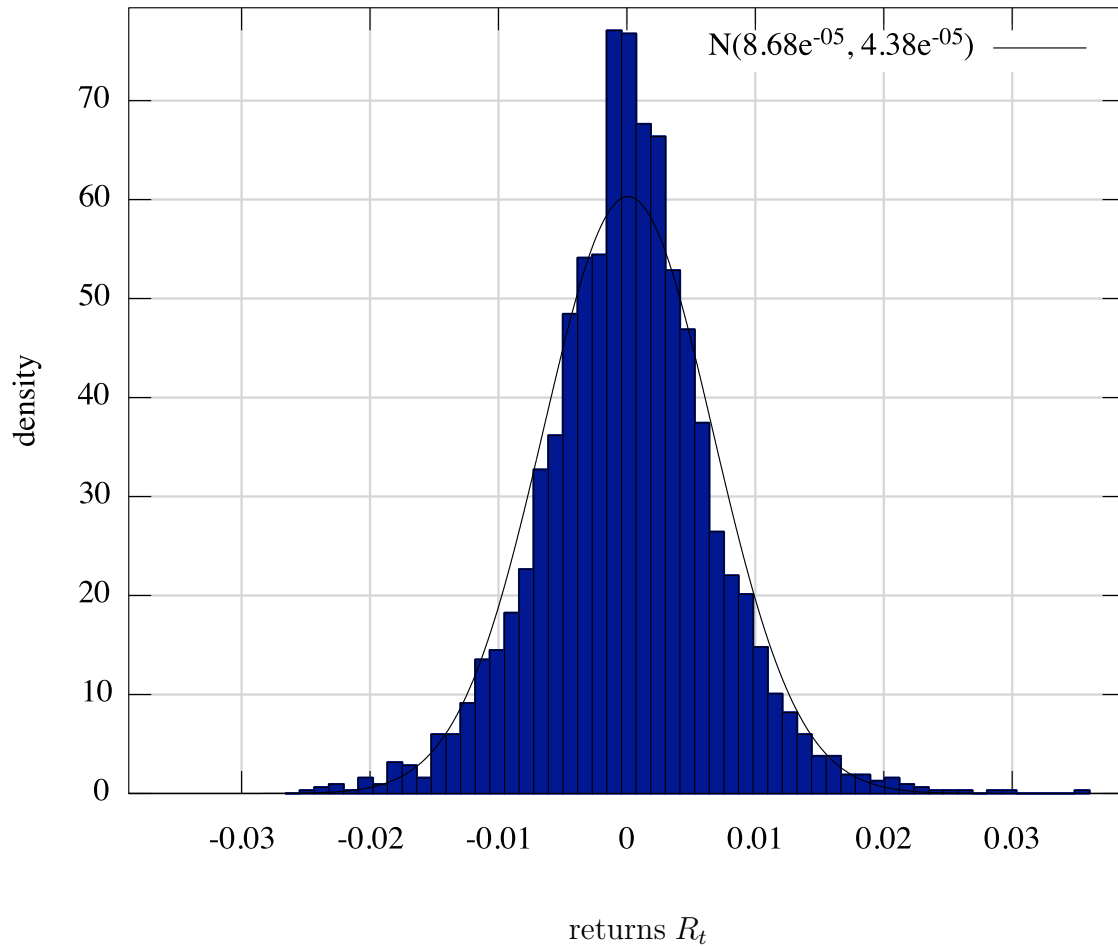


Figure 4.6.: Histogram of discrete returns R_t from time series as seen in Figure 4.5. The line represents the normal distribution with estimated mean and variance. Time series ranges from 04/01/1999 to 20/01/2010. The returns have a typical histogram found in financial data with a skew, fat tails, less frequency between the tail and the mean and larger frequency around the mean in comparison to the respective normal distribution.

models with closed form solutions. The two main models in this category are the Heston stochastic volatility model and the Heston-Nandi model which is based on a specific GARCH process for the volatility. The latter offers two different solutions as seen in Chapter 6, one is calculated by estimating via Maximum Likelihood and the other is subject to calibrating the model, as described in Section 4.3.

Stochastic volatility models have the great advantage of being able to explain why options with different strikes and maturities have different BSM implied volatilities, i.e. the volatility smile, c.f. [Gatheral06] ch.1. These models assume somewhat more realistic dynamics of the volatility which is also demonstrated in Figure 4.5 where the volatility is estimated by an NGARCH model introduced in Section 6.1.4. It is to be remembered that the BSM formulae are still used to calculate the implied volatility in order to quote the option prices in a different quantity as acknowledged in Section 3.3 and Section 4.2.2.

5. Heston's Stochastic Volatility Model

The main criticism on the Black-Scholes-Merton model is the assumed constant volatility. This might not be crucial when only an (approximate) estimate for plain vanilla stock option prices is needed. However, the unrealistic assumption of constant volatility (see Figure 7.3) in most cases has a significant impact on many derivatives in specific markets e.g. exotics currency options in the forex market. For this reason a *stochastic volatility* is introduced in the *Heston model*.

5.1. Heston's Stochastic Volatility Process

Unlike other stochastic volatility models, the Heston model has a closed-form solution applying the techniques of characteristic functions, cf. Appendix A.3. For this reason, the Heston model does not require extensive use of numerical methods to solve two dimensional PDEs, compare [Heston93]. Moreover, this model assumes that the stochastic volatility is correlated with the (stochastic) returns in order to implement skewness effects, and additionally, stochastic interest rates can be employed which is beneficial for pricing bond options and currency options accurately.

Similar to the price process used in the BSM model, one has a price process as in (5.1) where the only difference is the volatility $\sqrt{v_t}$, or variance v_t , which follows a further stochastic process. The underlying Wiener processes $W_{1,t}$ and $W_{2,t}$ are correlated and, with $\rho \in [-1, 1]$, one obtains

$$dS_t = \mu S_t dt + \sqrt{v_t} S_t dW_{1,t} \quad (5.1)$$

and

$$dv_t = \kappa (\bar{v} - v_t) dt + \sigma_v \sqrt{v_t} dW_{2,t}, \quad (5.2)$$

with

$$\rho = \text{Corr} [W_{1,t}, W_{2,t}]. \quad (5.3)$$

In this notation, $\kappa \geq 0$ represents the speed of reversion of the instantaneous variance $v_t > 0$ to its long-term mean $\bar{v} > 0$, and $\sigma_v > 0$ denotes the variance of variance (often

Simulated Price Process with Underlying Heston Volatility Process

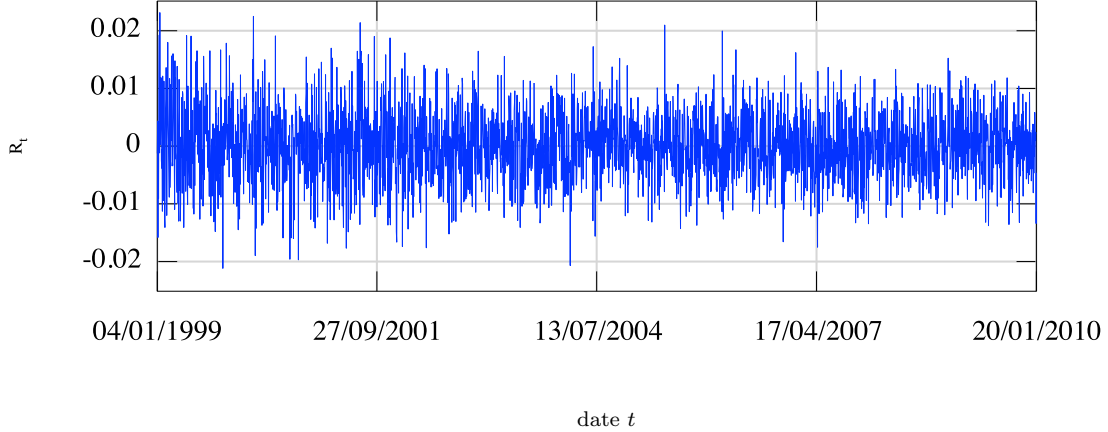


Figure 5.1.: Simulated price process with underlying stochastic volatility. Parameters are obtained from Table 7.2. The simulation has the same starting value and time interval as in Figure 4.5. The Returns have similar characteristics (e.g. clustering) as the time series in Figure 4.5.

referred to as volatility of volatility, as in [Gatheral06]). The model implies the variance to be mean reverting and autocorrelated which is a realistic assumption as the volatility-level clustering, seen in Figure 5.1, suggests. In order to guarantee the volatility process to be positive, the parameter restriction $2\kappa\bar{v} > \sigma_v^2$ is necessary, c.f. [Nögel03] p.2.

To be precise and adopting the definition from [Heston93], one actually employs the square root of the variance process, i.e. the standard error of volatility, into equation (5.1) which depicts an Ornstein-Uhlenbeck process or square root process, c.f. Appendix A.1.14,

$$d\sqrt{v_t} = -\xi\sqrt{v_t}dt + \vartheta dW_{2,t}.$$

However, for better interpretation, the preceding can be transformed into equation (5.2) by applying Ito's Lemma (similarly to Section 3.1.3) and setting the parameters to equal the variance process in (5.2) which constitutes a Cox-Ingersoll-Ross (CIR) process, c.f. Appendix A.1.15,

$$\begin{aligned} dv_t &= [\vartheta^2 - 2\xi v_t] dt + 2\vartheta\sqrt{v_t}dW_{2,t} \\ &=: \kappa[\bar{v} - v_t] dt + \sigma_v\sqrt{v_t}dW_{2,t}. \end{aligned}$$

5.2. Pricing Options Applying Heston's Stochastic Volatility Process

5.2.1. The Partial Differential Equation in the Heston Framework

Similarly to a *price* process, with $\mu(S_t, t)$ and $\sigma(S_t, t)$ being functions depending on the stock price S_t and time t , compare Section 3.1.3 and Appendix A.1.13, the general notation of a stochastic *volatility* process is given by, c.f. [Gatheral06],

$$dv_t = \alpha(S_t, v_t, t)dt + \sigma_v \beta(S_t, v_t, t) \sqrt{v_t} dW_{2,t}, \quad (5.4)$$

where $\alpha(S_t, v_t, t)$ and $\beta(S_t, v_t, t)$ additionally depend on the instantaneous variance v_t . The specific stochastic volatility process of Heston, as given in equation (5.2), the functionals $\alpha(S_t, v_t, t)$ and $\beta(S_t, v_t, t)$ are set to be $\kappa(\bar{v} - v_t)$ and 1, respectively.

In analogy to the derivation of the BSM-PDE, one needs to construct a risk-less portfolio for an infinitesimal small time dt which is given by

$$\begin{aligned} \Pi_t &= V_{\text{op},t} - \Delta_{\text{st},t} S_{\text{st},t} - \Delta_{\text{as},t} V_{\text{as},t,v_t} \\ &= V_{\text{op}} - \Delta_{\text{st}} S_{\text{st}} - \Delta_{\text{as}} V_{\text{as}}, \end{aligned} \quad (5.5)$$

where $V_{\text{op},t}$ denotes the value of the option (op) and V_{as,t,v_t} the value of a supplementary asset (as) which is dependent on the volatility. $\Delta_{\text{st},t}$ and $\Delta_{\text{as},t}$ refer to the quantities (the 'Delta's, see Section 3.4) of the underlying stock (st), respectively, of the extra asset which are needed to keep the portfolio risk-less. The only difference between the preceding equation and (3.13) is the amount $\Delta_{\text{as},t}$ of the asset $V_{\text{as},t}$, as one has an additional randomness for the *non*-constant volatility. In order to simplify the formulae, the specific time and volatility dependencies are omitted in the following derivation, as seen in equation (5.5). Applying Itô's Lemma for three dependant variables, the change of the portfolio is then given by

$$\begin{aligned} d\Pi \stackrel{\text{Itô}}{=} & \left(\frac{\partial V_{\text{op}}}{\partial t} + \frac{1}{2} v S^2 \frac{\partial^2 V_{\text{op}}}{\partial S^2} + \rho \sigma_v v \beta S \frac{\partial^2 V_{\text{op}}}{\partial v \partial S} + \frac{1}{2} \sigma_v^2 v \beta^2 \frac{\partial^2 V_{\text{op}}}{\partial v^2} \right) dt \\ & - \Delta_{\text{as}} \left(\frac{\partial V_{\text{as}}}{\partial S} + \frac{1}{2} v S^2 \frac{\partial^2 V_{\text{as}}}{\partial S^2} + \rho \sigma_v v \beta S \frac{\partial^2 V_{\text{as}}}{\partial v^2} \right) dt \\ & + \left(\frac{\partial V_{\text{op}}}{\partial S} - \Delta_{\text{as}} \frac{\partial V_{\text{as}}}{\partial S} - \Delta_{\text{st}} \right) dS \\ & + \left(\frac{\partial V_{\text{op}}}{\partial v} - \Delta_{\text{as}} \frac{\partial V_{\text{as}}}{\partial v} \right) dv, \end{aligned} \quad (5.6)$$

In order to make the portfolio risk-free, one must eliminate the dS and the dv terms by setting the two last terms to zero,

$$\frac{\partial V_{\text{op}}}{\partial S} - \Delta_{\text{as}} \frac{\partial V_{\text{as}}}{\partial S} - \Delta_{\text{op}} \stackrel{!}{=} 0, \quad (5.7)$$

and

$$\frac{\partial V_{\text{op}}}{\partial v} - \Delta_{\text{as}} \frac{\partial V_{\text{as}}}{\partial v} \stackrel{!}{=} 0, \quad (5.8)$$

which results in

$$\Delta_{\text{as}} = \frac{\frac{\partial V_{\text{op}}}{\partial v}}{\frac{\partial V_{\text{as}}}{\partial v}} \quad \text{and} \quad \Delta_{\text{op}} = \frac{\partial V_{\text{op}}}{\partial S} - \frac{\frac{\partial V_{\text{op}}}{\partial v}}{\frac{\partial V_{\text{as}}}{\partial v}} \frac{\partial V_{\text{as}}}{\partial S}. \quad (5.9)$$

This coincides to the derivation of the BSM-PDE, as equation (3.16) also does not consist of any dS terms which get cancelled out in a similar way. Considering the statements (5.8) and (5.7), the portfolio's fluctuation $d\Pi$ in an infinitesimal small time dt is then denoted by

$$\begin{aligned} d\Pi &\stackrel{\text{It}\hat{o}}{=} \left(\frac{\partial V_{\text{op}}}{\partial t} + \frac{1}{2} v S^2 \frac{\partial^2 V_{\text{op}}}{\partial S^2} + \rho \sigma_v v \beta S \frac{\partial^2 V}{\partial v \partial S} + \frac{1}{2} \sigma_v^2 v \beta^2 \frac{\partial^2 V_{\text{op}}}{\partial v^2} \right) dt \\ &\quad - \Delta_{\text{as}} \left(\frac{\partial V_{\text{as}}}{\partial S} + \frac{1}{2} v S^2 \frac{\partial^2 V_{\text{as}}}{\partial S^2} + \rho \sigma_v v \beta S \frac{\partial^2 V_{\text{as}}}{\partial v^2} \right) dt \\ &\stackrel{!}{=} r\Pi dt \\ &= r(V - \Delta_{\text{op}} S - \Delta_{\text{as}} V_{\text{as}}) dt. \end{aligned} \quad (5.10)$$

After substituting the equations in (5.9) into the PDE (5.10) and accumulating all the terms consisting of V_{op} on the LHS and all the terms containing V_{as} on the RHS, one obtains:

$$\begin{aligned} &\frac{\frac{\partial V_{\text{op}}}{\partial t} + \frac{1}{2} v S^2 \frac{\partial^2 V_{\text{op}}}{\partial S^2} + \rho \sigma_v v \beta S \frac{\partial^2 V_{\text{op}}}{\partial v \partial S} + \frac{1}{2} \sigma_v^2 v \beta^2 \frac{\partial^2 V_{\text{op}}}{\partial v^2} + r S \frac{\partial V_{\text{op}}}{\partial S} - r V}{\frac{\partial V_{\text{op}}}{\partial v}} \\ &= \frac{\frac{\partial V_{\text{as}}}{\partial t} + \frac{1}{2} v S^2 \frac{\partial^2 V_{\text{as}}}{\partial S^2} + \rho \sigma_v v \beta S \frac{\partial^2 V_{\text{as}}}{\partial v \partial S} + \frac{1}{2} \sigma_v^2 v \beta^2 \frac{\partial^2 V_{\text{as}}}{\partial v^2} + r S \frac{\partial V_{\text{as}}}{\partial S} - r V_{\text{as}}}{\frac{\partial V_{\text{as}}}{\partial v}} \end{aligned} \quad (5.11)$$

The latter is an interesting result, as both sides of the formula are identical *except* for the value of the option V_{op} to the left, respectively, of the asset V_{as} to the right of the equality. This can only hold, when both sides are equal to some function f of the *independent* variables S , v and t , i.e. $f_t(S, v, t)$, compare [Gatheral06]. This means that the function f has *no* dependency on the actual value of the option (V_{op}) *nor* to the asset (V_{as}). W.l.o.g, one can set the function to be, c.f. [Gatheral06],

$$\begin{aligned} f(S, v, t) &:= - \left(\alpha(S, v, t) - \lambda(S, v, t) \beta(S, v, t) \sqrt{v} \right) \\ &= - \left(\alpha - \lambda \beta \sqrt{v} \right), \end{aligned} \quad (5.12)$$

where $\alpha(S, v, t)$ and $\beta(S, v, t)$ denote the drift and the volatility functions as in equation (5.4). $\lambda(S, v, t)$ is referred to the *market price of volatility risk* and is outlined in following Section

5.2.2. After replacing the RHS of (5.11) by equation (5.12),

$$\begin{aligned} \frac{\partial V_{\text{op}}}{\partial t} + \frac{1}{2}vS^2\frac{\partial^2 V_{\text{op}}}{\partial S^2} + \rho\sigma_v\beta S\frac{\partial V_{\text{op}}}{\partial v\partial S} + \frac{1}{2}\sigma_v^2v\beta^2\frac{\partial^2 V_{\text{op}}}{\partial v^2} + rS\frac{\partial V_{\text{op}}}{\partial S} - rV_{\text{op}} \\ = -(\alpha - \lambda\beta\sqrt{v})\frac{\partial V_{\text{op}}}{\partial v}, \end{aligned} \quad (5.13)$$

and inserting the specific values of the Heston model, i.e. $\alpha(S_t, v_t, t) = \kappa(\bar{v} - v_t)$ and $\beta(S_t, v_t, t) = 1$, one obtains the following PDE which is the Heston counterpart to the BSM-PDE (3.18),

$$\begin{aligned} \frac{\partial V_{\text{op}}}{\partial t} + \frac{1}{2}vS^2\frac{\partial^2 V_{\text{op}}}{\partial S^2} + \rho\sigma_vvS\frac{\partial V_{\text{op}}}{\partial v\partial S} + \frac{1}{2}\sigma_v^2v\frac{\partial^2 V_{\text{op}}}{\partial v^2} + rS\frac{\partial V_{\text{op}}}{\partial S} - rV_{\text{op}} \\ = \kappa(v - \bar{v})\frac{\partial V_{\text{op}}}{\partial v}. \end{aligned} \quad (5.14)$$

5.2.2. The Market Price of Volatility Risk

The market price of volatility risk is acquired by comparing the previous PDE 5.14 with a PDE obtained by not considering the value of the additional volatility dependent asset as depicted in equation (5.5). So, the portfolio Π' is

$$\Pi' = V_{\text{op}} - \Delta_{\text{st}}S_{\text{st}}, \quad (5.15)$$

and again by applying Itô's Lemma, one receives the subsequent PDE

$$\begin{aligned} d\Pi' \stackrel{\text{It}\hat{o}}{=} & \left(\frac{\partial V_{\text{op}}}{\partial t} + \frac{1}{2}vS^2\frac{\partial^2 V_{\text{op}}}{\partial S^2} + \rho\sigma_vv\beta S\frac{\partial^2 V_{\text{op}}}{\partial v\partial S} + \frac{1}{2}\sigma_v^2v\beta^2\frac{\partial^2 V_{\text{op}}}{\partial v^2} \right) dt \\ & + \left(\frac{\partial V_{\text{op}}}{\partial S} - \Delta_{\text{st}} \right) dS \\ & + \frac{\partial V_{\text{op}}}{\partial v} dv. \end{aligned} \quad (5.16)$$

The preceding portfolio Π' is delta-hedged, therefore, the term containing dS drops out, as $\frac{\partial V_{\text{op}}}{\partial S} - \Delta_{\text{st}} \equiv 0$. After subtracting the amount one would achieve when investing Π' at a risk-free rate r , i.e. $r\Pi' = r(V_{\text{op}} - \Delta_{\text{st}}S_{\text{st}})$,

$$\begin{aligned} d\Pi' - r\Pi'dt = & \underbrace{\left(\frac{\partial V_{\text{op}}}{\partial t} + \frac{1}{2}vS^2\frac{\partial^2 V_{\text{op}}}{\partial S^2} + \rho\sigma_vv\beta S\frac{\partial^2 V_{\text{op}}}{\partial v\partial S} + \frac{1}{2}\sigma_v^2v\beta^2\frac{\partial^2 V_{\text{op}}}{\partial v^2} + rS\frac{\partial V_{\text{op}}}{\partial S} - rV_{\text{op}} \right)}_{\stackrel{(5.13)}{=} -(\alpha - \lambda\beta\sqrt{v})\frac{\partial V_{\text{op}}}{\partial v}} dt \\ & + \frac{\partial V_{\text{op}}}{\partial v} \underbrace{dv}_{\stackrel{(5.4)}{=} \alpha(S_t, v_t, t)dt + \sigma_v\beta(S_t, v_t, t)\sqrt{v_t}dW_{2,t}}, \end{aligned}$$

and substituting the two terms by the RHS of (5.13) and the RHS of (5.4), one receives

$$= \frac{\partial V_{\text{op}}}{\partial v} \beta \sqrt{v} (\lambda dt + \sigma_v dW_2). \quad (5.17)$$

From the preceding formula it can be seen that the portfolio Π' is *not* risk-less as the random term W_2 is present. Furthermore, the deterministic term λ may be interpreted as the *excess return* to the risk-free rate for accepting a certain level of risk, compare [Wilmott07b], p. 365. Therefore, for taking σ_v units of volatility risk dW_2 one acquires λdt units of extra return which is why λ is referred to as the *market price of volatility risk*.

Thus, to enable a risk-free portfolio Π' , one needs to employ a risk-neutral drift

$$\alpha^* = \alpha - \lambda \beta \sqrt{v}, \quad (5.18)$$

with the corresponding SDE for the volatility

$$dv = \alpha^* dt + \beta \sqrt{v} dW_2 \quad (5.19)$$

which would lead to the same results as the original SDE (5.2) without any explicit price of the risk term, c.f. [Gatheral06], p.7. This procedure corresponds to the changing of the risk measure of the real world \mathbb{P} to the risk-neutral world \mathbb{Q} , compare Appendix A.2. In order to simplify calculations, the latter will be applied in the following.

5.2.3. Pricing a European Option with the Heston Model

In analogy to the BSM call price solution, it can be shown that the price of a call option has to satisfy the following equation, as derived in Appendix A.4.2,

$$C_{t_0, T}(S_T, v) = SP_1 - Ke^{-r(T-t_0)}P_2, \quad (5.20)$$

where again, as in Section 3.2.3, the first term represents the pseudo-expectation¹ of the index level given that the option is in-the-money and the second term is the discounted strike price multiplied by the pseudo-probability of exercise, c.f. [Gatheral06]. After inserting the call price equation (5.20) into (5.14), with $V_{\text{op}} \stackrel{!}{=} C$, one obtains two PDEs for the respective pseudo probabilities P_j , $j = 1, 2$, c.f. Appendix A.4.3. After setting²

¹ P_1 itself is the pseudo-probability of exercising, as P_2 , but with respect to a different measure, compare Appendix A.4.1

²Note, to differentiate with respect to τ , one needs to employ the subsequent rule

$$\frac{\partial P_j}{\partial t} = \frac{\partial P_j}{\partial \tau} \underbrace{\frac{\partial \tau}{\partial t}}_{=-1} = -\frac{\partial P_j}{\partial \tau}$$

$\tau := T - t$ and $x := \ln(F_{t,T}/K)$, the j -th PDE is given by

$$-\frac{\partial P_j}{\partial \tau} + \frac{1}{2}v \frac{\partial^2 P_j}{\partial x^2} + w_j v \frac{\partial P_j}{\partial x} + \frac{1}{2}\sigma_v^2 v \frac{\partial^2 P_j}{\partial v^2} + \rho\sigma_v v \frac{\partial^2 P_j}{\partial x \partial v} + (a - b_j v) \frac{\partial P_j}{\partial v} = 0, \quad (5.21)$$

with $j = 1, 2$ and

$$w_1 = 0.5, \quad w_2 = -0.5, \quad a = \kappa \bar{v}, \quad b_1 = \kappa - \rho\sigma_v \quad \text{and} \quad b_2 = \kappa.$$

In order to satisfy the boundary conditions (A.42a) - (A.42e) in Appendix A.4.1, the preceding PDE (5.21) is subject to

$$\begin{aligned} \lim_{\tau \rightarrow 0} P_j(x, v, \tau) &= \begin{cases} 1 & \text{if } x > 0 \\ 0 & \text{if } x \leq 0 \end{cases} \\ &:= 1_{\{x > 0\}}. \end{aligned} \quad (5.22)$$

To be able to solve equation (5.21), with respect to the terminal conditions in (5.22), it is necessary to exploit the properties of characteristic functions, c.f. Appendix A.3. In this case, the characteristic functions³ of the respective probabilities P_j are depicted by

$$\tilde{P}_j(u, v, \tau) = \int_{-\infty}^{\infty} e^{-iux} P_j(x, v, \tau) dx, \quad (5.23)$$

so, for $\tau = 0$,

$$\tilde{P}_j(u, v, 0) = \int_{-\infty}^{\infty} e^{-iux} 1_{x > 0} dx = \frac{1}{iu}. \quad (5.24)$$

In Appendix A.3 it can be seen that the inverse transform is given by

$$P_j(x, v, \tau) = \frac{1}{2\pi} \int_{-\infty}^{\infty} e^{iux} \tilde{P}_j(u, v, \tau) du. \quad (5.25)$$

Substituting the pseudo probabilities P_j by the respective characteristic functions into PDE (5.21) the subsequent equation is obtained

$$\begin{aligned} \frac{1}{2\pi} \int_{-\infty}^{\infty} \left(-\frac{\partial \tilde{P}_j e^{iux}}{\partial \tau} + w_j v \frac{\partial \tilde{P}_j e^{iux}}{\partial x} + \frac{1}{2}v \frac{\partial^2 \tilde{P}_j e^{iux}}{\partial x^2} + \frac{1}{2}\sigma_v^2 v \frac{\partial^2 \tilde{P}_j e^{iux}}{\partial v^2} + \right. \\ \left. \rho\sigma_v v \frac{\partial^2 \tilde{P}_j e^{iux}}{\partial v \partial x} + (a - b_j v) \frac{\partial \tilde{P}_j e^{iux}}{\partial v} \right) du = 0 \end{aligned} \quad (5.26)$$

³In comparison to Appendix A.3, a negative sign in e^{-iux} is employed which is not relevant as it is an oscillating factor.

It is to be noted that after integrating the RHS of (5.23), the characteristic function $\tilde{P}_j(u,v,\tau)$ does not depend on the variable x . Thus the partial derivatives with respect to x are given by

$$\begin{aligned}\frac{\partial \tilde{P}_j e^{iux}}{\partial x} &= iu \tilde{P}_j e^{iux}, \\ \frac{\partial^2 \tilde{P}_j e^{iux}}{\partial x^2} &= -u^2 \tilde{P}_j e^{iux}.\end{aligned}$$

In order to simplify the notational expenditure, only the *integrand* of (5.26) is regarded until being solved at the end of the derivation in equation (5.34). Hence, after taking the partial derivatives w.r.t. x and dividing by e^{iux} , the integrand is given by

$$-\frac{\partial \tilde{P}_j}{\partial \tau} + iuw_j v \tilde{P}_j - \frac{1}{2}u^2 v \tilde{P}_j + \frac{1}{2}\sigma_v^2 v \frac{\partial^2 \tilde{P}_j}{\partial v^2} + iu\rho\sigma_v v \frac{\partial \tilde{P}_j}{\partial v} + (a - b_j v) \frac{\partial \tilde{P}_j}{\partial v} = 0 \quad (5.27)$$

The following shows that the characteristic function $\tilde{P}_j(u,v,\tau)$ is decomposed into two functions $\mathfrak{C}_j(u,\tau)$ and $\mathfrak{D}_j(u,\tau)$ which help to derive the price of a call option by reducing the preceding PDE to two ordinary differential equations (ODE). This substitution relies on a sophisticated guess which exploits the linearity of the coefficients in equation (5.27) and is depicted by

$$\begin{aligned}\tilde{P}_j(u,v,\tau) &= \tilde{P}_j(u,v,0) \cdot e^{\bar{v}\mathfrak{C}_j(u,\tau) + v\mathfrak{D}_j(u,\tau) + iux} \\ &= \frac{1}{iu} \cdot e^{\bar{v}\mathfrak{C}_j(u,\tau) + v\mathfrak{D}_j(u,\tau) + iux},\end{aligned} \quad (5.28)$$

subject to the terminal condition

$$\tilde{P}_j(u,v,\tau \doteq 0) = \frac{1}{iu} e^{iux}$$

which holds if, c.f. equation (5.28),

$$\mathfrak{C}_j(\tau \doteq 0, u) = 0 \quad \text{and} \quad \mathfrak{D}_j(\tau \doteq 0, u) = 0. \quad (5.29)$$

Thus, the partial differential equations of \tilde{P}_j are given by

$$\begin{aligned}\frac{\partial \tilde{P}_j}{\partial v} &= \mathfrak{D}_j \tilde{P}_j, \\ \frac{\partial^2 \tilde{P}_j}{\partial v^2} &= \mathfrak{D}_j^2 \tilde{P}_j, \\ \frac{\partial \tilde{P}_j}{\partial \tau} &= \left(\bar{v} \frac{\partial \mathfrak{C}_j}{\partial \tau} + v \frac{\partial \mathfrak{D}_j}{\partial \tau} \right) \tilde{P}_j.\end{aligned} \quad (5.30)$$

Substituting these results into equation (5.27) yields

$$\underbrace{\tilde{P}_j \left(-\frac{\partial \mathfrak{C}_j}{\partial \tau} + a \mathfrak{D}_j \right)}_{(*)} + \underbrace{\tilde{P}_j v \left(\frac{\partial \mathfrak{D}_j}{\partial \tau} + w_j i u - \frac{1}{2} u^2 + \frac{1}{2} \sigma_v^2 \mathfrak{D}_j^2 + \rho \sigma_v i u \mathfrak{D}_j - b_j \mathfrak{D}_j \right)}_{(**)} = 0. \quad (5.31)$$

It can easily be seen that equation (5.31) can only hold if (*) and (**) equal 0. Thus, as mentioned above, the PDE can be decomposed into two ordinary differential equations for the j -th pseudo probability

$$\begin{aligned} -\frac{d\mathfrak{C}_j}{d\tau} + a \mathfrak{D}_j &= 0, \\ \frac{d\mathfrak{D}_j}{d\tau} + w_j i u - \frac{1}{2} u^2 + \frac{1}{2} \sigma_v^2 \mathfrak{D}_j^2 + \rho \sigma_v i u \mathfrak{D}_j - b_j \mathfrak{D}_j &= 0, \end{aligned} \quad (5.32)$$

subject to the terminal conditions in (5.29). The functions \mathfrak{C}_j and \mathfrak{D}_j can now be calculated by integrating and by solving Riccati equations subject to the boundary conditions $\mathfrak{C}_j(u,0)$ and $\mathfrak{D}_j(u,0)$, as explicitly derived in [Desmettre07]. The respective values are given by

$$\begin{aligned} \mathfrak{C}_j(u, \tau) &= \tau r i u + \frac{a}{\sigma_v^2} \left((b_j - \rho \sigma_v i u + d_j) \tau - 2 \ln \left(\frac{1 - g_j e^{d_j \tau}}{1 - g_j} \right) \right), \\ \mathfrak{D}_j(u, \tau) &= \frac{b_j - \rho \sigma_v i u + d_j}{\sigma_v} \left(\frac{1 - e^{d_j \tau}}{1 - g_j e^{d_j \tau}} \right), \end{aligned} \quad (5.33)$$

where

$$g_j := \frac{b_j - \rho \sigma_v i u + d_j}{b_j - \rho \sigma_v i u - d_j} \quad \text{and} \quad d_j := \sqrt{(\rho \sigma_v i u - b_j)^2 - \sigma_v^2 (2w_j i u - u^2)}.$$

As the integrand of equation (5.26) has now been solved, one still needs to integrate to finally obtain the pseudo probabilities P_j , $j = 1, 2$. In Appendix A it is outlined that P_j has the following form

$$P_j(x, v, \tau) = \frac{1}{2} + \frac{1}{\pi} \int_0^\infty \Re \left\{ \frac{1}{iu} \cdot e^{\bar{v} \mathfrak{C}(u, \tau) + v \mathfrak{D}(u, \tau) + i u x} \right\} du \quad (5.34)$$

$$= \frac{1}{2} + \frac{1}{\pi} \int_0^\infty \Re \left\{ \tilde{P}_j(s_{t_0}, v, \tau, u) \right\}, \quad (5.35)$$

hence, the call option in equation (5.20) is derived.

5.3. Volatility Surface in the Heston Model

Having derived the Heston model for pricing options, it is of interest to see how this model performs in comparison to the BSM framework. As in Section 4.3 where the BSM

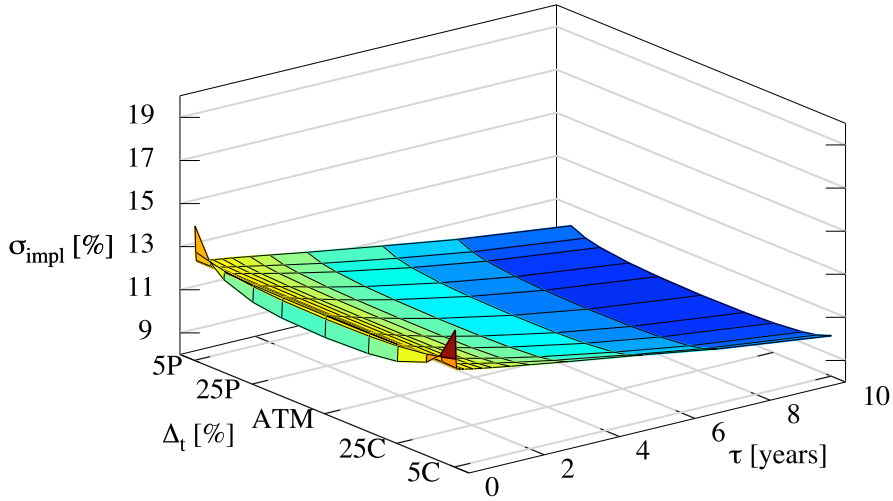


Figure 5.2.: Calibrated Heston model to call prices of EUR-USD, $t_0 = 23/09/2009$. Resulting implied volatility σ_{impl} denoted in % depending on the driftless delta $\Delta_{\text{dl},t}$ in % of the OTM option and maturity τ in years, c.f. Section 4.2.2

model is calibrated to the market prices, the squared differences of the market prices to the Heston call prices are minimised with respect to the Heston parameters κ , v_t , λ , \bar{v} , σ_v and ρ . Because the BSM model has only one parameter, i.e. the (implied) volatility, to minimise this the squared differences, it is obvious that the Heston model should perform better. Detailed results of the empirical analysis of the models are given in Chapter 7, as well as the exact specification of the optimisation procedure.

Figure 5.2 shows the resulting volatility surface after calibrating the Heston model to the market data on $t_0 = 23/09/2009$. Again, the implied volatility on the vertical axis is dependant on the respective driftless deltas $\Delta_{\text{dl},t}$ and the maturities τ , as acknowledged in Section 4.2.2. It can be seen that the volatility surface “imitates” the structure of the original data seen in Figure 4.1 to a large extent, especially when comparing it to the BSM model equivalent in Figure 4.3. This is why the deviations of the Heston prices relative to the spot S_{t_0} in Figure 5.3 are considerably smaller than the ones after calibrating the BSM model in Figure 4.4. Before comparing the outcomes in more details, another stochastic volatility model is introduced in the following chapter.

Deviation of Heston to Market Call Prices: EUR-USD, $t_0 = 18/09/2009$

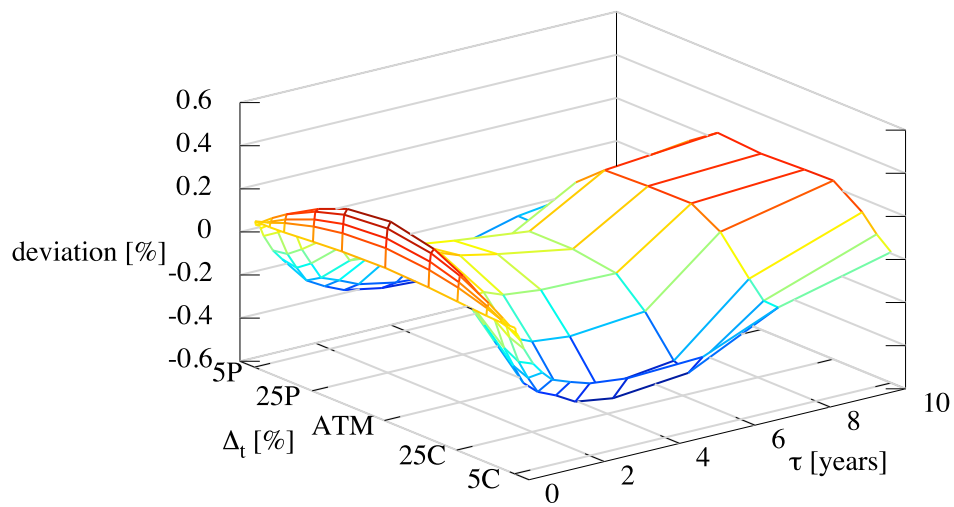


Figure 5.3.: Deviation of Heston to market call prices relative to the stock price in percent, i.e. $\frac{C_{model} - C_{market}}{S_t} [\%]$, depending on the driftless deltas $\Delta_{dl,t}$ in % of the OTM option and maturity τ in years, c.f. Section 4.2.2.

6. The GARCH Model

Estimating the volatility by employing the *GARCH* model (Generalized Autoregressive Conditional Heteroskedasticity) is another way of capturing the stochastic nature of the volatility as well as the correlation between the volatility and the spot returns, compare [Heston00]. Furthermore, it also simultaneously encapsulates the path dependency of the volatility being an autoregressive process. Although this model has a *discrete* (time) structure, the single lag version includes Heston's stochastic volatility approach as a continuous-time limit and also provides similar results. Besides, it is often easier to implement real data into this model.

6.1. The General GARCH Process

As mentioned, the GARCH model is generally motivated by similar arguments as Heston's stochastic volatility model, namely acquiring the *inconstant* volatility over time, as seen in Figure 6.1. The main differences of the GARCH in comparison to the Heston model are the discrete structure and the ability of taking path dependencies of time series into account (high levels of volatility often follow similarly high levels). The latter is done by examining *conditional* expectations and variances, given the history or filtration of a price process, c.f. Appendix A.1.1. The subsequent section follows [Bollerslev86].

6.1.1. Definition of the GARCH(p,q) Process

Let ϵ_t denote a real-valued discrete-time stochastic process, and let \mathcal{F}_t be the information set (σ -field, c.f. Appendix A.1.1) of all information through time $t \in T \subset \mathbb{N}_0$. The GARCH(p,q) process is then given by¹

$$\epsilon_t \mid \mathcal{F}_{t-1} \sim N(0, h_t), \quad (6.1)$$

$$\begin{aligned} h_t &= \alpha_0 + \sum_{j=1}^q \alpha_j \epsilon_{t-j}^2 + \sum_{j=1}^p \beta_j h_{t-j} \\ &= \alpha_0 + A(L)\epsilon_t^2 + B(L)h_t, \end{aligned} \quad (6.2)$$

where $p \geq 0$, $q > 0$, $\alpha_0 > 0$, $\alpha_j \geq 0$, $j = 1, \dots, q$, and $\beta_j \geq 0$, $j = 1, \dots, p$.

¹the conditional distribution of ϵ_t does not have to be normally distributed

Simulated Price Process with Underlying GARCH Variance h_t

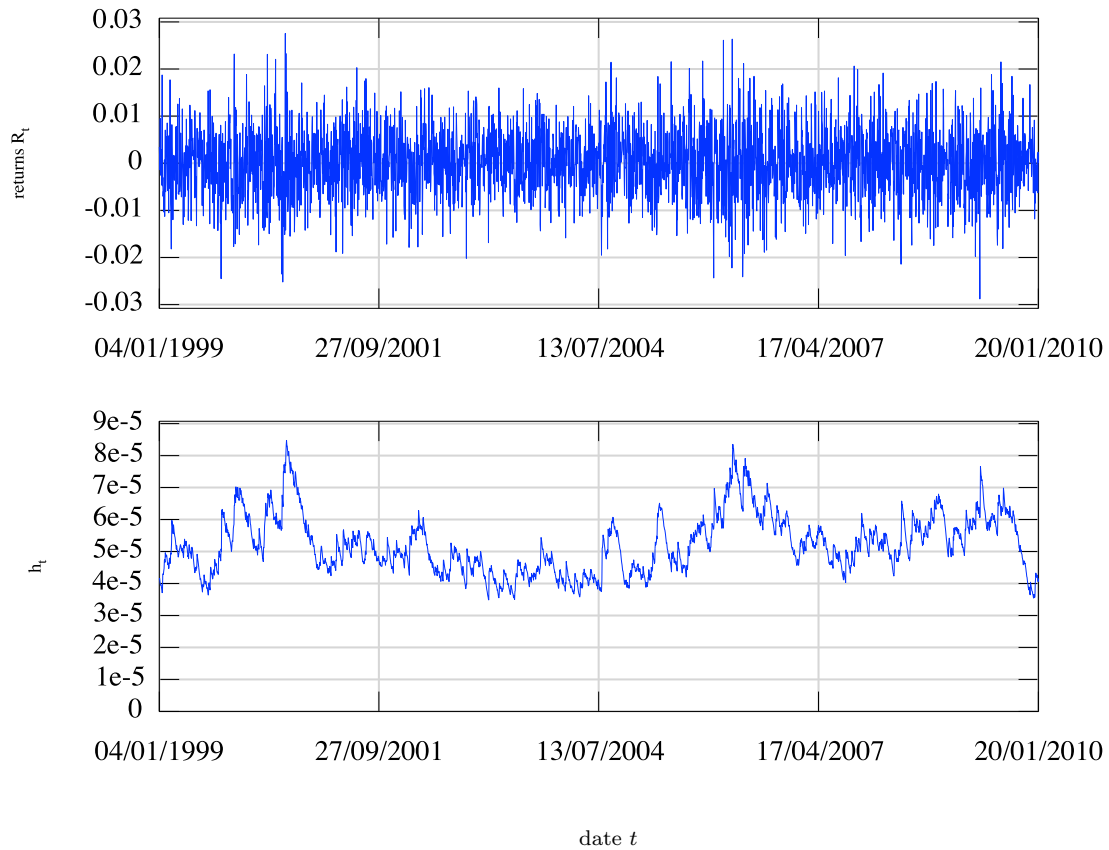


Figure 6.1.: Simulated price process with underlying GARCH variance h_t . Parameters are obtained from Table 7.5. The simulation has the same starting value and time interval as in Figure 4.5. The simulated variance process h_t is *inconstant* and has similar characteristics as the time series in Figure 4.5.

The error terms ϵ_t can be interpreted as some sort of innovation and the *conditional*² *variances*³ h_t can be seen as an adaptive learning mechanism, c.f. [Bollerslev86]. Note, for $p = 0$ one obtains an ARCH(q) process and for $p = q = 0$ the ϵ_t 's are simply white noise. Equation (6.1) implies that $E[\epsilon_t|\mathcal{F}_{t-1}] = 0$ and the conditional variance $h_t = E[\epsilon_t^2|\mathcal{F}_{t-1}]$ is a nontrivial positive-valued parametric function of \mathcal{F}_{t-1} , c.f. [Teräsvirta06].

The sequence $\{\epsilon_t\}$ can either be observed directly, or it can be seen as a sequence of errors or innovations of an econometric model, also compare [Teräsvirta06]. The latter case is denoted by a dependent variable y_t , a conditional mean of y_t given \mathcal{F}_{t-1} , i.e. $\mu(y_t) = E[y_t|\mathcal{F}_{t-1}]$, and the following equation

$$y_t = \mu_t(y_t) + \epsilon_t \quad \Leftrightarrow \quad \epsilon_t = y_t - \mu_t(y_t).$$

6.1.2. Properties of GARCH(p,q)

It can be shown that the GARCH(p,q) process is *weakly stationary* if and only if $A(1) + B(1) < 1$ or, equivalently,

$$\sum_{j=1}^q \alpha_j + \sum_{j=1}^p \beta_j < 1. \quad (6.3)$$

If a stationary GARCH(p,q) process is given, it is possible to simplify the model by replacing α_0 in (6.2) by

$$\underbrace{\left(1 - \sum_{j=1}^q \alpha_j - \sum_{j=1}^p \beta_j\right)}_{=: \alpha_0} \sigma^2,$$

where $\sigma^2 = E[\epsilon_t^2]$ can be estimated by $\hat{\sigma}^2 = T^{-1} \sum_{t=1}^T \epsilon_t^2$ before determining the other parameters. This results in the convergence of the conditional variance towards the *long-run unconditional variance* and having one less parameter to estimate.

6.1.3. Example: GARCH(1,1)

The GARCH(1,1) process is simple but very effective and popular. Setting $p = 1$ and $q = 1$ from equation (6.2), with $\alpha_0 > 0$, $\alpha_1 \geq 0$ and $\beta_1 \geq 0$, one obtains

$$h_t = \alpha_0 + \alpha_1 \epsilon_{t-1}^2 + \beta_1 h_{t-1},$$

²The *conditional* and the *unconditional* variance are not to be confused. The conditional variance can, in this context, change over time as a function of the past errors, $h_t \propto E[\epsilon_t^2|\mathcal{F}_{t-1}]$. However, the unconditional variance stays constant: $\text{Var}[\epsilon_t] = E[\epsilon_t^2] = \sigma^2$.

³It should be mentioned that in the GARCH framework one usually works with conditional *variance* processes instead of conditional *volatility* (square root of the variance) processes.

A GARCH(1,1) process is stationary (c.f. equation (6.3)) if and only if

$$\alpha_1 + \beta_1 < 1.$$

The exchange rate example shown earlier on can be modelled with a GARCH(1,1) process. The estimates are: $\alpha_0 = 0.0109$, $\alpha_1 = 0.1546$ and $\beta_1 = 0.8044$

6.1.4. GARCH Extensions

Various extensions of the original GARCH framework have been derived in order to increase the flexibility of the model. For Example, taking into account that shocks can be *asymmetric* or letting the conditional variance follow an *exponential GARCH (EGARCH)* process, can improve the fit significantly. These two amplifications are outlined in this unit as they are particular relevant in the context of valuating options. Further extensions can be viewed in the Appendix A.5 and in [Bollerslev86] and [Teräsvirta06].

The *GJR-GARCH* (Glosten, Jagannathan and Runkle in 1993) model has an additional indicator function $I_{\{\epsilon_{t-j} > 0\}}$ and a parameter γ in comparison to equation (6.2) to enable asymmetric shocks

$$h_t = \alpha_0 + \sum_{j=1}^q [\alpha_j + \gamma_j I_{\{\epsilon_{t-j} > 0\}}] \epsilon_{t-j}^2 + \sum_{j=1}^p \beta_j h_{t-j}.$$

The *nonlinear GARCH (NGARCH)* model developed by Engle and Ng shifts the centre of symmetry away from zero, also using an extra parameter γ ,

$$h_t = \alpha_0 + \alpha_1 (\epsilon_{t-1} - \gamma \sqrt{h_{t-1}})^2 + \beta_1 h_{t-1}, \quad \gamma \neq 0. \quad (6.4)$$

Another way to model asymmetric shifts can also be achieved by employing an *exponential GARCH (EGARCH)* process. In this framework, the positivity of the conditional variance process is always given as opposed to the standard GARCH model, where parameter restrictions are needed to ensure this condition, i.e. $p \geq 0$, $q > 0$, $\alpha_0 > 0$, $\alpha_j \geq 0, j = 1, \dots, q$, and $\beta_j \geq 0, j = 1, \dots, p$, confer Section 6.1.1. Robert F. Engle in [Engle82] assumes that ϵ_t can be decomposed by $\zeta_t h_t^{1/2}$, i.e.

$$\epsilon_t = \zeta_t h_t^{1/2}, \quad \text{with } \zeta_t \stackrel{i.i.d.}{\sim} D(0, 1). \quad (6.5)$$

D denotes the applied distribution which is often considered to be the normal distribution, so $\epsilon_t | \mathcal{F}_t = \zeta_t h_t^{1/2} \stackrel{!}{=} Z_t h_t^{1/2} \sim N(0, h_t)$. One can then define the EGARCH(p,q) model by

$$\ln h_t = \alpha_0 + \sum_{j=1}^q g_j (\zeta_{t-j}) + \sum_{j=1}^p \beta_j \ln h_{t-j}, \quad (6.6)$$

where $g_j(\zeta_{t-j})$ refers to some function of ζ_t . Ideally it is a function of both the magnitude and the sign of ζ_t to capture the negative correlation between stock returns and volatility changes, see [Nelson91]. In the following summary possible functions for $g_j(\zeta_{t_j})$ and further properties of EGARCH models are outlined, according to [Teräsvirta06].

- Nelson's original EGARCH model is obtained by setting

$$g_j(\zeta_{t-j}) := \alpha_j \zeta_{t-j} + \gamma_j (|\zeta_{t-j}| - \mathbb{E}|\zeta_{t-j}|), \quad j = 1, \dots, q,$$

into equation (6.6). It can easily be seen from above that no parameter restrictions are needed⁴.

- The logarithmic GARCH (LGARCH) model is acquired by

$$g_j(\zeta_{t-j}) := \alpha_j \ln \zeta_{t-j}^2, \quad j = 1, \dots, q.$$

- Similar to the standard GARCH case, the first order EGARCH model is the most popular model, i.e. EGARCH(1,1).
- Higher moments of the EGARCH process exist (under very weak conditions) and are fairly easy to compute which lies in contrast to the standard GARCH model.

6.2. Valuating Options Applying the GARCH Model

6.2.1. Model Derivation and Specification

Steven L. Heston and Saikat Nandi in [Heston00] were able to derive a *closed-form* GARCH model to value options. Various other attempts of pricing options with the GARCH framework only deliver numerical solutions. In many ways, this model is similar to Heston's stochastic volatility model which was derived in Chapter 5, except for being *discrete* instead of continuous. This is why the δ - as opposed to the d -notation is used to express the *discontinuity* of the process.

Note that the first equation in (6.7) is again the logarithmic price process corresponding to equations (3.1) and (5.1) in the BSM and the Heston model, respectively. Just as in the Heston case, an additional process for the variance (volatility) is modelled to account for the inconstant variance during time Δt .

Let r be the continuously compounded interest rate for the *unit* time interval $\delta t = const.$, h_t be the conditional variance of the log return between $t - \delta t$ and t , and λ be the

⁴After exponentiating equation 6.6, one attains h_t on the LHS and an exponentiated term on the RHS which is always positive.

constant unit risk premium⁵. The model consisting of a logarithmic price process and a GARCH(p,q) process for the conditional variance is given by

$$\delta \ln(S_t) = r + \lambda h_t + \sqrt{h_t} Z_t, \quad (6.7a)$$

$$h_t = \alpha_0 + \sum_{i=1}^q \alpha_i \left(Z_{t-i} - \gamma_i \sqrt{h_{t-i}} \right)^2 + \sum_{i=1}^p \beta_i h_{t-i}, \quad (6.7b)$$

where Z_t again denotes a standard normally distributed random variable, as defined in the preceding chapters, respectively, Appendix A.1.12. Hence, one random variable is drawn for one unit time interval δt , and no δ - or d -notation is needed for Z_t as opposed to the Wiener process. For $p = q = 1$ the conditional variance is stationary, i.e. mean reverting, if $\beta_1 + \alpha_1 \gamma_1^2 < 1$.

It can easily be seen that the conditional variance h_t in (6.7) is very similar to the NGARCH process depicted in Section 6.1.4, especially when recalling that $\epsilon_t = Z_t h_t^{1/2}$ holds when assuming standard normal random variables Z_t .

As the aim is to derive a GARCH option pricing model, one needs to generalize the conventional risk-neutral valuation relationship to enable heteroskedasticity of the asset return process, compare [Duan95]. This is done with the concept of the locally risk-neutral valuation relationship (LRNVR) which is depicted in Appendix A.5.1. According to [Heston00] it is equivalent to assume that the value of a call option with one period to expiration obeys the Black-Scholes-Bubinstein formula⁶. After rewriting the formulae in (6.7) to

$$\begin{aligned} \delta \ln(S_t) &= r - \frac{1}{2} h_t + \sqrt{h_t} Z_t^*, \\ h_t &= \alpha_0 + \sum_{i=1}^p \beta_i h_{t-i} + \sum_{i=2}^q \alpha_i \left(Z_{t-i} - \gamma_i \sqrt{h_{t-i}} \right)^2 + \alpha_1 \left(Z_{t-1}^* - \gamma_1^* \sqrt{h_{t-1}} \right)^2, \end{aligned} \quad (6.8)$$

and by substituting

$$\begin{aligned} Z_t^* &= Z_t + \left(\lambda + \frac{1}{2} \right) \sqrt{h_t}, \\ \gamma_1^* &= \gamma_1 + \lambda + \frac{1}{2}, \end{aligned}$$

with

$$Z_t^* \Big|_{\mathbb{Q}} \sim N(0, 1), \quad t \in T \subset \mathbb{N}_0,$$

⁵According to [Heston00], option prices are very insensitive to this parameter. The functional form of this risk premium, λh_t , prevents arbitrage by ensuring that the spot asset earns the risk-less interest rate when the variance equals zero. Also note that the term $r + \lambda h_t$ corresponds to $\mu - \frac{\sigma_t^2}{2}$ in the previous chapters and expresses the expected log return of an asset, i.e. $e^{r+\lambda h_t}$ when compounding continuously for one period.

⁶Similar to the LRNVR concept, a single-period framework is used, so one does not have to hedge continuously, c.f. [Wilmott07a], p.267-268

one acquires a risk-neutral version of the original. Note that without the LRNVR assumption from above, the latter statement does not need to hold and the substitutes Z_t^* and γ^* merely would depict simple rearrangements.

6.3. Pricing European Options in the GARCH framework

The derivation of the call price applying Heston and Nandi's GARCH model is comparable to the procedure in Heston's stochastic volatility model. Again, the call has to satisfy the following equation, c.f. Appendix A.4.2,

$$\begin{aligned} C &= e^{-r\tau} \mathbb{E}_t^{\mathbb{Q}} [\max(S_T - K, 0)] \\ &= S_t P_1 - e^{-r\Delta t} K P_2, \end{aligned} \quad (6.9)$$

with $\mathbb{E}_t^{\mathbb{Q}}$ denoting the expectation at time t under the risk-neutral measure \mathbb{Q} and P_1 and P_2 refer to the pseudo risk-neutral probabilities. Steven L. Heston and Saikat Nandi in [Heston00] show that the pseudo probabilities have the subsequent form

$$\begin{aligned} P_1 &= \frac{1}{2} + \frac{e^{-r\tau}}{\pi S_t} \int_0^\infty \Re \left\{ \frac{K^{-i\varphi} f^{\mathbb{Q}}(i\varphi+1)}{i\varphi} \right\} d\varphi, \\ P_2 &= \frac{1}{2} + \frac{1}{\pi} \int_0^\infty \Re \left\{ \frac{K^{-i\varphi} f^{\mathbb{Q}}(i\varphi)}{i\varphi} \right\} d\varphi, \end{aligned} \quad (6.10)$$

where $f^{\mathbb{Q}}(i\varphi) = \mathbb{E}_t^{\mathbb{Q}} [S_T^\varphi]$ is the generating function under the risk-neutral measure. Note that independent of the measure, the generating function of the price of the underlying asset is also the moment generating function of the log price of the asset, $\mathbb{E}_t [S_T^\varphi] = \mathbb{E}_t [\varphi \ln S_T]$, c.f. Appendix A. In [Heston00] it can be seen that the generating function $f(i\varphi)$ in general (without a risk-free measure) takes on the log-linear form

$$f(i\varphi) = S_t^\varphi \exp \left\{ A_t + \sum_{k=1}^p B_{k,t} h_{t+2-k} + \sum_{k=1}^{q-1} C_{k,t} \left(Z_{t+1-k} - \gamma_k \sqrt{h_{t+1-k}} \right)^2 \right\}, \quad (6.11)$$

where

$$A_t = A_{t+1} + \varphi r + B_{1,t+1} \alpha_0 - \frac{1}{2} \ln(1 - 2\alpha_1 B_{1,t+1}), \quad (6.12)$$

$$B_{1,t} = \varphi(\lambda + \gamma_1) - \frac{1}{2} \gamma_1^2 + \beta_1 B_{1,t+1} + \frac{\frac{1}{2} (\varphi \gamma_1)^2}{1 - 2\alpha_1 B_{1,t+1}}. \quad (6.13)$$

When dealing with the single lag case ($p = 1, q = 1$), the preceding coefficients can be computed recursively from the terminal conditions

$$A_T = B_{1,T} = 0. \quad (6.14)$$

6.4. Continuous Time Limit of the GARCH(1,1) Process

It is often crucial for a model to include the well established original types as a special case in order to be accepted, but also to be able to compare the models. Although the model depicted in equations (6.7) and (6.8) contains discrete processes for the stock price S_t and the conditional variance h_t , the *single lag* version of the GARCH family, i.e. GARCH(1,1) with $p = 1$ and $q = 1$, converges weakly to the Heston model given in Section 5.1 in the continuous time limit, c.f. [Duan95]. Therefore, the BSM framework is also received as a special case by additionally assuming the variance to be constant. The GARCH(1,1) variance process h_t is given by

$$h_t = \alpha_0 + \beta_1 h_{t-1} + \alpha_1 \left(Z_{t-1} - \gamma_1 \sqrt{h_{t-1}} \right)^2 \quad (6.15)$$

$$= \alpha_0 + \beta_1 h_{t-1} + \alpha_1 \left(Z_{t-1}^2 - 2Z_{t-1}\gamma_1\sqrt{h_{t-1}} + \gamma_1^2 h_{t-1} \right), \quad (6.16)$$

with the conditional mean and variance of h_t being, respectively,

$$E[h_{t+1}|\mathcal{F}_t] = \alpha_0 + \alpha_1 + (\beta_1 + \gamma_1^2) h_t, \quad (6.17)$$

$$\text{Var}[h_{t+1}|\mathcal{F}_t] = \alpha_1^2 (2 + 4\gamma_1^2 h_t). \quad (6.18)$$

There are different ways to acquire a continuous time limit for $\delta t \rightarrow 0$. The following shows the derivation according to [Heston00].

As h_t is defined as the conditional variance over a time interval δt , it should converge to zero for $\delta t \rightarrow 0$. In order to measure the variance per time unit with a well defined continuous time limit⁷, one defines

$$v_t := \frac{h_t}{\delta t}$$

Substituting v_t for h_t , the Heston-Nandi GARCH(1,1) process is then given by

$$v_{t+1} = \tilde{\alpha}_0 + \tilde{\beta}_1 v_t + \tilde{\alpha}_1 (Z_t - \tilde{\gamma}_1 \sqrt{v_t})^2, \quad (6.19)$$

with

$$\tilde{\alpha}_0 := \frac{\alpha_0}{\delta t}, \quad \tilde{\alpha}_1 := \frac{\alpha_1}{\delta t}, \quad \tilde{\beta}_1 := \beta_1 \quad \text{and} \quad \tilde{\gamma}_1 := \gamma_1 \sqrt{\delta t}. \quad (6.20)$$

⁷The well defined continuous time limit is similar to deriving a Wiener process as a continuous time limit of a binomial random walk, compare Appendix A.

After setting

$$\begin{aligned}
\alpha_0(\delta t) &\stackrel{!}{=} (\kappa\theta - \frac{1}{4}\sigma^2) \cdot (\delta t)^2, \\
\alpha_1(\delta t) &\stackrel{!}{=} \frac{1}{4}\sigma^2(\delta t)^2, \\
\beta_1(\delta t) &\stackrel{!}{=} 0, \\
\gamma_1(\delta t) &\stackrel{!}{=} \frac{2}{\sigma\delta t} - \frac{\kappa}{\sigma} \\
\lambda(\delta t) &\stackrel{!}{=} \lambda
\end{aligned} \tag{6.21}$$

the δt -dependant variance process v_t is given by

$$\begin{aligned}
v_{t+1} &= \left(\kappa\theta - \frac{1}{4}\sigma^2 \right) \delta t + \frac{1}{4}\sigma^2\delta t \left(Z_t - \left(\frac{2}{\sigma\sqrt{\delta t}} - \frac{\kappa\sqrt{\delta t}}{\sigma} \right) \sqrt{v_t} \right)^2 \\
&= \left(\kappa\theta - \frac{1}{4}\sigma^2 \right) \delta t + \frac{1}{4}\sigma^2\delta t \left(Z_t^2 - 2\sqrt{v_t} \left(\frac{2}{\sigma\sqrt{\delta t}} - \frac{\kappa\sqrt{\delta t}}{\sigma} \right) Z_t + \right. \\
&\qquad \qquad \qquad \left. \left(\frac{2}{\sigma\sqrt{\delta t}} - \frac{\kappa\sqrt{\delta t}}{\sigma} \right)^2 v_t \right).
\end{aligned}$$

The variance v_t is observable and, therefore, non-stochastic, given the information set \mathcal{F}_{t-1} . Hence, the conditional expected value $\mathbb{E}[\delta v_{t+1}|\mathcal{F}_{t-1}] = \mathbb{E}[v_{t+1} - v_t|\mathcal{F}_{t-1}]$ and the conditional variance⁸ $\text{Var}[\delta v_{t+1}|\mathcal{F}_{t-1}] = \text{Var}[v_{t+1}|\mathcal{F}_{t-1}]$ are

$$\begin{aligned}
\mathbb{E}[\delta v_{t+1}|\mathcal{F}_{t-1}] &= \tilde{\alpha}_0 + \tilde{\alpha}_1 \left(\underbrace{\mathbb{E}[Z_t^2|\mathcal{F}_{t-1}]}_{=\text{Var}[Z_t|\mathcal{F}_{t-1}]=1} - 2\tilde{\gamma}_1\sqrt{v_t} \cdot \underbrace{\mathbb{E}[Z_t|\mathcal{F}_{t-1}]}_{=0} + \tilde{\gamma}_1^2 v_t \right) - v_t \\
&= \tilde{\alpha}_0 + \tilde{\alpha}_1 (1 + \tilde{\gamma}_1^2 v_t) - v_t \\
&= \kappa(\theta - v_t)\delta t + \frac{1}{4}\kappa^2 v_t (\delta t)^2,
\end{aligned} \tag{6.22}$$

$$\begin{aligned}
\underbrace{\text{Var}[v_{t+1}|\mathcal{F}_{t-1}]}_{=\text{Var}[\delta v_{t+1}|\mathcal{F}_{t-1}]} &= \tilde{\alpha}_1^2 \left(\underbrace{\text{Var}[Z_t^2|\mathcal{F}_{t-1}]}_{\stackrel{!}{=}2, \text{ with } Z_t^2 \sim \chi^2(k=1)} - 4\tilde{\gamma}_1^2 v_t \underbrace{\text{Var}[Z_t|\mathcal{F}_{t-1}]}_{\stackrel{!}{=}1} \right) \\
&= 2\tilde{\alpha}_1^2 (1 - 2\tilde{\gamma}_1^2 v_t) \\
&= \sigma^2 v_t \delta t + \left(\frac{\sigma^4}{8} + \sigma^2 \kappa v_t + \frac{\sigma^2 \kappa^2}{4} v_t \delta t \right) (\delta t)^2.
\end{aligned} \tag{6.23}$$

⁸It is to be noted that v_t is a constant.

The conditional correlation between the variance process v_{t+1} and the continuously compounded stock return is depicted by the following, c.f. Appendix A.5.2

$$\text{Corr}[v_{t+1}, \ln(S_t) | \mathcal{F}_{t-1}] = \frac{-\text{sign}(\tilde{\gamma}_1) \sqrt{2\tilde{\gamma}_1^2 v_t}}{\sqrt{1 + 2\tilde{\gamma}_1^2 v_t}}. \quad (6.24)$$

Steven L. Heston and Saikat Nandi in [Heston00] argue that as the time interval δt shrinks, the skewness parameter $\tilde{\gamma}_1(\delta t)$ approaches positive or negative infinity¹⁰. Consequently the correlation in equation (6.24) approaches 1 (or¹⁰ negative 1 if $\sigma \in \mathbb{R}$) in the limit, c.f. [Heston00].

The variance process v_t has a continuous time diffusion limit following [Foster94]. As the observation interval δt shrinks, v_t converges weakly to the square-root process of Feller (1951), Cox, Ingersoll Ross (1985), and [Heston93]

$$d \ln(S_t) = (r + \lambda v_t) dt + \sqrt{v_t} dW_t, \quad (6.27)$$

$$dv_t = \kappa(\theta - v_t) dt + \sigma \sqrt{v_t} dW_t, \quad (6.28)$$

with W_t being a Wiener process. It is to be noted that the same Wiener process drives both the process of the asset's spot values and the variance process which gives the model its limiting behaviour. This is the substantial difference to other GARCH processes such as the GARCH(1,1) model by [Bollerslev86] where two different Wiener processes are given.

After deriving the well-defined continuous time limit of the data generating measure it still has to be shown that the risk-neutral process also converges to a continuous time limit when limiting the time intervals δt . Following Section 6.2.1, the risk-neutral version

⁹As Z_t is standard normally distributed, $Z_t \sim N(0, 1)$, the square of Z_t is χ^2 -distributed, $Z_t^2 \sim \chi^2(k=1)$, with the expected value being $E[Z_t^2] = k = 1$ and the variance $\text{Var}[Z_t^2] = 2k = 2$. Hence, the variance of $Z_t^2 \delta t$ is

$$\text{Var}(Z_t^2 \delta t) = (\delta t)^2 \text{Var}(Z_t^2) = 2(\delta t)^2.$$

¹⁰It is to be noted that the parameter σ without *any* assumptions can take on *any* positive or negative values, i.e. $\sigma \in \mathbb{R}$, and thus

$$\tilde{\gamma}(\delta t) = \gamma_1 \delta t = \underbrace{\frac{2}{\sigma \delta t}}_{\xrightarrow{\delta t \rightarrow 0} \pm \infty} - \underbrace{\frac{\kappa \sqrt{\delta t}}{\sigma}}_{\xrightarrow{\delta t \rightarrow 0} 0} \xrightarrow{\delta t \rightarrow 0} \pm \infty. \quad (6.25)$$

If, however, σ is assumed to be the volatility of volatility, i.e. $\sigma \stackrel{!}{=} \sigma_v > 0$, the parameter $\tilde{\gamma}(\delta t)$ in the limit approaches *positive* infinity, *only*,

$$\tilde{\gamma}(\delta t) \Big|_{\sigma > 0} \xrightarrow{\delta t \rightarrow 0} +\infty. \quad (6.26)$$

of the parameter γ is depicted by $\gamma_1^* = \gamma_1 + \lambda + \frac{1}{2}$ which, for $\tilde{\gamma}_1^*(\delta t) = \gamma_1^*(\delta t)\sqrt{\delta t}$, results in

$$\tilde{\gamma}_1^*(\delta t) = \frac{2}{\sigma\sqrt{\delta t}} - \left(\frac{\kappa}{\sigma} - \lambda - \frac{1}{2} \right) \sqrt{\delta t}. \quad (6.29)$$

This has an impact on the conditional expected value of δv_t under the risk-neutral measure which differs to the corresponding equation (6.22) of the data generating measure,

$$\mathbb{E}^{\mathbb{Q}} [\delta v_{t+1} | \mathcal{F}_t] = \left(\kappa(\theta - v_t) + \sigma \left(\lambda + \frac{1}{2} \right) v_t \right) \delta t + \frac{1}{4} \left(\kappa + \sigma \left(\lambda + \frac{1}{2} \right) \right)^2 v_t (\delta t)^2. \quad (6.30)$$

Again, by following [Foster94], one obtains the continuous time risk-neutral processes

$$d \ln(S_t) = \left(r - \frac{v_t}{2} \right) dt - \sqrt{v_t} dW_t^*, \quad (6.31)$$

$$dv_t = \left(\kappa(\theta - v_t) + \sigma \left(\lambda + \frac{1}{2} \right) v \right) dt + \sigma \sqrt{v_t} dW_t^*, \quad (6.32)$$

where W_t^* denotes a Wiener process under the risk-neutral measure. In analogy to the previous equations (6.27) and (6.28), both, the asset returns and the variance, are driven by the same Wiener process where the only difference is the specific measure. The risk-neutral stock price and variance process from above are equivalent to the risk-neutral processes in [Heston93] where the two underlying Wiener processes are perfectly correlated. This conclusion has also been asserted numerically, c.f. [Heston00].

6.5. Volatility Surfaces Containing NGARCH Processes

There are different ways to apply the NGARCH processes of the Heston-Nandi model in order to price options. Three of these are outlined in the following sections and are reviewed in more detail in Chapter 7. It is to be noted that there is a considerable difference between *estimating* the parameters of a (NGARCH) process via maximum likelihood estimation using *historic data* and *calibrating* a pricing model to the *current market prices*. The latter means that at a specific *point of time t*, the model parameters are adjusted until the (global) minimum of the squared differences between the model's call prices and the market's call prices is found. Whereas, parameter estimation refers to the maximum likelihood approach of finding the most likely parameters when fitting the model to a given *time series*. After this, the parameters are employed into the pricing model of [Heston00] which means that the parameters are not optimised to fit the current market assumptions.

6.5.1. Maximum Likelihood Estimation of the NGARCH Process

The first way to acquire the NGARCH parameters for pricing options with the Heston-Nandi model is to simply estimate these parameters by a maximum likelihood estimation (MLE). It is, therefore, assumed that the variance process of the underlying's historic returns is an NGARCH process. The formula of the process is defined by (6.4) in Section 6.1.4. The exact procedure of estimating the parameters via MLE is explained in Section 7.2.3.

As a result of not calibrating the model to the current market expectations, it is obvious that the volatility surface generated from the estimated parameters cannot match the results as in Section 5.3. It is quite remarkable though that the resulting volatility surface in Figure 6.2 is not too far from the actual market volatility surface at time $t_0 = 23/09/2009$ which is shown in Figure 4.1. Again, the implied volatility is depicted on the vertical axis and the respective driftless deltas $\Delta_{dl,t}$ and the maturities τ are on the horizontal axes, as acknowledged in Section 4.2.2. The deviations of the call prices relative to the spot S_{t_0} can be seen in Figure 6.3.

6.5.2. Applying Implied Volatilities for Fitting the NGARCH Process

Another possibility of obtaining the NGARCH parameters for the Heston-Nandi model is to use an implied volatility index and fit the NGARCH process to this index. This is an interesting approach as it combines the idea of estimating and calibrating the parameters. On the one hand it uses a time series and not current market prices, on the other it minimises the sum of squared differences between the index values and the volatility (i.e. the root of the variance) of the NGARCH process with respect to the parameters. This procedure could be referred to as “calibrating the NGARCH process to the implied volatility index time series”, raising the question whether this approach is sensible because the parameters are not optimised to the quantity of interest. This ambiguity is strengthened by the fact that the volatility index is also not the implied volatility of the currency pair but an indicator for the implied volatility of the entire forex market.

The results are not as close to the market volatility surface as in the preceding case. c.f. 6.3. This observation suggests that one needs to be able to calibrate to the implied volatility of the *currency pair* to give this approach further consideration. The deviation can be seen in Figures 6.4 and 6.5 when comparing the volatility surface of the model to that of the market in Figure 4.1. More details concerning the results of the models are found in Chapter 7 and 8.

*Heston-Nandi Volatility Surface with ML Estimated Parameters for EUR-USD,
 $t_0 = 23/09/2009$*

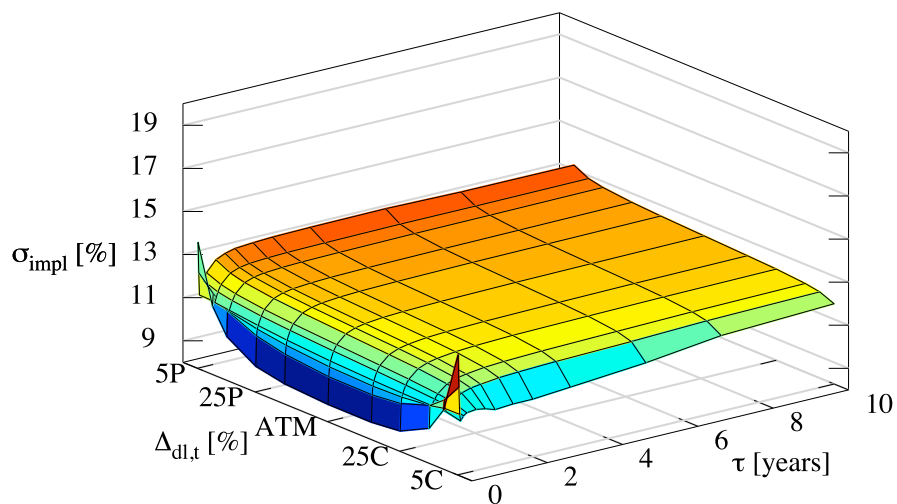


Figure 6.2.: Heston-Nandi Volatility Surface with ML Estimated Parameters for EUR-USD, $t_0 = 23/09/2009$. Resulting implied volatility σ_{impl} denoted in % depending on the driftless delta $\Delta_{\text{dl},t}$ in % of the OTM option and maturity τ in years, as stated in Section 4.2.2

Deviation of Heston to Market Call Prices: EUR-USD, $t_0 = 18/09/2009$

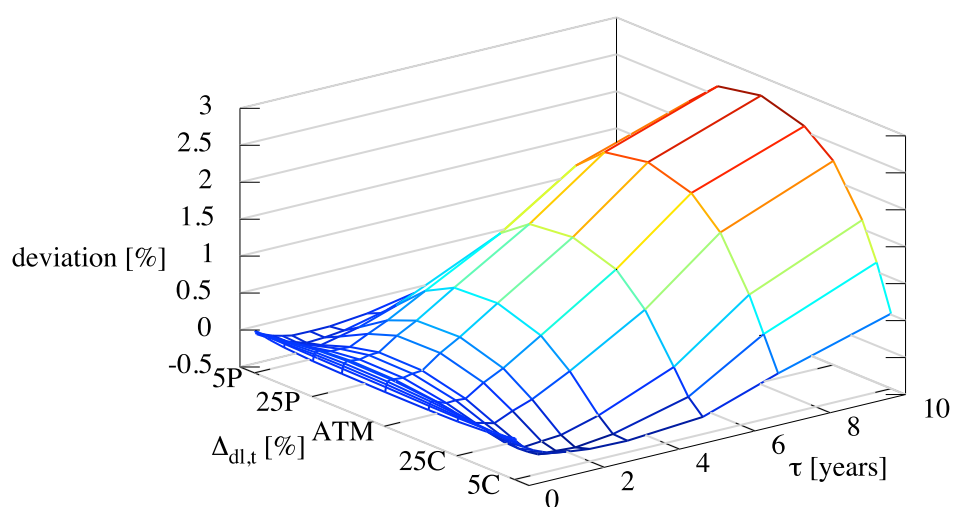


Figure 6.3.: Deviation of Heston-Nandi Call Prices with ML Estimated Parameters call prices to the market call prices relative to the stock price in percent, i.e. $\frac{C_{model} - C_{market}}{S_t} [\%]$, depending on the driftless delta $\Delta_{dl,t}$ in % of the OTM option and maturity τ in years, c.f. Section 4.2.2.

*Volatility Surface of Calibrated NGARCH Parameters to a Volatility Index,
 $t_0 = 23/09/2009$*

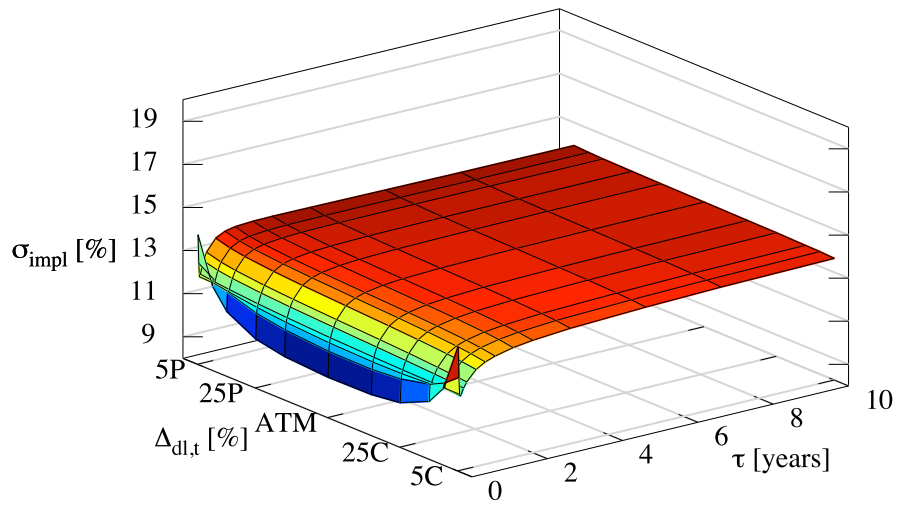


Figure 6.4.: Volatility Surface of Calibrated NGARCH Parameters to a Volatility Index, $t_0 = 23/09/2009$. Resulting implied volatility σ_{impl} denoted in % depending on the driftless delta $\Delta_{\text{dl},t}$ in % of the OTM option and maturity τ in years, as stated in Section 4.2.2

Deviation of Heston-Nandi with Calibrated Volatility Index Parameters to Market Call Prices: EUR-USD, $t_0 = 18/09/2009$

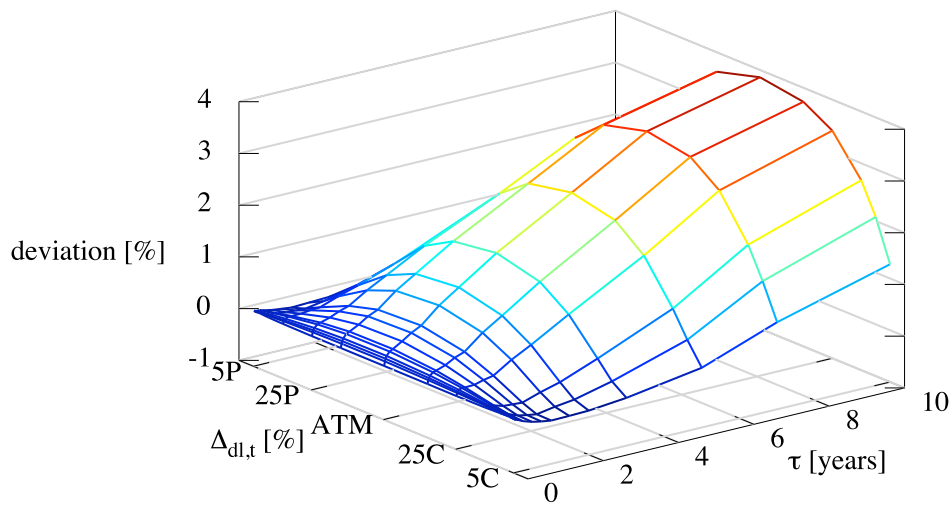


Figure 6.5.: Deviation of Heston-Nandi with Calibrated Volatility Index Parameters to Market Call Prices relative to the stock price in percent, i.e. $\frac{C_{model} - C_{market}}{S_t} [\%]$, depending on the driftless deltas $\Delta_{dl,t}$ in % of the OTM option and maturity τ in years, c.f. Section 4.2.2.

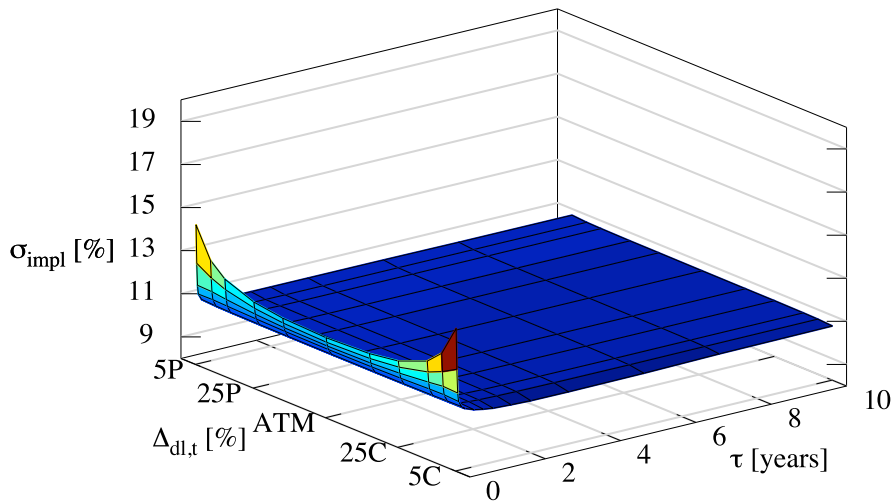


Figure 6.6.: Calibrated Heston-Nandi model to call prices of EUR-USD, $t_0 = 23/09/2009$. Resulting implied volatility σ_{impl} denoted in % depending on the driftless deltas $\Delta_{dl,t}$ in % of the OTM option and maturity τ in years, c.f. Section 4.2.2

6.5.3. Calibration of the Heston-Nandi Model

The third approach to obtain the parameters of the volatility process for the Heston-Nandi pricing representation is to calibrate the model to the respective market volatility surfaces just as in the case of Section 5.3. Although the procedure is practically equal to the one described in the Heston case, it is not recommended in this framework. The reasons for this outcome are explained in Chapter 7. An example of calibrating the Heston-Nandi model to the market volatility surface is found in Figure 6.6.

7. Empirical Analysis

The empirical analysis examines the derived models when fitted to real data. Thereby, the emphasis is laid on how the individual models are estimated, respectively calibrated, and what the results of the models and their parameters are. Summaries of the results are presented as tables and figures in this chapter, further graphical details of *all* presented models are found in the Appendix B. Moreover, the data used in these sections is described in the following unit.

7.1. Description of the Data

As the main focus of this thesis is laid on the forex market, c.f. Chapter 2 and 4, the models described in the preceding chapters are fitted to forex data. However, it is to be noted that these models are used for numerous different markets and asset classes such as equities but also weather and energy derivatives.

Section 2.1 also states that the forex market is particularly suitable for comparing different models and derivatives as it is one of the most liquid financial markets. For a similar reason the empirical analysis concentrates on the currency pair USD-EUR which is the most traded pair, as stated in Table 4.1. However, other exchange currencies have been examined with similar outcomes.

All the data applied in this research is obtained from [Bloomberg10], i.e. market volatility surfaces with the respective exchange and forward interest rates, as well as historic time series of exchange rates, volatility indices and LIBOR-rates which are used for historic interest rates, c.f. Section 2.3.4. The data is always given by the closed values of the respective trading day.

The starting point of all model fitting is, of course, the individual volatility surface implied by the market at a specific date t . These are given by [Bloomberg10] in the same way as the volatility surfaces are depicted in Section 4.2.2. The introduced notations are also conform with most market conventions as described for example in [Wystup07], ch.1. This means that the volatility surface is displayed as a three dimensional plot with the implied volatility on the vertical axis depending on the maturity τ and the (dirftless) delta $\Delta_{(dl),t}$ on the horizontal axes. The collected market volatility surfaces are pretty much arbitrarily chosen throughout the time interval 23/09/2009-20/10/2010 with no more than 14 days (approximately 10 trading days) in between.

The implied volatility being the wrong quantity inserted into the BSM call price formula (4.5) to obtain the right price and applying the wrong formula, c.f. Section 4.3.1, is unambiguously defined just as the maturity τ . However, there are various different deltas for a number of different purposes, e.g. hedging, pricing etc. Amongst others, there are driftless, forward, dual and spot deltas, c.f. [Wystup07] ch.1. The latter is the usual textbook definition seen in [Hull02] p.304 and has been introduced in Section 3.4 and is reviewed in Section 4.2.2. It is, however, an inconvenience that [Bloomberg10] fails to clearly state which of these deltas are given. It is strongly assumed and also partly verified that the deltas employed by [Bloomberg10] have to be driftless deltas $\Delta_{dl,t}$ in this context which is also concluded by [Wilmott10]. Furthermore, it can be shown that the given deltas must be driftless by calculating the strike K from equation (4.25) and inserting the values back into the BSM formulae to acquire the delta.

Each examined volatility surface has $11 \cdot 15 = 165$ data points with 11 different driftless deltas $\Delta_{dl,t}$ including the ATM price and 15 different maturities τ . The series of driftless deltas is given by

$$\left[5P-\Delta_t, 10P-\Delta_t, 15P-\Delta_t, 25P-\Delta_t, 35P-\Delta_t, \text{ATM}, 35C-\Delta_t, 25C-\Delta_t, 15C-\Delta_t, 10C-\Delta_t, 5C-\Delta_t \right]$$

and the maturities are

$$\left[1w, 2w, 3w, 1m, 2m, 3m, 6m, 9m, 1y, 18m, 2y, 3y, 5y, 7y, 10y \right],$$

where w denotes a week, m a month and y a year.

The domestic and foreign forward interest rates which are needed to calibrate the models and to compute K , are given by the currencies' deposit rates and can be obtained from [Bloomberg10] together with the respective volatility surfaces. The spot S_t for the volatility surface at t is obtained from exchange rate time series. With these values it is possible to retrieve the strike K from (4.25).

[Bloomberg10] offers different volatility surfaces with different amounts of data points. For example, there is also a volatility surface with the additional maturities $4m$ and $4y$ and with equidistant (driftless) delta points in 5% intervals. However, it is believed that these supplementary points are only interpolations of the surrounding points. This is why the volatility surfaces used in this research are the ones with less data points, as the models should only be calibrated to real existing data.

Another reason for working with this data set is the fact that the calibration is a very computational-intensive process which is seen in the following sections. Moreover, the differences between calibrating the "larger" volatility surfaces and the "smaller" ones turned out to be minor and can be neglected. Though, it should be noted that there is one disadvantage when employing the surfaces with less data points, as the points are not equidistant which automatically give the optimisation a certain loading or weighting, c.f. Section 10.1.1.

For the Maximum Likelihood estimation of the GARCH process further data is needed. Next to the already mentioned time series of the exchange rates, also the respective historic interest rates and implied volatility indices are needed. The historic interest rates are LIBOR-rates as seen in Section 2.3.4. [Bloomberg10] offers various implied volatility indices for the forex market. Many of them measure the implied volatility of the most traded currency pairs with some kind of weighting to account for the different volumes of the respective pair, c.f. for example [DB07]. The volatility indices, therefore, do not specify the implied volatilities of a specific currency pair but rather indicate the implied volatility of the entire forex market. For the data analysis in this research, the “BNP Paribas FX Realised Volatility Index” is used, because it has a similarly long time series as the currency pair USD-EUR.

The particular time series of the currency pair, the interest rate and the implied volatility index are perfectly consistent except for specific holidays which accumulate to about 5 days in the year and are treated the same way as weekends for *all* time series. These holidays are, therefore, assumed to be nonexistent and the next trading day follows the previous. This results in the year having approximately 253 trading days. The time horizon of the applied data starts from 04/01/1999 and ends 20/01/2010. Again, the data-sets consist of closed values only and are all acquired from [Bloomberg10].

7.2. Estimating and Calibrating the Models

The basic idea of how to calibrate a (BSM) model to the data has been introduced in Section 4.3.1. The subsequent sections give an exact description of how the models are calibrated and estimated in detail. Section 6.5 already describes how the terms estimation and calibration are used in this context. Estimation refers to a maximum likelihood maximisation with the data being obtained from a time series. Calibration denotes the parameter fit which is acquired when minimising the model results to current market data.

A major difference between these two approaches is that the MLE over an entire time series delivers global parameters which are used for *all* examined volatility surfaces. Calibrated parameters, however, are only fitted to the respective current volatility surfaces and are, therefore, different for each set.

7.2.1. Calibrating the BSM Model

As mentioned in Section 4.3.1, calibrating the BSM model to the given market data only involves a one dimensional minimisation problem. The starting point is the volatility surface given by [Bloomberg10] as depicted in Section 4.3.1 and 7.1, and seen for example in Figure 4.1. The surface is given by a $[11 \times 15]$ -matrix with 165 points where the rows denote the different deltas and the 15 columns symbolise the maturities.

From this matrix, together with the values of the respective interest rates (foreign and domestic), maturities, deltas and also the price of the underlying stock, the strike values of every volatility data point is calculated by equation (4.25). The individual strike values are again stored in another matrix of the same dimension. Now the matrix of all call (and/ or put) prices anticipated by the market can be calculated, as all of the needed parameters are given to apply the BSM formulae (4.5) and (4.6) in Section 4.1.2. It is to be remembered that the volatility surfaces given by [Bloomberg10] are in fact implied volatilities of the market call prices. All what is done in the preceding procedure is to retrieve the original market call prices from the collected implied volatilities from [Bloomberg10]. It is irrelevant what currency is used as the numéraire, because the implied volatility is the same for both, c.f. Section 4.2.1. It is, however, vital to stay consistent once the foreign and domestic currency have been chosen.

Once the market call price matrix has been computed, it is possible to calibrate the model call prices to the market call prices. This is done by the least squared error (LSE) method. Let $C_{m,n}$ be market call price of the m -th delta and n -th maturity and $\hat{C}_{m,n}(\hat{\sigma})$ the corresponding call price of the BSM model, $m = 1, \dots, M$ and $n = 1, \dots, N$. The LSE function is minimised w.r.t. the only free parameter $\hat{\sigma}$ which means that only *one* volatility exists for the whole “surface”. It is to be remembered that the BSM model assumes constant volatility, c.f. Chapter 3. The least squared error function $\text{LSE}_{(\hat{\sigma})}$ is, thus, depicted by

$$\text{LSE}_{(\hat{\sigma})} = \arg \min_{\hat{\sigma}} \sum_{m=1}^M \sum_{n=1}^N \left(C_{m,n} - \hat{C}_{m,n}(\hat{\sigma}) \right)^2. \quad (7.1)$$

In Section 4.3 the implied volatility which minimises the LSE function in Figure 4.3 is $\hat{\sigma}_{\text{impl},t} = 10.63\%$. The results of calibrating the parameters, i.e. the implied volatilities, for the respective volatility surfaces during the period of 23/09/2009 and 20/01/2010 can be found in Table 7.1 and Figure 7.1. It is to be remembered that the BSM model assumes constant volatilities and that the volatility surfaces are planes. This is why these “surfaces” all more or less look like the one in Figure 4.3 and the deviations seen in Figure 4.4 are relatively similar, too, and no further graphical analyses are, therefore, undertaken. Instead, the differences to the market volatility surfaces are examined by statistical measures in Chapter 8.

In the case of the BSM model calibration any minimisation algorithm can be used as it is a simple one dimensional optimisation problem with one global minimum. For example the Newton-Raphson method can be applied. Nevertheless, as especially the Heston model needs to be minimised differently, another algorithm is used and employed in all implementations to be able to compare the models more consistently¹. This is why a

¹Generally, the Newton-Raphson method is more precise than the simulated annealing method which only gives the an acceptable good solution rather than the best possible solution, c.f. [Wikipediary]. In this context and especially with any one dimensional optimisation problem the error can be neglected, since the error can also be minimised.

Calibrated BSM Implied Volatilities

date t	23/09/09	07/10/09	21/10/09	04/11/09	18/11/09
$\hat{\sigma}_{\text{impl}}$	0.1063	0.1071	0.1098	0.1164	0.1148
date t	02/12/09	16/12/09	30/12/09	06/01/10	20/01/10
$\hat{\sigma}_{\text{impl}}$	0.1149	0.1147	0.1163	0.1126	0.1103

Table 7.1.: Resulting BSM implied volatility of the calibrated BSM model for each examined market volatility surface, c.f. Section 7.2.1. With these parameters the calibrated volatility surfaces as seen in Appendix B are calculated. The results are also shown in Figure 7.1.

Progression of the Calibrated BSM Implied Volatilities

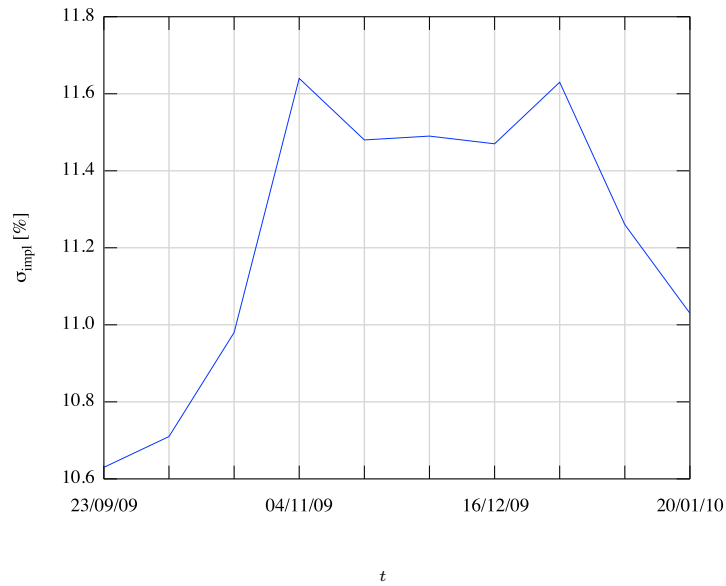


Figure 7.1.: The progression of the calibrated BSM implied volatility is shown as depicted in Table 7.1.

simulated annealing minimisation method is applied which is explained in more detail in the following section. In Octave, which is the open source version of Matlab, the function is given by `samin()`.

7.2.2. Calibrating the Heston Model

The underlying calibration idea for the Heston model is practically the same as for the BSM model. Again the strikes are acquired from equation (4.25) to calculate the market call prices. The big difference between the BSM and the Heston calibration is that *six* parameters κ , v_t , λ , \bar{v} , σ_v and ρ instead of one parameter are used to minimise the LSE function which is due to the Heston volatility being a process instead of a constant, c.f. equations (5.2) and (5.3) in Section 5.1 and also (5.19) in Section 5.2.2. It should be noted that in the Heston framework it is more or less irrelevant whether the parameter λ is estimated with the model, or set to be 0 assuming to be in the risk-less world, as the risk-neutral parameters can be retrieved by, c.f. [Heston93] p.335,

$$\kappa^* = \kappa + \lambda \quad \text{and} \quad \bar{v}^* = \frac{\kappa \bar{v}}{\kappa + \lambda} \quad (7.2)$$

This phenomena can be seen in Figure 7.2 where the calibrated values $\hat{\kappa}$ and $\hat{\lambda}$ take on diverging values, i.e. when $\hat{\kappa}$ is relatively large then $\hat{\lambda}$ is comparatively small and vice versa. Let $\hat{\Theta}_H$ denote the vector of the Heston parameters, $\hat{\Theta}_H = [\kappa, v_t, \lambda, \bar{v}, \sigma_v, \rho]'$, the LSE function to be minimised is thus given by

$$\text{LSE}(\hat{\Theta}_H) = \arg \min_{\hat{\Theta}_H} \sum_{m=1}^M \sum_{n=1}^N \left(C_{m,n} - \hat{C}_{m,n}(\hat{\Theta}_H) \right)^2. \quad (7.3)$$

In Section 5.1 it is mentioned that the parameter restriction $2\kappa\bar{v} > \sigma_v^2$ is needed to guarantee a positive volatility process. When minimising the LSE function w.r.t. the Heston parameters, this constraint has to be considered. There are different ways to take this restriction into account, one is to give the LSE function some sort of penalty when optimising the problem. In this case, the LSE is multiplied by some factor if the restriction is violated. It is found that the resulting solutions often just about fulfil the parameter constraint. The formulae for the adjusted minimisation can be given by

$$\text{LSE}^*(\hat{\Theta}_H) = \begin{cases} \text{LSE}(\hat{\Theta}_H) & , 2\kappa\bar{v} > \sigma_v^2 \\ \text{LSE}(\hat{\Theta}_H) \cdot p_f & , 2\kappa\bar{v} \leq \sigma_v^2 \end{cases}, \quad (7.4)$$

where p_f denotes some kind of penalty factor, e.g. $p_f = 10$.

As the optimisation problem is no longer one dimensional, more complex minimisation algorithms need to be employed. It is, however, a nontrivial problem to find the *global* minimum. In fact most minimisation algorithms fail, as the LSE function has a large

number of local minimums and these algorithms get stuck in one of them. One way out of this problem is to implement the simulated annealing algorithm which is a generic probabilistic metaheuristic for global optimisation, c.f. [Wikipediary].

The basic idea behind this method is that the current point is compared to a different point in the search space. This point is accepted either because it lowers the function value or it is chosen with a certain probability regardless of the function value. The probability can be influenced by a so called temperature parameter. The probability is also dependant on the amount of steps taken and decreases by the increasing number of steps. Because of this probability the next point can jump to an “arbitrary” location in the search space and the algorithm does not get stuck in some local minimum so easily. For the same reason the precision of the optimisation result is only finite and also *identical* results cannot be reproduced when repeating the minimisation procedure. This is only a very basic idea of the functionality. A good summary of this procedure is found in [Wikipediary]. As mentioned, the octave command for this optimisation is `samin()`.

Even though the simulated annealing algorithm is a very powerful tool to find a minimum which is bordering on the global minimum, it is still possible to get stuck in a local optimum. In order to cancel out this probability, it is recommended to choose different starting regions and to alter the lower and upper bounds of the search space. This should guarantee finding a very accurate optimum eminently close to the global minimum.

Instead of minimising the difference between the market call price and the model’s call price, the differences between the market volatility surface and the model’s implied volatility surface can be minimised. Even though this is another possibility of obtaining a calibrated model, it has the computational disadvantage of having to calculate the implied volatility to *each* Heston call price. It is to be remembered that the implied volatility can only be obtained by another minimisation problem, c.f. Section 3.3 and that the calculation of a matrix of Heston call prices in each step of the simulated annealing algorithm already is a computational-intensive process.

The calibration of the Heston model in Figure 5.2 delivers the parameters $\hat{\kappa} = 0.1489$, $\hat{\lambda} = 0.0663$, $\hat{v}_t = 0.0158$, $\hat{v} = 0.0064$, $\hat{\sigma}_v = 0.0438$ and $\hat{\rho} = -0.0486$. The results of the parameters from all calibrated volatility surfaces during the period of 23/09/2009 and 20/01/2010 can be found in Table 7.2 and Figure 7.2. The figures of the individual calibrated surfaces can be found in Appendix B.

7.2.3. Maximum Likelihood Estimation of the NGARCH Process

Section 6.5.1 describes the underlying idea of this approach to obtain the parameters for the Heston-Nandi model. Before being able to estimate the parameters of the NGARCH process it is necessary to collect a consistent time series containing the level values of the underlying and the respective foreign and domestic interest rates to the same dates. As mentioned in Section 7.1 the data often has to be adjusted on certain holidays which

Calibrated Heston Parameters

date t	23/09/09	07/10/09	21/10/09	04/11/09	18/11/09
$\hat{\kappa}$	0.1489	0.0928	0.0581	0.0366	0.0667
$\hat{\lambda}$	0.0663	0.1383	0.1586	0.2307	0.1460
\hat{v}_t	0.0158	0.0158	0.0177	0.0215	0.0198
\hat{v}	0.0064	0.0142	0.0135	0.0304	0.0117
$\hat{\sigma}_v$	0.0438	0.0514	0.0397	0.0472	0.0396
$\hat{\rho}$	-0.0486	-0.0838	-0.1194	-0.2013	-0.3187

date t	02/12/09	16/12/09	30/12/09	06/01/10	20/01/10
$\hat{\kappa}$	0.2007	0.1213	0.0194	0.0847	0.0370
$\hat{\lambda}$	0.0323	0.1145	0.2271	0.1338	0.1691
\hat{v}_t	0.0201	0.0194	0.0202	0.0177	0.0167
\hat{v}	0.0053	0.0106	0.0661	0.0151	0.0314
$\hat{\sigma}_v$	0.0460	0.0507	0.0506	0.0506	0.0482
$\hat{\rho}$	-0.3688	-0.4098	-0.3970	-0.3846	-0.3682

Table 7.2.: Resulting parameters of the calibrated Heston model for each examined market volatility surface, c.f. Section 7.2.2. With these parameters the calibrated volatility surfaces as seen in Appendix B are calculated. Due to rounding the parameters it is possible that the restriction $2\kappa\bar{v} > \sigma_v^2$ as seen in 5.1 is not fulfilled. The results are also shown in Figure 7.2.

Progression of the Calibrated Heston Parameters

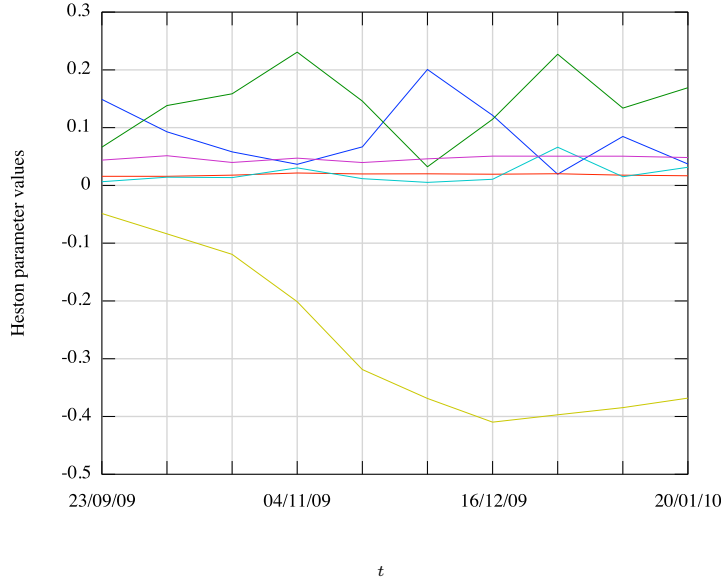


Figure 7.2.: The progression of the calibrated Heston parameters is shown as depicted in Table 7.2, with $\hat{\kappa}$ —, $\hat{\lambda}$ —, \hat{v}_t —, \hat{v} —, $\hat{\sigma}_v$ — and $\hat{\rho}$ —

is achieved by leaving out the extra days. The historic interest rates are given by the LIBOR rates of the respective country which need to be annualised, i.e. divided by the number of trading days in one year. In the given data sets this is approximately 253 days.

Once the time series is homogeneous, the maximum likelihood estimation can be undertaken, with the log-likelihood function l being

$$\arg \max_{\hat{\Theta}_{ML}} l(\hat{\Theta}_{ML}) = \sum_t -0.5 (\log (h_t(\hat{\Theta}_{ML}) + Z_t^2)) . \quad (7.5)$$

The values h_t and Z_t are defined as in the formulae of (6.7) in Section 6.2.1, with $p = q = 1$. The error variable Z_t is retrieved by inverting the first of these equations. $\hat{\Theta}_{ML}$ is the vector of all the NGARCH parameters to be estimated by the likelihood maximisation, i.e. $\hat{\Theta}_{ML} = [\alpha_0, \alpha_1, \beta_1, \gamma_1]'$. Subsequently, the variable λ is estimated by minimising the sum of squared errors of the underlying asset's level values S_t and the values resulting from the price process (6.7a) with the ML-estimated variance h_t from the first step, i.e. $\hat{S}_t(\lambda, h_t)$. This approach is also consistent with the one found in [Heston00] p.597. The sum in equation (7.5) and (7.6) is over all dates t in the time series. The latter shows the minimisation formula to estimate the parameter λ which is given by

$$\arg \min_{\lambda} \sum_t \left(S_t - \hat{S}_t(\lambda, h_t) \right)^2 \quad (7.6)$$

Estimated Heston-Nandi Parameters by MLE

$$\begin{array}{l} \hat{\alpha}_0 \\ \hat{\alpha}_1 \\ \hat{\beta}_1 \\ \hat{\gamma} \\ \hat{\lambda} \end{array} \parallel \begin{array}{l} 5.079e - 20 \\ 9.394e - 07 \\ 0.9728 \\ 73.0832 \\ -0.4520 \end{array}$$

Table 7.3.: Heston-Nandi Parameters are obtained by estimating the NGARCH process via maximum likelihood estimation (MLE), c.f. Section 7.2.3.

The Heston-Nandi process is also subject to a parameter restriction which is given by $\beta_1 + \alpha_1 \gamma_1^2 < 1$, as seen in Section 6.2.1. In order to consider this constraint in the log-likelihood function, again a penalty factor is added to the maximisation problem. In this case the log-likelihood function is simply set to a small number p_c if the restriction is violated, e.g. $p_c = 0$. The log-likelihood function is then depicted by

$$l^*(\hat{\theta}_{ML}) = \begin{cases} l(\hat{\theta}_{ML}) & , \beta_1 + \alpha_1 \gamma_1^2 < 1 \\ p_c & , \beta_1 + \alpha_1 \gamma_1^2 \geq 1 \end{cases} . \quad (7.7)$$

As a result of estimating the parameters to the time series, the parameters are constant for all volatility surfaces which is another major difference between estimating the parameters from a time series and calibrating the pricing model to current market prices. In Section 6.2.1 it is mentioned that the prices are very sensitive to the parameter λ . This statement is also observed in this research.

After estimating the parameters from the MLE and the second step minimisation procedure, the Heston-Nandi model as in Section 6.3 is used to price the options. Again, a matrix of all call prices dependent on the respective driftless deltas and maturities is generated to obtain the implied volatilities of the surface as seen in Figure 6.2 in Section 6.5.1. The results of the parameter estimation according to this approach can be found in Table 7.3 which are also used in *every* volatility surface to be computed, as shown in the mentioned figure for $t_0 = 23/09/2009$. The variance is of course given by the respective values of the variance process h_t at each date t as seen in Table 7.4.

7.2.4. Fitting the NGARCH Process to an Implied Volatility Index

As stated in Section 6.5.2, fitting an NGARCH process to a time series of implied volatilities is another possibility to obtain the parameters in order to price options with the Heston-Nandi model. The idea is to minimise the squared differences of the NGARCH process to the implied volatility index. The values of this index need to be squared and annualised (i.e. divided by the amount of days in a year) for this procedure, as

Values of the NGARCH Variance Process at Specific Dates

date t	23/09/09	07/10/09	21/10/09	04/11/09	18/11/09
\hat{h}_t	$2.935e - 05$	$2.867e - 05$	$2.579e - 05$	$3.182e - 05$	$3.367e - 05$
date t	02/12/09	16/12/09	30/12/09	06/01/10	20/01/10
\hat{h}_t	$3.331e - 05$	$4.038e - 05$	$4.038e - 05$	$3.811e - 05$	$3.749e - 05$

Table 7.4.: Estimated values at the respective date t of the NGARCH process \hat{h}_t generated from the parameters in Table 7.3.

the NGARCH process delivers *variances* at certain *points of time* which in this case are the closing times of the individual trading days. Let $\sigma_{IV,t}^2$ denote the implied annualised variances of the index. The NGARCH parameters are again stored in a vector $\Theta_{IV} = [\alpha_0, \alpha_1, \beta_1, \gamma_1]'$ which underlie $h_t(\Theta_{IV})$. Thus, the minimisation is given by

$$\arg \min_{\Theta_{IV}} \sum_t (\sigma_{IV,t}^2 - h_t(\Theta_{IV}))^2. \quad (7.8)$$

Again, the sum applies to all given dates t in the time series. It is to be noted that the parameter λ being the variable for the risk premium does not have to be estimated in this framework and is set to $\lambda = -0.5$ as the implied volatilities already contain this premium. This is why implied volatilities are normally higher than the estimated volatilities in the time series. During the financial crises in 2008-2009, the implied volatility index was so high that the NGARCH process cannot fit the index values appropriately during this period. This can be seen in Figure 7.3 where the peaks of $\sigma_{IV,t}^2$ are more than twice as high as the estimated NGARCH variances.

In Section 6.5.2 it is mentioned that this approach is questionable, as the model is fitted to the wrong quantity. The implied volatility, or variance, is not that of the respective currency but that of the entire market. Figure 7.3 also shows large discrepancies between the actual time series and the fitted NGARCH process. Also, the differences between the relative market prices of an option to the prices of the model are larger than in the previous solution which is discussed in more detail in Chapter 8. The results should be somewhat more sophisticated, if the implied volatility index were more adequate. The parameters which are obtained from this particular calibration are given in Table 7.5.

7.2.5. Calibrating the Heston-Nandi Model

It has been shown in Section 6.5.3 that the calibration of the Heston-Nandi model does not deliver satisfying results, c.f. Figure 6.6. It can be seen from the preceding attempts to produce volatility surfaces with the NGARCH process that the volatilities become very flat for long termed options. This should be the reason why it does not seem to be possible to calibrate this approach to the market data properly as the approximate

*Comparison of the Implied Volatility Index to the Fitted NGARCH Process, during
04/01/1999 – 20/01/2010*

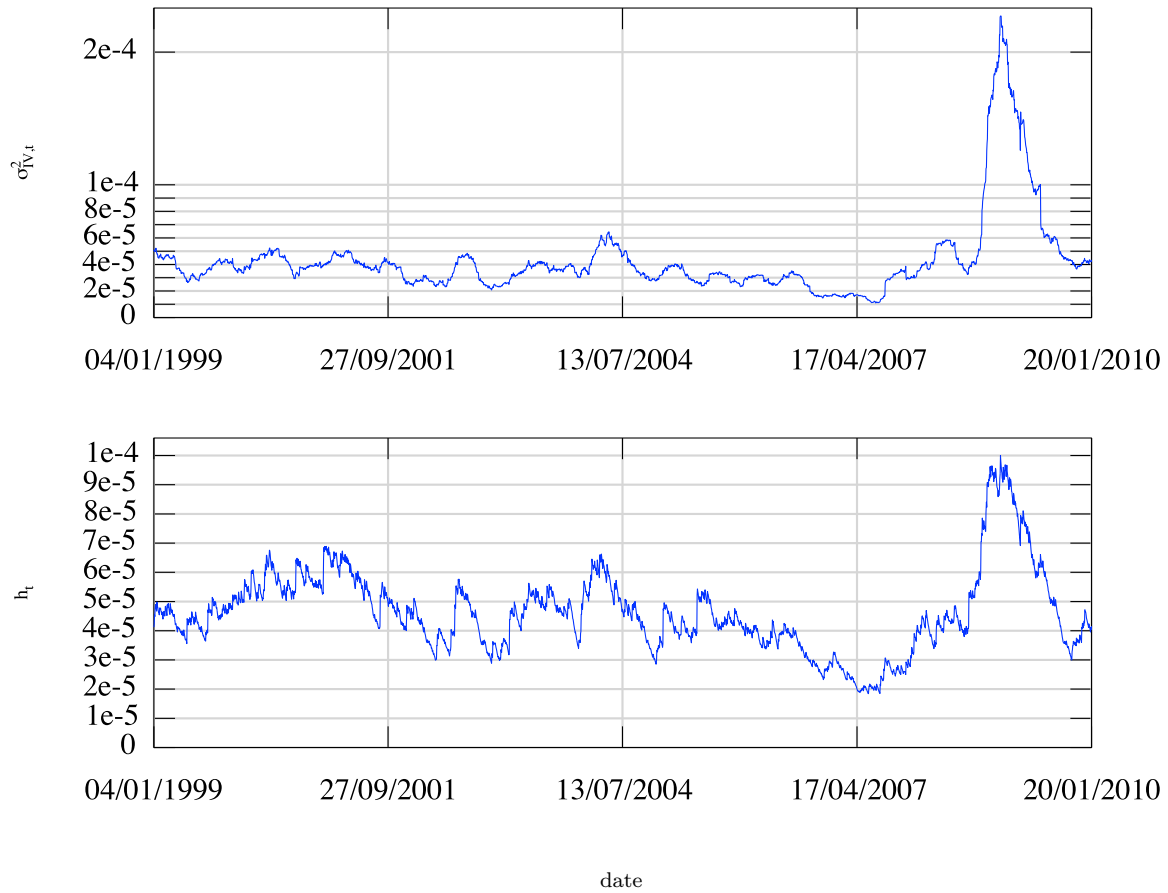


Figure 7.3.: During the financial crises in 2008-2009, the squared implied volatility $\sigma_{IV,t}^2$ index was so high that the NGARCH process cannot fit the index values appropriately during this period. The peaks of $\sigma_{IV,t}^2$ are more than twice as high as the fitted NGARCH variances h_t .

Calibrated NGARCH Parameters to a Volatility Index

$\hat{\alpha}_0$	$1.126e - 21$
$\hat{\alpha}_1$	$8.773e - 07$
$\hat{\beta}_1$	0.9790
$\hat{\gamma}$	70.0852

Table 7.5.: Heston-Nandi Parameters are obtained by fitting the NGARCH process to a volatility index, c.f. Section 7.2.4.

Values of the NGARCH Variance Process at Specific Dates

date t	23/09/09	07/10/09	21/10/09	04/11/09	18/11/09
\hat{h}_t	$3.587e - 05$	$3.454e - 05$	$3.128e - 05$	$3.577e - 05$	$3.716e - 05$
date t	02/12/09	16/12/09	30/12/09	06/01/10	20/01/10
\hat{h}_t	$3.685e - 05$	$4.336e - 05$	$4.388e - 05$	$4.204e - 05$	$4.159e - 05$

Table 7.6.: Estimated values at the respective date t of the NGARCH process \hat{h}_t generated from the parameters in Table 7.5.

plane as from the middle of the surface takes too much weight in the minimisation. However, it may also be possible that the outcome of the minimisation is stuck in some local minimum. In either of the cases, without further restrictions the results do not perform well.

Apart from the fact that the optimisation process seems to need further adjustments, this approach to obtain the NGARCH parameters is not feasible in practice. This statement is due to the fact that the computational expenditure is very large to obtain just one matrix of call prices when applying the Heston-Nandi model. With relatively fast hardware it took a few minutes to calculate one call matrix and over one week for the calibration to deliver some output. In comparison, the Heston model, which is based on similar characteristic functions and a totally equal optimisation procedure, takes an instant to deliver one matrix of option prices and approximately four hours to present a calibrated model.

As the LSE function is minimised by six parameters in both frameworks with similar parameter ranges, this possibility obviously is not the cause for the differences. However, some explanations are found in the specific properties of the Heston-Nandi characteristic functions. The main reason for the extensive computational expenditure is the recursive computation of A_t and $B_{1,t}$ seen in Section 6.3 which has to be computed for *each* integrand and *each* ϕ . In order to have a certain precision for the numeric integration, the number of ϕ 's is relatively large.

If the computational effort is of no importance, the calibration of the Heston-Nandi framework can be carried out the same way as described in Section 7.2.2 for the Heston model. The strikes are acquired from equation (4.25) and the market call prices are retrieved by the BSM formulae (4.5). The Heston-Nandi model is then calibrated to the market call prices by minimising the LSE function w.r.t. the parameter vector $\hat{\Theta}_{HN} = [\alpha_0, \alpha_1, \beta_1, \gamma, h_t, \lambda]'$,

$$\text{LSE}(\hat{\Theta}_{HN}) = \arg \min_{\hat{\Theta}_{HN}} \sum_{m=1}^M \sum_{n=1}^N \left(C_{m,n} - \hat{C}_{m,n}(\hat{\Theta}_{HN}) \right)^2. \quad (7.9)$$

Calibrated Heston-Nandi Model at $t_0 = 23/09/2009$

$\hat{\alpha}_0$	$7.818e - 06$
$\hat{\alpha}_1$	$2.301e - 06$
$\hat{\beta}_1$	0.6708
$\hat{\gamma}$	0.1001
$\hat{\lambda}$	-0.4932
\hat{h}_t	$6.586e - 05$

Table 7.7.: Resulting parameters of the calibrated Heston-Nandi model at $t = 23/09/2009$. $\hat{\lambda}$ is close to the value -0.5 which is expected as the model is calibrated to the (implied) market volatility surface. The calibration does not seem to be feasible without further assumptions, c.f. Section 7.2.5.

The parameter results of the calibration from Figure 6.6 are given in Table 7.7. However, because the computational effort is so large and the results are not convincing the model is not calibrated to all the examined market volatility surfaces like in the Heston case. The Heston-Nandi model does not seem to be able to represent the prices adequately which have long term maturities. In all the examined Heston-Nandi/ NGARCH approaches, no matter how the parameters are estimated, the volatility surface becomes very flat for options expiring in the far future. The characteristics of the outcomes from all the different models are examined in the following chapter.

8. Valuations and Comparisons of the Different Models

Having introduced, and fitted the Heston and the Heston-Nandi model to data, the latter also in some variations, it is of interest to analyse the differences of the individual models and their modifications. Their performance is valued by graphical comparisons, statistical measures and by examining the underlying processes of the respective concepts.

8.1. Model Valuations

8.1.1. Graphical Comparison

It can easily be determined how well the models' option prices perform by simply calculating the deviations to the real market prices. However, instead of considering the level differences, it is useful to investigate the relative difference of the option prices to the price of the underlying asset. This makes sense as the level differences of highly priced options are naturally larger than lower priced options and the price of an option is generally only of interest relative to the price of its underlying asset. Therefore, the errors should also be expressed in this relative quantity which is depicted in percent. The graphical version of this procedure has already been introduced in Section 4.3 and is also seen in many textbooks, see for example Figure 4.4.

Examining the results of these graphical comparisons and also the models' volatility surfaces with the given market volatilities, it can generally be concluded that the calibrated Heston model fits the best even though it has deficiencies for short termed options which are reviewed in Section 10.1.3. The model "imitates" the basic structure of the market volatility surface which is one main aim of the model constructions. In comparison, the Heston-Nandi framework, regardless of which procedure is used, seems to be able to fit the options with short termed maturities better but with the disadvantage of approximately constant volatilities for middle and long termed maturities. These observations can be seen throughout all the volatility surfaces and deviation plots which are presented in Appendix B.

MSE Values of the Examined Models

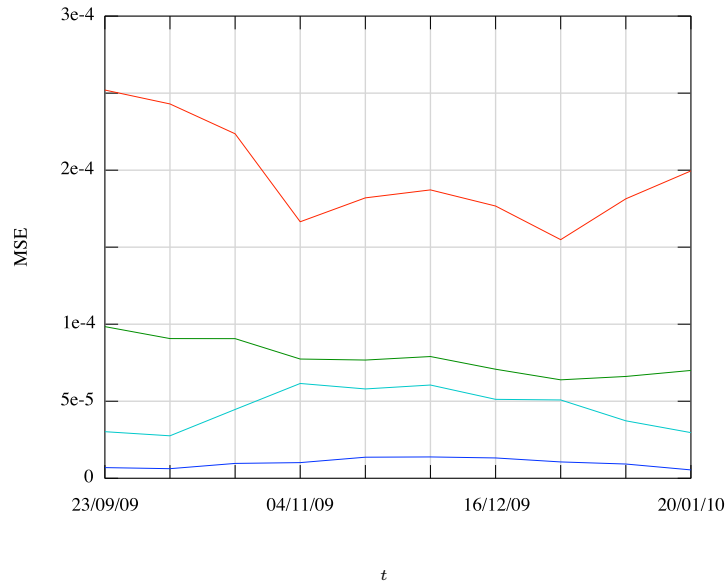


Figure 8.1.: The chart shows the mean squared errors (MSE) of the respective models which are given by the calibrated Heston framework (—), the ML estimated parameters of Heston-Nandi model (—), the Heston-Nandi version with calibrated NGARCH process to the implied volatility index (—) and, as a comparison, the calibrated BSM model (—). The MSE is computed by the mean squared difference of each calculated call price to every market call price w.r.t. all maturities and (driftless) deltas is computed. It can be seen that the options priced by the Heston approach have the smallest mean squared errors, c.f. Table 8.1.

8.1.2. Mean Square Error

The *mean square error (MSE)* is a widely used statistical measure which specifies how close an estimator is to the true value. In this case, it is irrelevant whether the mean or the simple sum of squares is examined, as the volatility surfaces all have the same amount of data points. In this context, the MSE of the same call price matrix as in Chapter 7 is calculated. This means that the difference of each calculated call price to every market call price w.r.t. all maturities and (driftless) deltas is computed.

It should be mentioned that it is not surprising that the calibrated Heston model performs the best as the sum of squared errors is also used to calibrate the model to *each* examined volatility surface. The mean square error of each model and volatility surface can be seen in Table 8.1 and also in Figure 8.1 where the progression throughout the time is visualised.

MSE Values of the Examined Models

date t	23/09/09	07/10/09	21/10/09	04/11/09
Heston, calibration	$6.904e - 06$	$6.205e - 06$	$9.639e - 06$	$1.016e - 05$
NGARCH, MLE	$9.844e - 05$	$9.068e - 05$	$9.065e - 05$	$7.741e - 05$
NGARCH, fitted vola index	$2.520e - 04$	$2.430e - 04$	$2.236e - 04$	$1.665e - 04$
BSM, calibration	$3.023e - 05$	$2.757e - 05$	$4.464e - 05$	$6.155e - 05$

date t	18/11/09	02/12/09	16/12/09	30/12/09
Heston, calibrated	$1.369e - 05$	$1.386e - 05$	$1.320e - 05$	$1.061e - 05$
NGARCH, MLE	$7.676e - 05$	$7.903e - 05$	$7.079e - 05$	$6.388e - 05$
NGARCH, fitted vola index	$1.820e - 04$	$1.872e - 04$	$1.767e - 04$	$1.549e - 04$
BSM, calibration	$5.800e - 05$	$6.053e - 05$	$5.124e - 05$	$5.082e - 05$

date t	06/01/10	20/01/10
Heston, calibrated	$9.250e - 06$	$5.415e - 06$
NGARCH, MLE	$6.608e - 05$	$7.000e - 05$
NGARCH, fitted vola index	$1.814e - 04$	$1.995e - 04$
BSM, calibration	$3.729e - 05$	$2.962e - 05$

Table 8.1.: The table shows the mean squared errors (MSE) of the respective models which are given by the calibrated Heston framework, the ML estimated parameters of Heston-Nandi model, the Heston-Nandi version with calibrated NGARCH process to the implied volatility index and, as a comparison, the calibrated BSM model. The MSE is computed by the mean squared difference of each calculated call price to every market call price w.r.t. all maturities and (driftless) deltas is computed. It can be seen that the options priced by the Heston approach have the smallest mean squared errors, c.f. Figure 8.1.

It can be concluded that the calibrated Heston model *always* outperforms the other concepts clearly. It can also be seen that the Heston-Nandi approach with the NGARCH process fitted to the volatility index has the largest MSE at all times and thus delivers worse results than the BSM options pricing scheme.

8.2. Comparing the Return Densities of the Individual Models

Another way to analyse the different models is to examine how close the driving processes are in comparison to the observed market returns of the underlying asset. This can be done by comparing the returns of the given time series with the ones produced by a Monte Carlo (MC) simulation from the processes of the respective model. This is an interesting approach as the basic characteristics of the model are analysed, i.e. it is checked whether the price process of the underlying asset delivers the same characteristics as the market. As seen in Section 4.7, the market returns are not normally distributed as the given data has fat tails, a higher frequency around the mean and also seems to have a skew. This also means that the standard BSM model fails to meet these occurrences as the underlying process is normally distributed, c.f. equation (3.2) in Section 3.1.1.

It is, therefore, a good indicator of the model's performance to see whether the model suffices the basic asset path and return characteristics. Moreover, a good and consistent comparison to the BSM model is given because it assumes normally distributed returns. In order to have the same conditions for all the models and to be able to compare the results with the collected time series, an equally long time period with the same amount of level values is produced for the MC simulations of each model. Also, the estimated parameters from Chapter 7 are used as these parameters have been used to fit the respective models to the given market data.

The returns of the simulated price paths are shown in the resulting histograms in the Figures 8.2-8.4. It can be seen that the underlying processes also differ from the normal distribution in a similar way as the original data seen in Figure 4.6 in Section 4.7. Hence, it can be stated that these underlying processes are more realistic and closer to reality than the price process given by the BSM model.

Return Histogram of MC Simulation Generated by Calibrated Heston Parameters

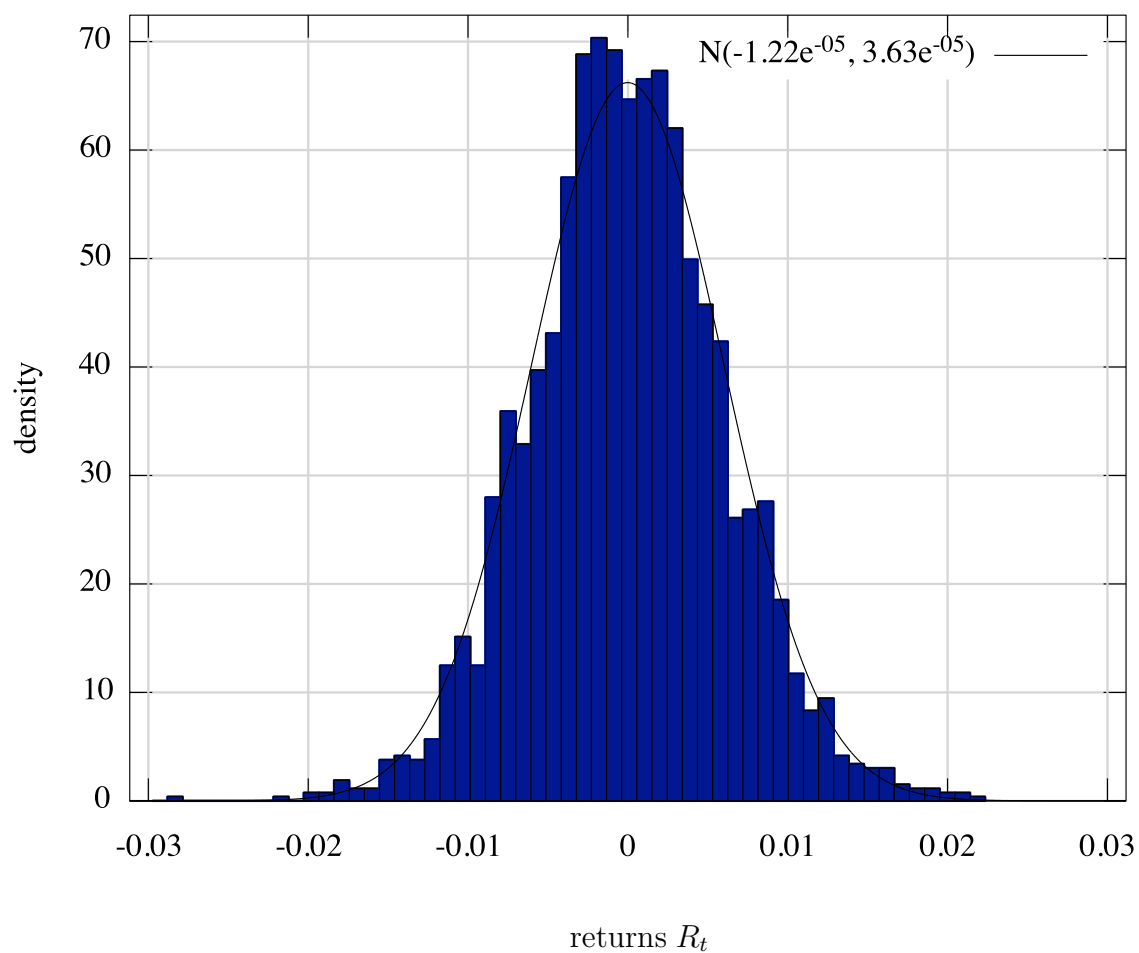


Figure 8.2.: Histogram of discrete returns R_t generated from the processes in equations (5.1)-(5.3) and the same starting value as the original time series in Figure 7.3. The parameters for the Heston model are obtained from the calibrated parameters of $t = 20/01/2010$ in Table 7.2. The histogram differs from the normal density in a similar way as the market returns in Figure 4.6.

Return Histogram of MC Simulation Generated by NGARCH Parameters from MLE

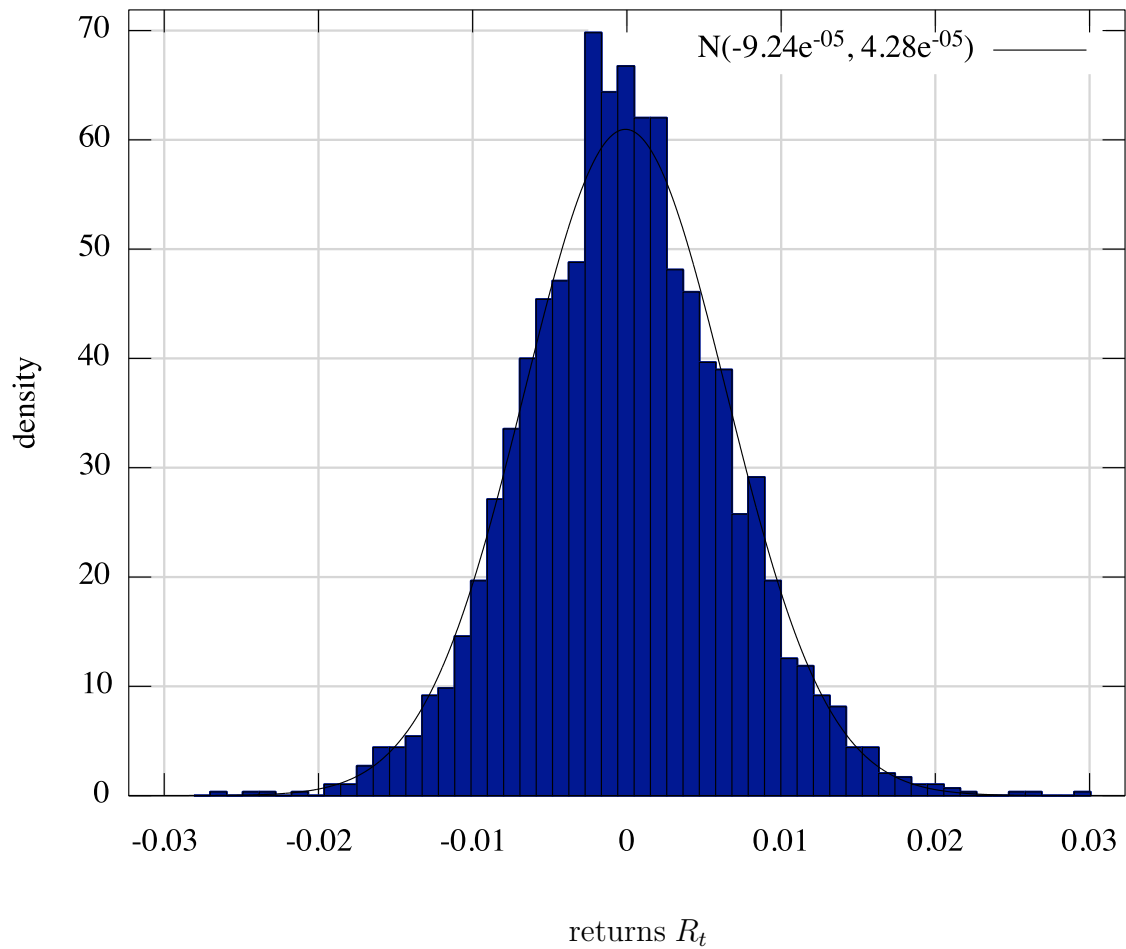


Figure 8.3.: Histogram of discrete returns R_t generated from the processes in equation (6.7) and the same starting value as the original time series in Figure 7.3. The parameters of the NGARCH process are obtained from the maximum likelihood estimated (MLE) parameters in Table 7.3. The histogram differs from the normal density in a similar way as the market returns in Figure 4.6.

Return Histogram of MC Simulation Generated by NGARCH Parameters from Fitting the Volatility Index

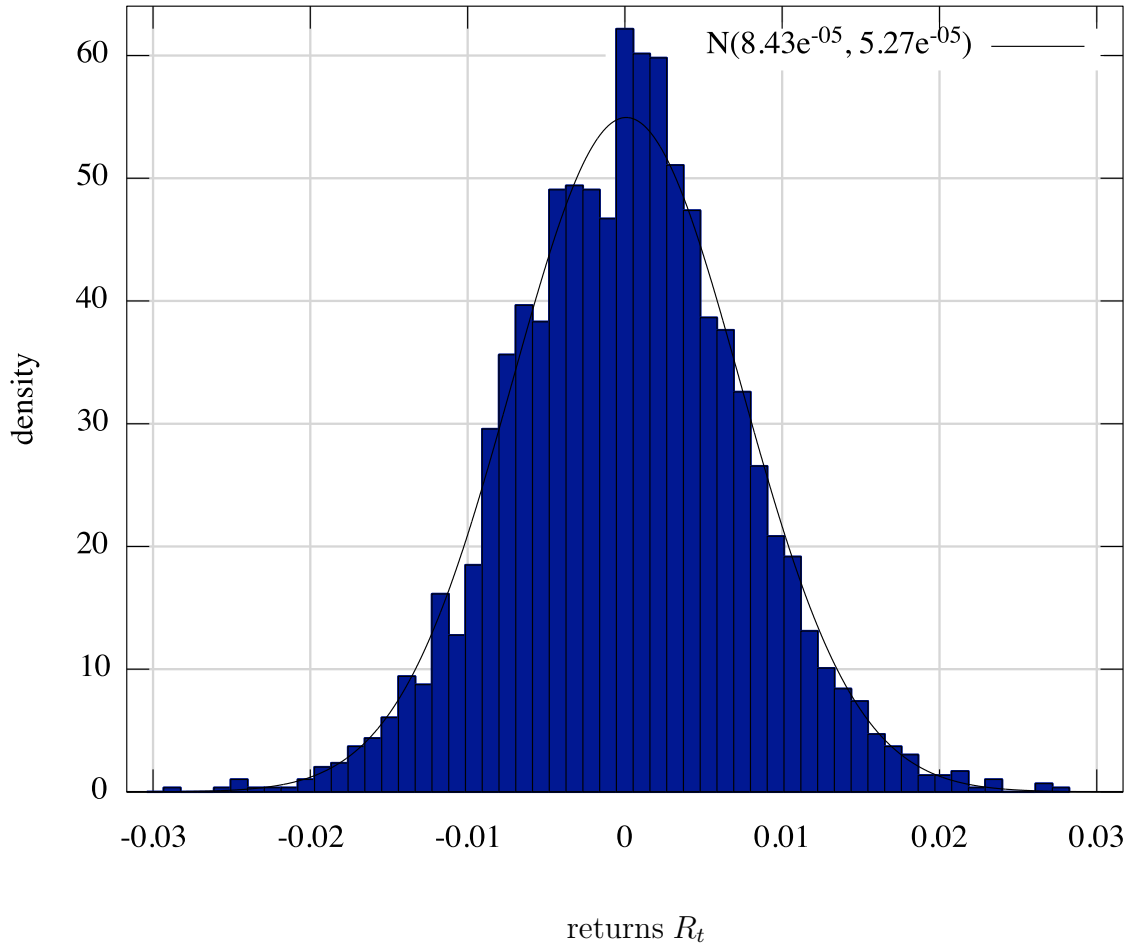


Figure 8.4.: Histogram of discrete returns R_t generated from the processes in equation (6.7) and the same starting value as the original time series in Figure 7.3. The parameters of the NGARCH process are obtained from the fitted NGARCH process to the implied volatility index in Table 7.5. The histogram differs from the normal density in a similar way as the market returns in Figure 4.6.

9. Pricing Exotic Options

The topic of pricing exotic options is continued in this Chapter, as seen in Section 4.6. This issue is one of the reasons for using stochastic volatility models as the BSM model does not seem to be able to deliver convincing prices for exotics. Different possibilities of pricing barrier options are outlined and an approach for valuating cliquet options is described in the following units.

9.1. Pricing Barrier Options with Stochastic Volatility Models

The basics of barrier options are explained in Section 4.6.1 as well as the formulae to price these options in the BSM framework. [Cont04] illustrates different ways of pricing barriers for different kinds of processes. The theory of pricing barrier options is vast and is beyond the scope of this research. However, one possibility is always given by a simple Monte Carlo simulation which is easily implemented by simulating the price processes with Heston or GARCH volatilities. At the end of the path, each simulation is examined to determine the respective payoff function from the min and max terms. By repeating this procedure sufficiently often, a good estimate of the barrier price is given. This approach of determining the price of an (exotic) option is performed in the next section.

The reason why it is necessary to price barrier options with stochastic volatility or similar models is given by the fact that the BSM model underestimates the probability of hitting the barrier. Further explanations for why it is essential to use more sophisticated models other than the BSM model are found in Section 4.7 and in [Cont04].

Even if the prices of barrier options are only estimated by MC simulations, the results should be more trustworthy than the BSM closed form prices. The accuracy can be improved by various variance reduction methods such as mirroring the paths and control variate. Nevertheless, it should be emphasised that the prices of barrier options is very model dependent and further investigations have to be undertaken to obtain consistent prices, c.f. [Gatheral06] ch.9. In fact the barrier prices differ considerably which is possibly the reason why bid and ask prices of market participants also differ to a large extent. These analyses are not the focal point of this research and can be observed in the latter citations.

9.2. Pricing Cliquets with Stochastic Volatility Models

The basic concept of pricing options with MC simulations has been outlined in the preceding section. This section shows an example of this procedure by pricing call cliquets with the payoff function (4.48) as seen in Section 4.6.3. The reason why these specific options have been chosen to be analysed is that it is also not possible to price these options with a closed form solution in any model so the comparisons have the same precision. The results of this pricing example can be viewed in Table 9.1. As stated in [Gatheral06] ch.9, the obtained prices are very model dependant.

Example of Pricing Cliquets with Stochastic Volatility Models

Model	Cliquets Call Price
BSM	2.213
Heston	2.316
Heston-Nandi	6.266

Table 9.1.: Fictive example of pricing Cliquets with Stochastic Volatility Models. The parameters are chosen from the fitted models of the Sections 7.2.1, 7.2.2 and 7.2.3 with $t = 20/01/2010$. The prices are calculated by Monte Carlo (MC) simulation with 10000 different paths, 253 trading days, total maturity of 10 years, 10 individual cliquets and $\nu = 1$, c.f. Section 4.6.3.

10. Extensions of the Models

This chapter gives an outlook on extensions of the models examined in the preceding chapters and presents further approaches. It is shown that some extensions are only relevant in theory and do not have a practical value, e.g. it is not possible to hedge the resulting option prices properly, or the model loses its initial purpose. The main focus lies on Heston model extensions, also because there is more literature available and it is the more established model for pricing options.

10.1. Heston Model Extensions

10.1.1. Adjustment of the Least Squared Error Function

It has been shown that the Heston Model seems to be the most feasible model which is why extensions of this approach will be discussed first. The simplest form of improving the fit of the model is to employ weights $w_{m,n}$ into the least square error function in equation (7.3) resulting in

$$\text{LSE}(\hat{\theta}_H) = \arg \min_{\hat{\theta}_H} \sum_{m=1}^M \sum_{n=1}^N w_{m,n} \left(C_{m,n} - \hat{C}_{m,n}(\hat{\theta}_H) \right)^2. \quad (10.1)$$

Weights enable one to focus the optimisation on a “relevant” or more important area of the volatility surface, such as options being close to ATM because they are traded more frequently. This would also account for the higher accuracy of the markets’ option prices (or implied volatilities) when being closer to ATM as when options are far OTM or ITM they are usually not so liquid and vary to a greater extent. Another adjustment which can be undertaken to improve the fit is to alter the measure of the price differences. This is done by replacing the square with another value $q > 0$ and applying absolute differences

$$\text{LQE}(\hat{\theta}_H) = \arg \min_{\hat{\theta}_H} \sum_{m=1}^M \sum_{n=1}^N \left| C_{m,n} - \hat{C}_{m,n}(\hat{\theta}_H) \right|^q. \quad (10.2)$$

Also, a general penalty function $\text{pen}(\theta_H, \theta_0)$, as seen in [Nögel03] p.4, can be added to favour parameters that lie close to each other or to a initial parameter value θ_0 . This

has the advantage that parameters are not likely to suddenly “jump” to a somewhat different scale. The least squared error function can thus be given by

$$\text{LSE}'(\hat{\theta}_H) = \arg \min_{\hat{\theta}_H} \sum_{m=1}^M \sum_{n=1}^N \left(C_{m,n} - \hat{C}_{m,n}(\hat{\theta}_H) \right)^2 + \text{pen}(\hat{\theta}_H, \Theta_0). \quad (10.3)$$

Various combinations of the latter adjustments are possible.

10.1.2. Time Dependant Parameters

The latter extensions are very easy to implement and offer a simple way to improve the fit but also parameter consistency. A very different approach is given by making the Heston parameters dependant on the time in some way. One example is given by making the mean reversion parameter \bar{v} time dependent, i.e. \bar{v}_t , for example $\bar{v}_t = \mathbf{m} + (\bar{v}_0 - \mathbf{m}) e^{-\alpha t}$ as seen in [Overhaus07] p.46. The Heston variance process v_t in equation (5.2) is then given by

$$dv_t = \kappa (\bar{v}_t - v_t) dt + \sigma_v \sqrt{v_t} dW_{2,t}. \quad (10.4)$$

A similar idea is to make all the parameters piecewise constant, i.e. $\kappa_{\delta t_j}$, $\bar{v}_{\delta t_j}$, $\sigma_{\delta t_j}$ and $\rho_{\delta t_j}$. This results in

$$dv_{\delta t_j} = \kappa_{\delta t_j} (\bar{v}_{\delta t_j} - v_t) dt + \sigma_{\delta t_j} \sqrt{v_t} dW_{2,t} \quad (10.5)$$

and

$$\rho_{\delta t_j} = \text{Corr}_{\delta t_j} [W_{1,t}, W_{2,t}]. \quad (10.6)$$

In [Nögel03] and [Overhaus07] ch.2 it is shown that these extensions can be solved practically the same way already described in Chapter 5 with minor alterations. Therefore, these are also closed form solutions. It is obvious that the fit of the model increases the more parameters are included in the model. However, there is a considerable trade-off involved when applying these proposals which is also outlined in [Overhaus07] ch.2. By employing piecewise constant time dependant parameters the model’s structure gets lost which defeats the purpose of the whole model. The model is practically turned into an “arbitrage-free interpolation of market data” instead of giving a “view” on the build of the volatility, c.f. [Overhaus07] p.47. Additional parameter restrictions similar to the ones seen in equation (10.3) can again be used to smooth the parameters over the time period.

Another drawback of such models for practitioners is the problem of hedging. When inserting time dependant parameters into the model one needs to additionally hedge against movements of the parameters, c.f. [Overhaus07] ch.2. Therefore, the less consistent the parameters are and the more parameters involved, the less dependable the model gets which is a good reason to continue with the original model. whether the extension is reasonable.

10.1.3. Jumps

A very popular way of extending stochastic volatility models and, in particular the Heston stochastic volatility model, is to add *jumps* to the models. The idea of jumps arises when noticing that a certain amount of the volatility is due to overnight and also weekend shifts which is not explicitly modelled by ordinary stochastic volatility processes. Adding jumps can improve the fit considerably which is seen in [Gatheral06] ch.5 and [Cont04]. It is shown that adding jumps particularly helps to improve the short term volatility structure, i.e. options with close expiry dates. In this research, c.f. Chapter 8, it is also observed that the volatility surfaces of the Heston model is comparatively poor which is why jumps seem to be a promising solution.

[Gatheral06] argues that it is not without reason why stochastic volatility models perform badly for short term options as the volatility process does not vary much during short time periods. This is why the returns from the Heston model should be close to the normal distribution and the volatility smiles consequently are relatively flat. The proposed approach can work against this behaviour by adding jumps to the *price process*

$$dS_t = \mu S_t dt + \sigma S_t dW_t + (J - 1) S_t d\mathbf{q}, \quad t > 0. \quad (10.7)$$

where $d\mathbf{q}$ denotes a Poisson process

$$d\mathbf{q} = \begin{cases} 0 & , \text{ with probability } 1 - \lambda(t)dt \\ 1 & , \text{ with probability } \lambda(t)dt \end{cases}. \quad (10.8)$$

The price process is equivalent to equation (3.1) in Section 3.1.1, except for the additional jump process. $\lambda(t)$ depicts the hazard rate of the Poisson process which can be interpreted as the “pseudo-probability” per unit time for a jump to occur, c.f. [Fahrmeir05] ch.5. and [Gatheral06] p.54. The Heston version of the price process from equation (5.1) is

$$dS_t = \mu S_t dt + \sqrt{v_t} S_t dW_{1,t} + (J - 1) S_t d\mathbf{q}, \quad t > 0. \quad (10.9)$$

In [Gatheral06] ch.5 it is shown that the derivation of the PDE is very similar to the one shown in Section 5.2.1 and, therefore, has a closed form solution. It is also shown in a worked example that the Heston stochastic volatility process with added jumps to the price process is superior to the standard Heston model as seen in Chapter 5. There are also different versions of jump processes which can be supplemented.

Again, one can argue that because there are more parameters, the model should perform better. Moreover, the same problems arise as in Section 10.1.2, i.e. difficulties of assigning consistent and reproduceable parameters when calibrating the model. This is because both the volatility process and the jump process both model a certain amount of the varying volatility. However, the jumps are included for a convincing reason and do not simply “over-fit” the model. Besides, the problems of calibrating seem to be minor,

as the Table 5.4 in [Gatheral06] indicates where the Heston model is fitted by different authors with different data. The result is that the Heston parameters only differ to a certain extent which speaks for this approach.

10.1.4. Further GARCH Models

As the Heston-Nandi model has not become as established as the Heston model, there are also fewer attempts (practically none) of extending it. At least for the calibrated version of the Heston-Nandi model, c.f. Section 6.5 and Chapter 7, some of the approaches outlined in the previous subsections can be taken into consideration to improve the fit.

However, there are various attempts of non-closed form solutions by using Monte-Carlo (MC) simulations and exploiting all possible GARCH extensions. In fact, these approaches have existed before the closed form frameworks due to the simpler implementation (no characteristic functions are involved). Especially [Duan95] shows how this approach can be applied for pricing options using a basic GARCH(p,q) process for the variance. This is enabled by the LRNVR concept which is described in Chapter 6.

It has been stated that there are numerous GARCH extensions which can improve the fit of the variance process considerably. For example the EGARCH process as depicted in Section 6.1.4 has some distinctive advantages over the standard GARCH model which also seem to improve the fit volatility smiles and skews, c.f. [Schmitt96]. Nevertheless, the advantages of closed form solutions are considerable especially as one is able to price an option with the highest possible accuracy.

11. Conclusions and Summary

In the preceding chapters a detailed analysis on option pricing in the context of stochastic volatility models has been given. Concentrating on the foreign exchange market, the general theory has been derived as well as showing examples and further specifics of this particular market. The drawbacks and failures of the Black-Scholes-Merton framework and also pricing more complex option strategies motivate the necessity of using stochastic volatility models which do not wrongly assume constant volatility. Two of these concepts are introduced, both having the unique advantage of possessing closed form solutions to price plain vanilla options, i.e. the Heston and the Heston-Nandi model.

An interesting relationship between the models is that the Black-Scholes-Merton pricing scheme is a special case of the Heston framework which in turn is a special case of the Heston-Nandi pricing approach when limiting the time lags to zero. However, the empirical results after calibrating the respective models are quite different which is mainly due to the different assumption made in the respective models. This is partly seen when the underlying price processes are compared to each other, c.f. Section 8.2. Moreover, further dissimilarities are found after comparing the volatility surfaces which are a direct result of the different underlying processes as well as investigating the actual path of these processes which is continuous for BSM and Heston and discrete for Heston-Nandi. The characteristic functions of the two latter models also differ which particularly have a large effect on the empirical analysis where it turns out that the Heston-Nandi framework is not suitable for efficient calibration results.

The main conclusion to be made after comparing the different models as well as several sub-models is that the Heston framework generates a volatility surface which is closest to the market conditions and delivers the most accurate option prices, c.f. Section 8.1.2. This approach is also applicable to calibrate the model to the market. Although this characteristic might seem natural at first, it is shown that the Heston-Nandi approach is not suitable for this procedure due to a considerably high computational expenditure. Instead, this model can be fitted either by the maximum likelihood estimation or to an implied volatility index. It turns out that only the former operation delivers satisfying results and outperforms the original BSM option pricing scheme.

Although the Heston-Nandi model provides more precise prices for short termed options, overall the Heston framework can be declared to be the most consistent. Especially when taking possible improvements and extensions into consideration to correct the weaknesses in the short term, the Heston model can be considered to be the best performing approach. Together with the fitted parameters of the respective framework, plain vanilla

and exotic options can thus be priced under more realistic assumptions than the original BSM pricing scheme.

A. The Statistical Basis

This chapter reviews the statistical basis for some techniques applied in the preceding chapters following [Cont04], [Fahrmeir05] and [Grimmett01].

A.1. Stochastic Processes

A.1.1. Theory and Notation

A family of random variables $\{X_t, t \in \Delta t = [t_0, T]\}$, where t denotes the time index, is referred to as a *stochastic process*, or *random process*. The codomain of the random variable is the set S .

More precisely (see also [Cont04]), one needs to define a *probability space* $(\Omega, \mathcal{F}, \mathbb{P})$, where Ω specifies a set of scenarios and \mathbb{P} denotes the *probability measure* which assigns a *probability* between 0 and 1 to each event (scenario) $A \in \mathcal{F}$:

$$\begin{aligned} \mathbb{P} : \mathcal{F} &\rightarrow [0, 1] \\ A &\mapsto \mathbb{P}(A). \end{aligned} \tag{A.1}$$

\mathcal{F} is the σ -algebra which is a collection of the subsets, satisfying:

- \mathcal{F} contains the empty set: $\emptyset \in \mathcal{F}$,
- is stable under unions:

$$A_n \in \mathcal{F}, (A_n)_{n \geq 1} \text{ disjoint} \quad \Rightarrow \quad \bigcup_{n \geq 1} A_n \in \mathcal{F},$$

- contains the complementary of every element: $\forall A \in \mathcal{F}, A^c \in \mathcal{F}$.

Applying the notation of [Fahrmeir05], a family of random variables $\{X_t, t \in \Delta t\}$ is a *measurable function*, with the codomain S , and σ -algebra \mathcal{S} ,

$$X_t : (\Omega, \mathcal{F}, \mathbb{P}) \rightarrow (S, \mathcal{S}). \tag{A.2}$$

S is in general equal to \mathbb{R}^d , however, often applied in the one dimensional space, \mathbb{R} .

Definition A.1.1 (Stochastic Process) *A stochastic process is the quadruplet*

$$X = (\Omega, \mathcal{F}, \mathbb{P}, (X_t, t \in \Delta t)), \quad (\text{A.3})$$

where Δt denotes the parameter space and S the codomain space, cf. [Fahrmeir05].

The Wiener process ($W_t \equiv X_t$) in Section A.1.12 is an example of a stochastic process with continuous paths.

Definition A.1.2 (Finite-Dimensional Distributions and Distribution Families)

Let X be a stochastic process and let $\{t_1, \dots, t_n, n \in \mathbb{N}\} \subset \Delta t$ be arbitrary. Then,

$$P_{t_1, \dots, t_n}(A_1 \times \dots \times A_n) = P(X_{t_1} \in A_1, \dots, X_{t_n} \in A_n) \quad (\text{A.4})$$

are the finite-dimensional distributions of the stochastic process with the events $A_1, \dots, A_n \in \mathcal{B}$, and \mathcal{B} being the Borel σ -algebra (the σ -algebra generated by all open subsets). For real valued random variables, one obtains the finite-dimensional distribution functions of the stochastic process S :

$$F_{t_1, \dots, t_n}(x_1, \dots, x_n) = P(X_{t_1} \leq x_1, \dots, X_{t_n} \leq x_n). \quad (\text{A.5})$$

The set of all finite-dimensional distributions (distribution functions) is called the family of the finite dimensional distributions (distribution functions).

Definition A.1.3 (Consistent Distribution Families) *A finite-dimensional distribution family is consistent if and only if the following equations hold:*

$$F_{t_{k_1}, \dots, t_{k_n}}(x_{k_1}, \dots, x_{k_n}) = F_{t_1, \dots, t_n}(x_1, \dots, x_n), \quad (\text{A.6})$$

for every permutation k_1, \dots, k_n of $1, \dots, n$

$$F_{t_1, \dots, t_k}(x_1, \dots, x_k) = F_{t_1, \dots, t_n}(x_1, \dots, x_k, \infty, \dots, \infty), \quad (\text{A.7})$$

$\forall 1 \leq k < n$ and $x_1, \dots, x_k \in \mathbb{R}$

Definition A.1.4 (Path, Trajectory, Realization) *For every (fixed) $\omega \in \Omega$, the function*

$$\begin{aligned} X(\omega) : T &\rightarrow S \\ t &\mapsto X_t(\omega) \end{aligned} \quad (\text{A.8})$$

is called path, trajectory or realization of a stochastic process X .

In many cases the probability space $(\Omega, \mathcal{F}, \mathbb{P})$ cannot be explicitly specified, e.g. when applying stock prices. The Kolmogorov existence theorem shows it is sufficient to establish a finite-dimensional distribution in a *consistent* way.

Definition A.1.5 (Kolmogorov Existence theorem) *Let $\{F_{t_1, \dots, t_n}\}$, or $\{P_{t_1, \dots, t_n}\}$ be a consistent system of finite-dimensional distribution (functions). Then a probability space $(\Omega, \mathcal{F}, \mathbb{P})$ and a stochastic process*

$$X = \{\Omega, \mathcal{F}, \mathbb{P}, (X_t, t \in \Delta t)\} \quad (\text{A.9})$$

exist, with F_{t_1, \dots, t_n} being a system of finite-dimensional distributions, i.e.,

$$F_{t_1, \dots, t_n}(x_1, \dots, x_n) = P(X_{t_1} \leq x_1, \dots, X_{t_n} \leq x_n). \quad (\text{A.10})$$

Note, the stochastic process is not uniquely specified by the existence theorem. However, it ensures the existence of a probability space $(\Omega, \mathcal{F}, \mathbb{P})$ to a given joint distribution $F(x_1, \dots, x_p)$, with

$$F(x_1, \dots, x_p) = P(X_{t_1} \leq x_1, \dots, X_{t_p} \leq x_p). \quad (\text{A.11})$$

Because the Kolmogorov existence theorem *only* ensures a stochastic process S_t which allows discontinuous paths, a version with continuous paths has to be constructed when applying a Wiener process W_t [Fahrmeir05].

Definition A.1.6 (Cadlag function) *A function $f : \Delta t \rightarrow \mathbb{R}$ is said to be cadlag (compare [Cont04]) if it is right-continuous with left limits: for each $t \in \Delta t$ the limits*

$$f(t^-) = \lim_{s \nearrow t} f(s) \quad f(t^+) = \lim_{s \searrow t} f(s) \quad (\text{A.12})$$

exist and $f(t) = f(t^+)$.

A cadlag function, therefore, does not have to be continuous at every point of its domain, allowing a countable amount of certain discontinuities of the form:

$$\delta f(t) = f(t) - f(t^-). \quad (\text{A.13})$$

The left-continuous analogon is referred to as *caglag*.

To account for the time dependent information given to a certain time $t > 0$, the concept of *filtration* is applied, which can be interpreted as a sequence of non-declining information sets in the notation of σ -algebras, $\mathcal{F}_{t_0} \subseteq, \dots, \subseteq \mathcal{F}_t \subseteq, \dots, \subseteq \mathcal{F}_T \subseteq \mathcal{F}$.

Definition A.1.7 (Filtration) *A filtration or information flow on $(\Omega, \mathcal{F}, \mathbb{P})$ is an increasing family of σ -algebras $(\mathcal{F}_t)_{t \in \Delta t} : \forall t \geq s \geq 0, \mathcal{F}_s \subseteq \mathcal{F}_t \subseteq \mathcal{F}$.*

A stochastic process is referred to as being *adapted* or *non-anticipating* if and only if the value X_t is revealed at time t by the information \mathcal{F}_t . Therefore, it cannot “see into the future”.

Definition A.1.8 (Non-Anticipating Process) *A stochastic process $(X_t)_{t \in \Delta t}$ is said to be non-anticipating with respect to the information structure $(\mathcal{F}_t)_{t \in \Delta t}$ or \mathcal{F}_t -adapted if, for each $t \in \Delta t$, the value of X_t is revealed at time t : the random variable X_t is \mathcal{F}_t -measurable.*

Definition A.1.9 (Previsible Process) *A process $(X_t)_{t \in \Delta t}$ is called previsible if, for each $t \in \Delta t$, X_t is \mathcal{F}_{t-1} -measurable.*

The information is said to be the *natural history* or its *history* if it only depends on the past values of the stochastic process X .

Definition A.1.10 (History of a Process) *The history of a process X is the filtration $(\mathcal{F}_t^X)_{t \in \Delta t}$, where (\mathcal{F}_t^X) is the σ -algebra generated by the past values of the process, completed by the null sets \mathcal{N} :*

$$\mathcal{F}_t^X = \sigma(X_s, s \in [0, t]) \vee \mathcal{N} \quad (\text{A.14})$$

The random time (positive random variable) at which an event has taken place is called the *stopping time* τ and only depends on its history \mathcal{F}_t (and not its future).

$$\{\tau \leq t\} \in \mathcal{F}_t \quad (\text{A.15})$$

Definition A.1.11 (Martingale) *A cadlag process $(X_t)_{t \in \Delta t}$ is said to be a martingale if X is nonanticipating (adapted to \mathcal{F}_t), $E[|X_t|]$ is finite for any $t \in \Delta t$ and*

$$E[X_s | \mathcal{F}_t] = X_t, \quad \forall s > t. \quad (\text{A.16})$$

Theorem A.1.1 (Sampling Theorem) *If $(M_t)_{t \in \Delta t}$ is a martingale and T_1, T_2 are nonanticipating random times (stopping times) with $T \geq T_2 \geq T_1 \geq 0$ a.s. then*

$$E[M_{T_2} | \mathcal{F}_{T_1}] = M_{T_1}. \quad (\text{A.17})$$

A.1.2. Examples of Stochastic Processes

Definition A.1.12 (Wiener Process) A stochastic process $W = \{W_t, t \in \mathbb{R}^+\}$, taking values in \mathbb{R} , is called a Wiener process, if [Fahrmeir05]:

- increments are normally distributed and stationary:

$$W_{t+s} - W_s \sim W_t - W_0 \sim N(0, \sigma^2 t), \quad \text{for all } s, t \geq 0,$$

- for all $0 \leq t_1 < t_2 < \dots < t_n$, $n \geq 3$ the increments are independent:

$$W_{t_2} - W_{t_1}, \dots, W_{t_n} - W_{t_{n-1}},$$

- $W_{t_0} = 0$,
- paths are continuous.

Note, that the initial condition $W_{t_0} = 0$ can be extended by $W_t^* = W_t + c$, with $W_{t_0}^*$.

Further properties of the Wiener process and normally distributed variables:

- The process \tilde{W} is called a *standard* Wiener process if $\sigma^2 = 1$ and $W_{t_0} = 0$, if the process W is non-standard, then $\tilde{W}_t = (W_t - W_{t_0})/\sigma$ is standard normally distributed, c.f. [Grimmett01].
- A constant c multiplied to a standard normally distributed random variable $Z_t \sim N(0, 1)$ delivers: $Z_t \cdot c \sim N(0, c^2)$.
- When dealing with transformations of the variance, such as $\sigma^2 dt$, one also obtains: $Z_t \cdot \sigma \sqrt{dt} \sim N(0, \sigma^2 dt)$.

Definition A.1.13 (Itô Process) A generalized Wiener process using an additional drift $\mu(S_t, t)$ and a multiplier $\sigma(S_t, t)$ on the standard normal Wiener process is referred to as an Itô Process (see, [Hull02]). Both variables are dependant on time t and the underlying variable, S_t ¹. When assuming the drift rate and the volatility are constant, $\mu(S_t, t) := \mu S_t$ and $\sigma(S_t, t) := \sigma S_t$, then equation (A.19) also holds,

$$dS_t = \mu(S_t, t)dt + \underbrace{\sigma(S_t, t) d\tilde{W}_t}_{= Z_t \sqrt{dt}} \quad (\text{A.18})$$

$$dS_t \stackrel{!}{=} \mu S_t dt + \sigma S_t d\tilde{W}_t, \quad (\text{A.19})$$

¹Here, the stock price S_t and the time t are the depending variables. In general, the Ito process can be applied by any variables x and y .

and when dealing with time periods of arbitrary length $\delta t = t_2 - t_1, \forall t_2 \geq t_1 \geq 0 \wedge t_1, t_2 \in \mathbb{R}_0^+$, one obtains,

$$\delta S_t = \mu(S_t, t)\delta t + \underbrace{\sigma(S_t, t) \delta \tilde{W}_t}_{= Z_t \sqrt{\delta t}}. \quad (\text{A.20})$$

More precisely (compare [Grimmett01]), the general notation of the Ito process is given by:

$$dS_t = \int_0^t \mu(S_s, s)ds + \int_0^t \sigma(S_s, s)d\tilde{W}_s, \quad (\text{A.21})$$

Definition A.1.14 (Ornstein-Uhlenbeck (OU) Process) *The Ornstein-Uhlenbeck (OU) process has the following form, c.f. [Cont04],*

$$dS_t = -\beta S_t dt + \sigma^2 d\tilde{W}_t. \quad (\text{A.22})$$

Definition A.1.15 (Cox-Ingersoll-Ross (CIR) Process) *The solution of the following stochastic differential equation is referred to as the Cox-Ingersoll-Ross (CIR) or square root process:*

$$S_{t_j} - S_{t_i} = \lambda \int_{t_i}^{t_j} (\eta - S_s) ds + \theta \int_{t_i}^{t_j} \sqrt{S_s} dW_s, \quad (\text{A.23})$$

for all $t_i > t_j \geq 0$ and $\lambda, \eta, \theta > 0$.

The CIR process is continuous and positive. The latter can easily be seen as when the value of the process S_t becomes small (close to 0), then $2\lambda\eta > \theta$. Therefore, the drift rate $\lambda(\eta - S_t)$ is larger than the amplitude of the diffusion term. The instantaneous version of the CIR process is

$$dS_t = \lambda(\eta - S_s) ds + \theta\sqrt{S_s}dW_s. \quad (\text{A.24})$$

It can easily be seen that the OU process and the CIR process are special cases of the Itô process with the parameters being $\mu(S_t, t) = -\beta S_t, \sigma(S_t, t) = \sigma^2$ and $\mu(S_t, t) = \lambda(\eta - S_s), \sigma(S_t, t) = \theta\sqrt{S_s}$, respectively.

A.2. Change of the Measure & Numeraire

A.2.1. Measure

A basic introduction into measure theory is given by [Wilmott07a].

Theorem A.2.1 (Girsanov's Theorem) *Let W_t be a Wiener process with measure \mathbb{P} and sample space Ω . If u_t is a previsible process satisfying the constraint $\mathbb{E}_{\mathbb{P}} \left[e^{\frac{1}{2} \int_0^T u_t^2} \right] < \infty$ then there exists an equivalent measure \mathbb{Q} on Ω such that*

$$W_t^* = W_t + \int_0^t u_s ds \quad (\text{A.25})$$

is a Wiener process.

Another way of writing the above is in differential form, compare [Wilmott07a],

$$dW_t^* = dW_t + u_t dt. \quad (\text{A.26})$$

A.2.2. A Numéraire

In general, a numéraire is a standard by which values are measured [Wikipediaerc]. The most present numéraires are currencies which are used to value other goods *relative* to its monetary worth. However, many other assets, e.g. gold, can be used for this purpose which is a key tool in finance, c.f. [Henry-Labordère08], p. 34.

Definition A.2.1 (Numéraire) *A numéraire is any positive continuous asset.*

A.2.3. Change of the Numéraire

The technique of changing the numéraire is a key tool in finance which simplifies calculations to a great extent, as one can constrain an asset to be the instantaneous interest rate r_t under a risk-neutral measure \mathbb{Q} , c.f. [Henry-Labordère08], p 34. Following [Wikipediaerc], let $p_{t_0,t}(r_i) = \exp \left\{ \int_{t_0}^t r_t dt \right\}$ be the price of one monetary unit which is invested at time t_0 and compounded in the money market to time $t \in [t_0, T]$. After applying the risk-neutral measure \mathbb{Q} , all money market priced assets S_t are martingales, so

$$\frac{S_t}{p_{t_0,t}} = \mathbb{E}_{\mathbb{Q}} \left[\frac{S_T}{p_{t_0,T}} \middle| \mathcal{F}_t \right] \quad \forall t \leq T. \quad (\text{A.27})$$

Supposing that $m_{t_0,t}$ is another strictly positive traded asset (and hence a martingale when priced in terms of the money market), then one can define a new probability measure \mathbb{Q}_m

$$\frac{d\mathbb{Q}_m}{d\mathbb{Q}} = \frac{p_{t_0,t_0} m_{t_0,T}}{p_{t_0,T} m_{t_0,t_0}}. \quad (\text{A.28})$$

After applying the Bayes' rule, one obtains a martingale S_t priced in terms of the new numéraire $m_{t_0,t}$

$$\begin{aligned}
\mathbb{E}_{\mathbb{Q}_N} \left[\frac{S_T}{m_{t_0,T}} \middle| \mathcal{F}_t \right] &= \mathbb{E}_{\mathbb{Q}} \left[\frac{S_T}{m_{t_0,T}} \frac{p_{t_0,t_0} m_{t_0,T}}{p_{t_0,T} m_{t_0,t_0}} \middle| \mathcal{F}_t \right] / \mathbb{E}_{\mathbb{Q}} \left[\frac{p_{t_0,t_0} m_{t_0,T}}{p_{t_0,T} m_{t_0,t_0}} \middle| \mathcal{F}_t \right] \\
&= \frac{p_{t_0,t}}{m_{t_0,t}} \mathbb{E}_{\mathbb{Q}} \left[\frac{S_T}{p_{t_0,T}} \middle| \mathcal{F}_t \right] = \frac{p_{t_0,t}}{m_{t_0,t}} \frac{S_t}{p_{t_0,t}} \\
&= \frac{S_t}{m_{t_0,t}}.
\end{aligned} \tag{A.29}$$

A.3. Characteristic Functions and Fourier Transformation

The Characteristic function is the Fourier transform analogon to the distribution of a random variable. As stated in [Cont04], many *probabilistic* properties of random variables can be obtained by computing the *analytical accessible* properties of the corresponding characteristic functions, which simplifies many calculations. Moreover, some properties can only be obtained using characteristic functions and in some cases, the distribution of a random variable does not exist, whereas the characteristic function always exists (compare [Held06]).

Definition A.3.1 (Characteristic function) *The characteristic function of the \mathbb{R}^d -valued random variable X is the function $\varphi_X : \mathbb{R}^d \rightarrow \mathbb{C}$ defined by:*

$$\varphi_X(u) = \mathbb{E} [\exp(iuX)] = \int_{\mathbb{R}^d} e^{iuX} d\mu_F \quad \forall u \in \mathbb{R}^d, \tag{A.30}$$

where $i = \sqrt{-1}$, and μ_F denotes the probability measure on the Borel sets of \mathbb{R} .

The second term in the above equation, $\int_{\mathbb{R}^d} e^{iuX} d\mu_F$, reveals the relatedness to Fourier transforms. Further properties of the characteristic function φ_X are:

- $\varphi_X(0) = 1$, $|\varphi(u)| \leq 1 \quad \forall u$,
- φ_X is uniformly continuous in \mathbb{R} ,
- φ_X is non-negative definite, which is to say that $\sum_{j,k} \phi(u_j - u_k) z_j \bar{z}_k \geq 0$ for all $t_1, \dots, t_n \in \mathbb{R}$, $z_1, \dots, z_n \in \mathbb{C}$, and \bar{z}_k denotes the complex conjugate of z_k ,
- applying complex analysis, one obtains: $\varphi_X(u) = \mathbb{E} [\exp(iuX)] = \mathbb{E} [\cos(uX)] + i\mathbb{E} [\sin(uX)]$,
- two random variables with same characteristic function are identically distributed.

- given a sequence of independent random variables $(X_i, i = 1, \dots, n)$, then the characteristic function of $S_n = X_1 + \dots + X_n$ is the *product* of the individual random variables' characteristic functions,

$$\varphi_{S_n}(u) = \prod_{i=1}^n \varphi_{X_i}(u). \quad (\text{A.31})$$

The n th moment of a random variable X on \mathbb{R} , $m_n(X) = \mathbb{E}[X^n]$, the n th absolute moments, $m_n(|X|) = \mathbb{E}[|X|^n]$ and the n th centered moment, $\mu_n(X) = \mathbb{E}[(X - \mathbb{E}[X])^n]$, can be calculated by taking the derivatives at 0 of the underlying characteristic function. The moments do not have to exist, depending on how fast the distribution μ_F decays at infinity.

Theorem A.3.1 (Moments of Character Function)

- If $\mathbb{E}[|X|^n] < \infty$ then φ_X has n continuous derivatives at $u = 0$ and

$$m_k \equiv \mathbb{E}[X^k] = \frac{1}{i^k} \frac{\partial^k \varphi_X}{\partial u^k}(0), \quad \forall k = 1, \dots, n. \quad (\text{A.32})$$

- If φ_X has $2n$ continuous derivatives at $u = 0$ then $\mathbb{E}[|X|^{2n}] < \infty$ and

$$m_k \equiv \mathbb{E}[X^k] = \frac{1}{i^k} \frac{\partial^k \varphi_X}{\partial u^k}(0), \quad \forall k = 1, \dots, 2n. \quad (\text{A.33})$$

- X possesses finite moments of all orders if $u \mapsto \varphi_X(u)$ is C^∞ at $u = 0$. Then the moments of X are related to the derivatives of φ_X by:

$$m_n \equiv \mathbb{E}[X^n] = \frac{1}{i^n} \frac{\partial^n \varphi_X}{\partial u^n}(0). \quad (\text{A.34})$$

Moments of order n can be often computed by applying *moment generating functions* which, however, are not always defined.

Definition A.3.2 (Moment Generating Function) *The moment generating function of \mathbb{R}^d -valued random variable X is the function M_X defined by*

$$M_X(u) = \mathbb{E}[\exp(uX)] \quad \forall u \in \mathbb{R}^d. \quad (\text{A.35})$$

If the moment generating function M_X is well defined, the relatness to the underlying characteristic function φ_X is given by:

$$M_X(u) = \varphi_X(-iu). \quad (\text{A.36})$$

If $M_X(u)$ is finite on an open interval which contains zero, then it can be shown that:

$$m_n = \frac{\partial^n M_X}{\partial u^n}(0). \quad (\text{A.37})$$

The following theorems allow one to obtain density and distribution functions from the characteristic functions. The first *only* refers to *continuous* random variables.

Theorem A.3.2 *If X is continuous with density function f and characteristic function φ then*

$$f(x) = \frac{1}{2\pi} \int_{-\infty}^{\infty} e^{iux} \varphi(u) du \quad (\text{A.38})$$

at every point x at which f is differentiable.

A sufficient, but not necessary condition (cf. [Grimmett01]) that a characteristic function φ be the characteristic function of a continuous variable is that

$$f(x) = \int_{-\infty}^{\infty} |\varphi(u)| du < \infty. \quad (\text{A.39})$$

The general case, i.e. X is not continuous, can be seen below, however, it is more complex.

Theorem A.3.3 (Inversion Theorem) *Let X have distribution function F and characteristic function φ . Define $\bar{F} : \mathbb{R} \rightarrow [0, 1]$ by*

$$\bar{F}(x) = \frac{1}{2} \left\{ F(x) + \lim_{y \nearrow x} F(y) \right\}. \quad (\text{A.40})$$

Then

$$\bar{F}(b) - \bar{F}(a) = \lim_{N \rightarrow \infty} \int_{-N}^N \frac{e^{-iau} - e^{-ibu}}{2\pi i u} \varphi(u) du. \quad (\text{A.41})$$

In the case of a continuous distribution one has $\bar{F}(x) = F(x)$.

Theorem A.3.4 *Random variables X and Y have the same characteristic function if and only if they have the same distribution function.*

Theorem A.3.5 (Continuity Theorem) *Suppose that F_1, F_2, \dots is a sequence of distribution functions with corresponding characteristic functions $\varphi_1, \varphi_2, \dots$*

- *If $F_n \rightarrow F$ for some distribution function F with characteristic function φ , then $\varphi_n(u) \rightarrow \varphi(u)$ for all u .*
- *Conversely, if $\varphi(u) = \lim_{n \rightarrow \infty} \varphi_n(u)$ exists and is continuous at $u = 0$, then φ is the characteristic function of some distribution function F , and $F_n \rightarrow F$.*

A.4. Heston

A.4.1. Boundary Conditions of the Heston Model

It can easily be seen that a European call option maturing at T with a strike price K has the subsequent boundary conditions, c.f. [Heston93] and [Desmettre07],

$$V(S_t, v, T) = \max(0, S_t - K), \quad (\text{A.42a})$$

$$V(0, v, t) = 0, \quad (\text{A.42b})$$

$$\frac{\partial V(\infty, v, t)}{\partial S_t} = 1, \quad (\text{A.42c})$$

$$rS_t \frac{\partial V(S_t, 0, t)}{\partial S_t} + \kappa \bar{v} \frac{\partial V(S_t, 0, t)}{\partial v} - rV(S_t, 0, t) + V(S_t, 0, t) = 0, \quad (\text{A.42d})$$

$$V(S_t, \infty, t) = S_t. \quad (\text{A.42e})$$

A.4.2. Deriving the Call Equation by Changing the Numéraire

Following [Heston93] and [Desmettre07], one can derive equation (5.20) by changing the numéraire of the subsequent formula. Note that K is a constant and $\mathbf{p}_{T,T} = 1$ is the $\delta t = 0$ discount factor as seen in Appendix A.2.3. Assuming that $(S_t/\mathbf{p}_{\mathfrak{s},t})_{t \geq 0}$ is a \mathbb{Q}_s -martingale and that $(p_{T,t}/\mathbf{p}_{\mathfrak{s},t})_{t \geq 0}$ is a \mathbb{Q}_p -martingale, one obtains

$$\begin{aligned} C_{t_0, T}(S_t, v) &= \mathbf{p}_{T,t} \cdot \mathbb{E}_{\mathbb{Q}} \left[\frac{\max(S_T - K, 0)}{\mathbf{p}_{T,T}} \right] \\ &= \mathbf{p}_{T,t} \cdot \mathbb{E}_{\mathbb{Q}} \left[\frac{S_T}{\mathbf{p}_{T,T}} 1_{\{S_T > K\}} \right] - \mathbf{p}_{T,t} K \cdot \mathbb{E}_{\mathbb{Q}} \left[\frac{1}{\mathbf{p}_{T,T}} 1_{\{S_T > K\}} \right] \\ &= S_t \cdot \mathbb{E}_{\mathbb{Q}_s} \left[\frac{S_T}{S_T} 1_{\{S_T > K\}} \right] - p_{T,t} K \cdot \mathbb{E}_{\mathbb{Q}_p} \left[\frac{1}{p_{T,T}} 1_{\{S_T > K\}} \right] \\ &= S_t \cdot \mathbb{E}_{\mathbb{Q}_s} \left[\frac{S_T}{S_T} 1_{\{S_T > K\}} \right] - p_{T,t} K \cdot \mathbb{E}_{\mathbb{Q}_p} \left[\frac{1}{p_{T,T}} 1_{\{S_T > K\}} \right] \\ &= S_t \cdot \mathbb{E}_{\mathbb{Q}_s} [1_{\{S_T > K\}}] - p_{T,t} K \cdot \mathbb{E}_{\mathbb{Q}_p} [1_{\{S_T > K\}}] \\ &= S_t \cdot P_1(S_T > K) - p_{T,t} K \cdot P_0(S_T > K) \end{aligned} \quad (\text{A.43})$$

The preceding is a general result which can be used for any equity price model (c.f. [Desmettre07]), but also, to derive the BSM-PDE which is shown e.g. in [Wilmott07a] in a similar form.

A.4.3. Deriving the Pseudo-Probability PDE

To be able to derive equation (5.21) from (5.14), the partial derivatives need to be calculated. As the variables $x = \ln(F_{t,T}/K) = \ln(S_t e^{r(T-t)}/K)$ and $\tau = T - t$ in PDE (5.21) are functions of the original variables S_t and t in (5.14), the subsequent relations are necessary

$$\begin{aligned}\frac{\partial V_{\text{op}}}{\partial t} &= \frac{\partial V_{\text{op}}}{\partial \tau} \cdot \frac{\partial \tau}{\partial t} = \frac{\partial V_{\text{op}}}{\partial \tau} \cdot (-1) \\ \frac{\partial V_{\text{op}}}{\partial S_t} &= \frac{\partial V_{\text{op}}}{\partial x} \cdot \frac{\partial x}{\partial S_t} = \frac{\partial V_{\text{op}}}{\partial x} \cdot \frac{1}{S_t}\end{aligned}$$

A.5. GARCH

A.5.1. Locally Risk-Neutral Valuation Relationship

Compare [Duan95]:

Definition A.5.1 (Locally Risk-Neutral Valuation Relationship (LRNVR)) *A pricing measure \mathbb{Q} is said to satisfy the locally risk-neutral valuation relationship (LRNVR) if measure \mathbb{Q} is mutually absolutely continuous with respect to measure \mathbb{P} , with lognormal distribution of $\frac{S_t}{S_{t-1}}|\mathcal{F}_{t-1}$ (under \mathbb{Q}),*

$$\mathbb{E}_{\mathbb{Q}} \left[\frac{S_t}{S_{t-1}} \middle| \mathcal{F}_{t-1} \right] = e^r, \quad (\text{A.44})$$

and

$$\text{Var}_{\mathbb{Q}} \left[\ln \left(\frac{S_t}{S_{t-1}} \right) \middle| \mathcal{F}_{t-1} \right] = \text{Var}_{\mathbb{P}} \left[\ln \left(\frac{S_t}{S_{t-1}} \right) \middle| \mathcal{F}_{t-1} \right] \quad (\text{A.45})$$

almost surely with respect to measure \mathbb{P} .

A.5.2. Derivation of the Correlation

$$\text{Corr}[v_{t+1}, \ln(S_t)|\mathcal{F}_{t-1}] = \frac{\text{Cov}[v_{t+1}, \ln(S_t)|\mathcal{F}_{t-1}]}{\sqrt{\text{Var}[v_{t+1}|\mathcal{F}_{t-1}] \text{Var}[\ln(S_t)|\mathcal{F}_{t-1}]}} \quad (\text{A.46})$$

with the $\text{Cov}[v_{t+1}, \ln(S_t)|\mathcal{F}_{t-1}]$ being

$$\text{Cov}[v_{t+1}, \ln(S_t)|\mathcal{F}_{t-1}] = \mathbb{E}[v_{t+1} \cdot \ln(S_T)|\mathcal{F}_{t-1}] - \mathbb{E}[\delta v_{t+1}|\mathcal{F}_{t-1}] \cdot \mathbb{E}[\ln(S_T)|\mathcal{F}_{t-1}] \quad (\text{A.47})$$

As can be seen in Section 6.4 the expected value is

$$\begin{aligned} \mathbb{E}[v_{t+1}|\mathcal{F}_{t-1}] &= \tilde{\alpha}_0 + \tilde{\alpha}_1 \left(\underbrace{\mathbb{E}[Z_t^2|\mathcal{F}_{t-1}]}_{=\text{Var}[Z_t|\mathcal{F}_{t-1}]=1} - 2\tilde{\gamma}_1\sqrt{v_t} \cdot \underbrace{\mathbb{E}[Z_t|\mathcal{F}_{t-1}]}_{=0} + \tilde{\gamma}_1^2 v_t \right) \\ &= \tilde{\alpha}_0 + \tilde{\alpha}_1 (1 + \tilde{\gamma}_1^2 v_t) \end{aligned} \quad (\text{A.48})$$

and

$$\begin{aligned} \text{Var}[v_{t+1}|\mathcal{F}_{t-1}] &= \tilde{\alpha}_1^2 \left(\underbrace{\text{Var}[Z_t^2|\mathcal{F}_{t-1}]}_{=2, \text{ with } Z_t^2 \sim \chi^2(k=1)} - 4\tilde{\gamma}_1^2 v_t \underbrace{\text{Var}[Z_t|\mathcal{F}_{t-1}]}_{=1} \right) \\ &= 2\tilde{\alpha}_1^2 (1 - 2\tilde{\gamma}_1^2 v_t) \end{aligned} \quad (\text{A.49})$$

Now,

$$\mathbb{E}[\ln(S_t)|\mathcal{F}_{t-1}] = \ln(S_{t-1}) + r + \lambda v_t + \sqrt{v_t} \underbrace{\mathbb{E}[Z_t|\mathcal{F}_{t-1}]}_{=0} \quad (\text{A.50})$$

and

$$\text{Var}[\ln(S_t)|\mathcal{F}_{t-1}] = (\sqrt{v_t})^2 \underbrace{\text{Var}[Z_t|\mathcal{F}_{t-1}]}_{=1} = v_t \quad (\text{A.51})$$

and also,

$$\begin{aligned} \mathbb{E}[v_{t+1} \cdot \ln(S_t)|\mathcal{F}_{t-1}] &= \mathbb{E} \left[(\tilde{\alpha}_0 + \tilde{\alpha}_1 (Z_t^2 - 2\tilde{\gamma}_1\sqrt{v_t}Z_t + \tilde{\gamma}_1^2 v_t)) \cdot \right. \\ &\quad \left. (\ln(S_{t-1}) + r + \lambda v_t + \sqrt{v_t}Z_t) \mid \mathcal{F}_{t-1} \right] \\ &= \tilde{\alpha}_0 (\ln(S_{t-1}) + r + \lambda v_t + \sqrt{v_t} \mathbb{E}[Z_t|\mathcal{F}_{t-1}]) + \\ &\quad \tilde{\alpha}_1 \left((\ln(S_{t-1}) + r + \lambda v_t) \mathbb{E}[Z_t^2|\mathcal{F}_{t-1}] - \right. \\ &\quad \left. 2\tilde{\gamma}_1\sqrt{v_t} (\ln(S_{t-1}) + r + \lambda v_t) \mathbb{E}[Z_t|\mathcal{F}_{t-1}] + \right. \\ &\quad \left. \tilde{\gamma}_1^2 v_t (\ln(S_{t-1}) + r + \lambda v_t) \right) + \tilde{\alpha}_1 \left(\mathbb{E}[Z_t^3|\mathcal{F}_{t-1}] \sqrt{v_t} - \right. \\ &\quad \left. 2\tilde{\gamma}_1 v_t \mathbb{E}[Z_t^2|\mathcal{F}_{t-1}] + \tilde{\gamma}_1^2 v_t \sqrt{v_t} \mathbb{E}[Z_t|\mathcal{F}_{t-1}] \right) \\ &\stackrel{3}{=} \tilde{\alpha}_0 (\ln(S_{t-1}) + r + \lambda v_t) + \\ &\quad \tilde{\alpha}_1 (\ln(S_{t-1}) + r + \lambda v_t) (1 + \tilde{\gamma}_1^2 v_t) + \tilde{\alpha}_1 (-2\tilde{\gamma}_1 v_t) \end{aligned} \quad (\text{A.52})$$

²As Z_t is standard normally distributed, $Z_t \sim N(0, 1)$, the square of Z_t is χ^2 -distributed, $Z_t^2 \sim \chi^2(k=1)$, with the expected value being $\mathbb{E}[Z_t^2] = k = 1$ and the variance $\text{Var}[Z_t^2] = 2k = 2$. Hence, the variance of $Z_t^2 \delta t$ is

$$\text{Var}(Z_t^2 \delta t) = (\delta t)^2 \text{Var}(Z_t^2) = 2(\delta t)^2.$$

Hence,

$$\begin{aligned}
\text{Cov}[v_{t+1}, \ln(S_t) | \mathcal{F}_{t-1}] &= \tilde{\alpha}_0 (\ln(S_{t-1}) + r + \lambda v_t) + \\
&\quad \tilde{\alpha}_1 (\ln(S_{t-1}) + r + \lambda v_t) (1 + \tilde{\gamma}_1^2 v_t) + \tilde{\alpha}_1 (-2\tilde{\gamma}_1 v_t) - \\
&\quad (\tilde{\alpha}_0 + \tilde{\alpha}_1 (1 + \tilde{\gamma}_1^2 v_t)) (\ln(S_{t-1}) + r + \lambda v_t) \\
&= \tilde{\alpha}_1 (-2\tilde{\gamma}_1 v_t)
\end{aligned} \tag{A.53}$$

and finally,

$$\begin{aligned}
\text{Corr}[v_{t+1}, \ln(S_t) | \mathcal{F}_{t-1}] &= \frac{\tilde{\alpha}_1 (-2\tilde{\gamma}_1 v_t)}{\sqrt{v_t} \sqrt{2\tilde{\alpha}_1^2 (1 - 2\tilde{\gamma}_1^2 v_t)}} = \frac{-\tilde{\gamma}_1 \sqrt{2v_t}}{\sqrt{1 - 2\tilde{\gamma}_1^2 v_t}} \\
&= \frac{-\text{sign}(\tilde{\gamma}_1) \sqrt{2\tilde{\gamma}_1^2 v_t}}{\sqrt{1 + 2\tilde{\gamma}_1^2 v_t}}.
\end{aligned} \tag{A.54}$$

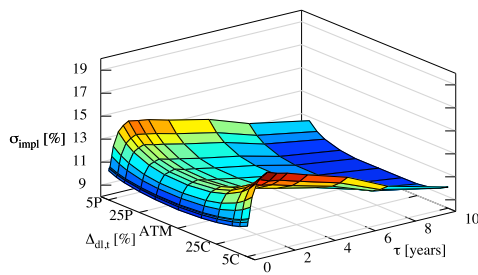
³The third central moment of the normal distribution is 0

B. Volatility Surfaces

All volatility surfaces and deviation plots of the examined models are presented in this unit with two exceptions. One is the BSM model where only the deviation plots are given as the volatility surfaces in this framework are plains which do not differ much in value, c.f. Section 4.3 and 7.2.1. The other is the calibrated Heston-Nandi approach as it could not be implemented properly, c.f. Section 7.2.5.

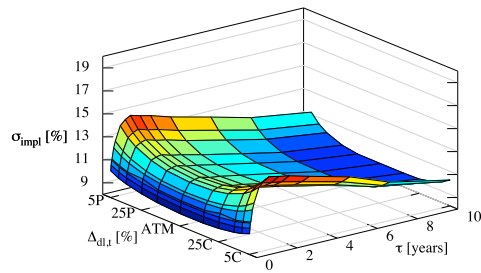
B.1. Market Volatility Surfaces

Market Volatility Surface: EUR-USD, $t_0 = 23/09/2009$



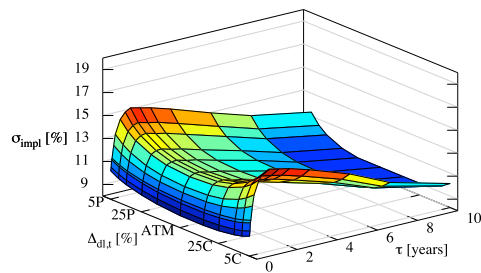
Implied volatility σ_{impl} denoted in %, depending on the driftless delta $\Delta_{\text{dl},t}$ in % of the OTM option and maturity τ in years, c.f. Section 4.2.2.

Market Volatility Surface: EUR-USD, $t_0 = 07/10/2009$



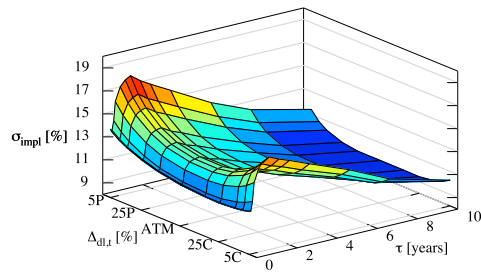
Implied volatility σ_{impl} denoted in %, depending on the driftless delta $\Delta_{\text{dl},t}$ in % of the OTM option and maturity τ in years, c.f. Section 4.2.2.

Market Volatility Surface: EUR-USD, $t_0 = 21/10/2009$



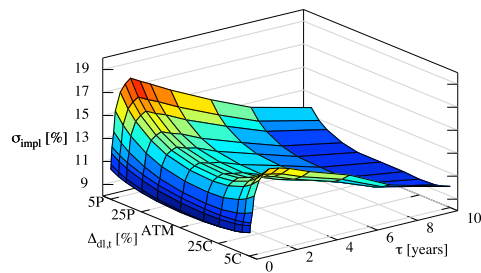
Implied volatility σ_{impl} denoted in %, depending on the driftless delta $\Delta_{\text{dl},t}$ in % of the OTM option and maturity τ in years, c.f. Section 4.2.2.

Market Volatility Surface: EUR-USD, $t_0 = 04/11/2009$



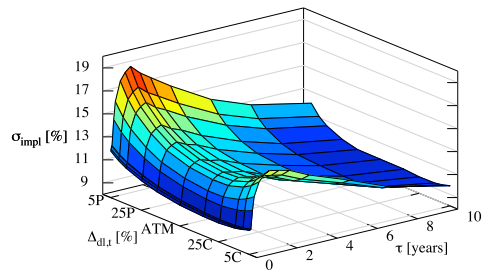
Implied volatility σ_{impl} denoted in %, depending on the driftless delta $\Delta_{\text{dl},t}$ in % of the OTM option and maturity τ in years, c.f. Section 4.2.2.

Market Volatility Surface: EUR-USD, $t_0 = 18/11/2009$



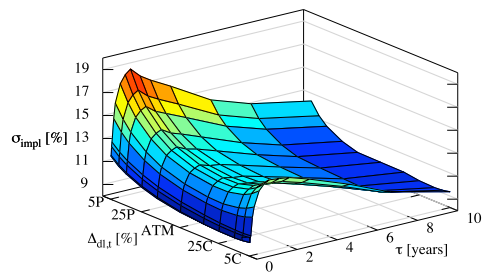
Implied volatility σ_{impl} denoted in %, depending on the driftless delta $\Delta_{\text{dl},t}$ in % of the OTM option and maturity τ in years, c.f. Section 4.2.2.

Market Volatility Surface: EUR-USD, $t_0 = 02/12/2009$



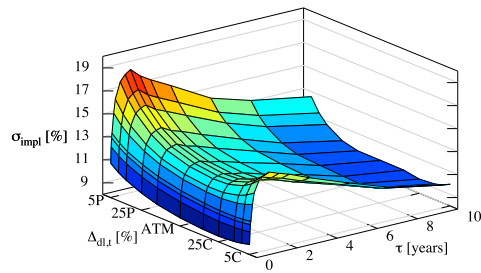
Implied volatility σ_{impl} denoted in %, depending on the driftless delta $\Delta_{\text{dl},t}$ in % of the OTM option and maturity τ in years, c.f. Section 4.2.2.

Market Volatility Surface: EUR-USD, $t_0 = 16/12/2009$



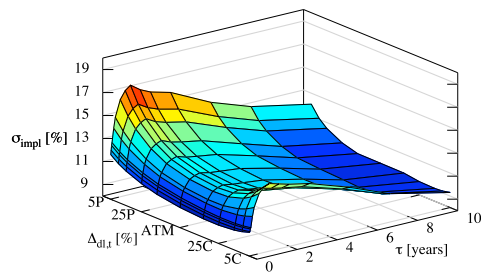
Implied volatility σ_{impl} denoted in %, depending on the driftless delta $\Delta_{\text{dl},t}$ in % of the OTM option and maturity τ in years, c.f. Section 4.2.2.

Market Volatility Surface: EUR-USD, $t_0 = 30/12/2009$



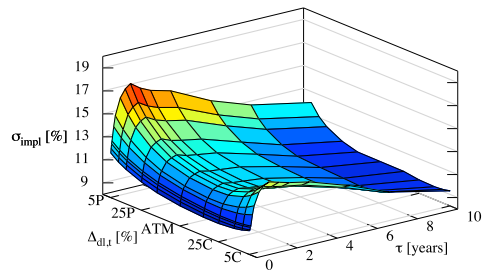
Implied volatility σ_{impl} denoted in %, depending on the driftless delta $\Delta_{\text{dl},t}$ in % of the OTM option and maturity τ in years, c.f. Section 4.2.2.

Market Volatility Surface: EUR-USD, $t_0 = 06/01/2010$



Implied volatility σ_{impl} denoted in %, depending on the driftless delta $\Delta_{\text{dl},t}$ in % of the OTM option and maturity τ in years, c.f. Section 4.2.2.

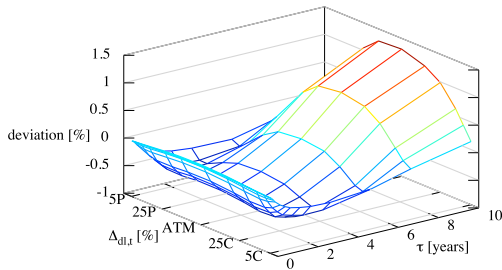
Market Volatility Surface: EUR-USD, $t_0 = 20/01/2010$



Implied volatility σ_{impl} denoted in %, depending on the driftless delta $\Delta_{\text{dl},t}$ in % of the OTM option and maturity τ in years, c.f. Section 4.2.2.

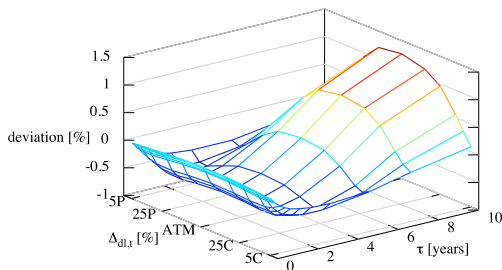
B.2. Deviations of the Calibrated BSM Call Prices to the Market Call Prices

Deviation of BSM to Market Call Prices: EUR-USD, $t_0 = 23/09/2009$



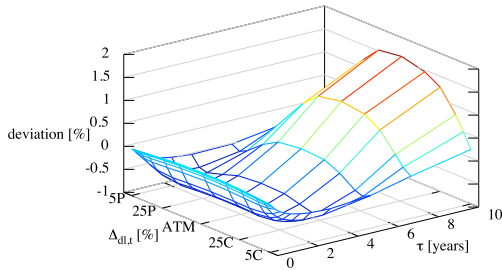
Deviation of BSM call prices to the market call prices relative to the stock price in percent, i.e. $\frac{C_{model} - C_{market}}{S_t} [\%]$, depending on the driftless delta $\Delta_{dl,t}$ in % of the OTM option and maturity τ in years, c.f. Section 4.2.2.

Deviation of BSM to Market Call Prices: EUR-USD, $t_0 = 07/10/2009$



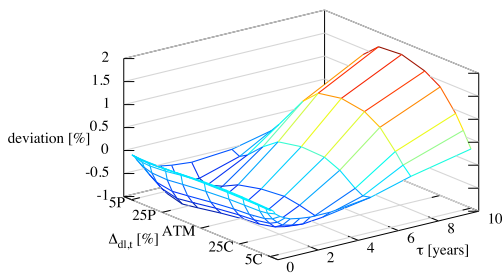
Deviation of BSM call prices to the market call prices relative to the stock price in percent, i.e. $\frac{C_{model} - C_{market}}{S_t} [\%]$, depending on the driftless delta $\Delta_{dl,t}$ in % of the OTM option and maturity τ in years, c.f. Section 4.2.2.

Deviation of BSM to Market Call Prices: EUR-USD, $t_0 = 21/10/2009$



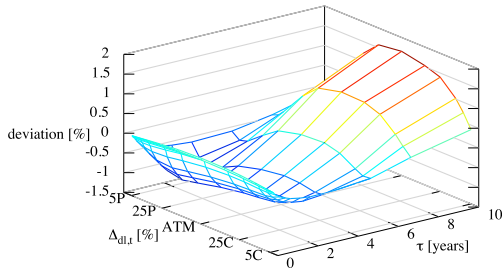
Deviation of BSM call prices to the market call prices relative to the stock price in percent, i.e. $\frac{C_{model} - C_{market}}{S_t} [\%]$, depending on the driftless delta $\Delta_{dl,t}$ in % of the OTM option and maturity τ in years, c.f. Section 4.2.2.

Deviation of BSM to Market Call Prices: EUR-USD, $t_0 = 04/11/2009$



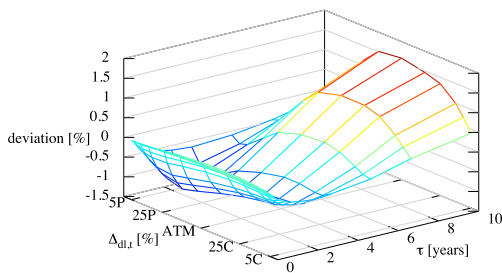
Deviation of BSM call prices to the market call prices relative to the stock price in percent, i.e. $\frac{C_{model} - C_{market}}{S_t} [\%]$, depending on the driftless delta $\Delta_{dl,t}$ in % of the OTM option and maturity τ in years, c.f. Section 4.2.2.

Deviation of BSM to Market Call Prices: EUR-USD, $t_0 = 18/11/2009$



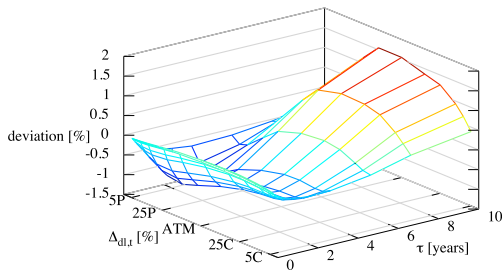
Deviation of BSM call prices to the market call prices relative to the stock price in percent, i.e. $\frac{C_{model} - C_{market}}{S_t} [\%]$, depending on the driftless delta $\Delta_{dl,t}$ in % of the OTM option and maturity τ in years, c.f. Section 4.2.2.

Deviation of BSM to Market Call Prices: EUR-USD, $t_0 = 02/12/2009$



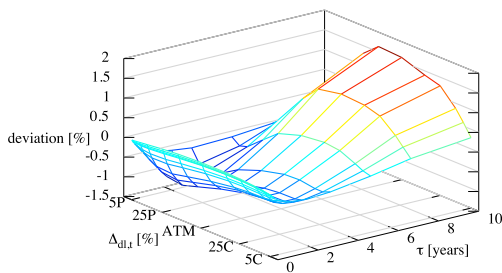
Deviation of BSM call prices to the market call prices relative to the stock price in percent, i.e. $\frac{C_{model} - C_{market}}{S_t} [\%]$, depending on the driftless delta $\Delta_{dl,t}$ in % of the OTM option and maturity τ in years, c.f. Section 4.2.2.

Deviation of BSM to Market Call Prices: EUR-USD, $t_0 = 16/12/2009$



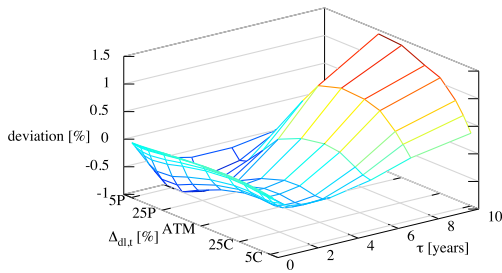
Deviation of BSM call prices to the market call prices relative to the stock price in percent, i.e. $\frac{C_{model} - C_{market}}{S_t} [\%]$, depending on the driftless delta $\Delta_{dl,t}$ in % of the OTM option and maturity τ in years, c.f. Section 4.2.2.

Deviation of BSM to Market Call Prices: EUR-USD, $t_0 = 30/12/2009$



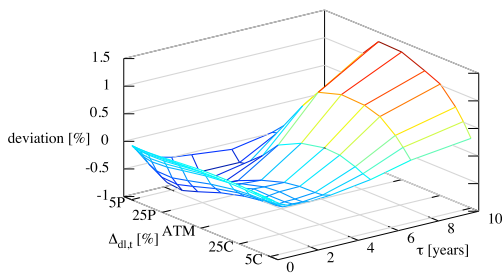
Deviation of BSM call prices to the market call prices relative to the stock price in percent, i.e. $\frac{C_{model} - C_{market}}{S_t} [\%]$, depending on the driftless delta $\Delta_{dl,t}$ in % of the OTM option and maturity τ in years, c.f. Section 4.2.2.

Deviation of BSM to Market Call Prices: EUR-USD, $t_0 = 06/01/2010$



Deviation of BSM call prices to the market call prices relative to the stock price in percent, i.e. $\frac{C_{model} - C_{market}}{S_t}$ [%], depending on the driftless delta $\Delta_{dl,t}$ in % of the OTM option and maturity τ in years, c.f. Section 4.2.2.

Deviation of BSM to Market Call Prices: EUR-USD, $t_0 = 20/01/2010$

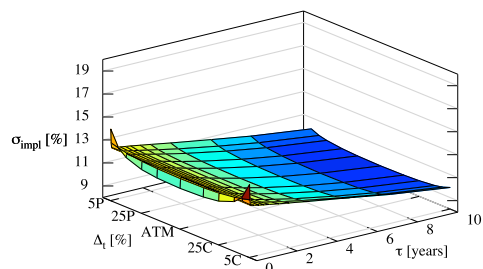


Deviation of BSM call prices to the market call prices relative to the stock price in percent, i.e. $\frac{C_{model} - C_{market}}{S_t}$ [%], depending on the driftless delta $\Delta_{dl,t}$ in % of the OTM option and maturity τ in years, c.f. Section 4.2.2.

B.3. Grafical Results of the Calibrated Heston Model

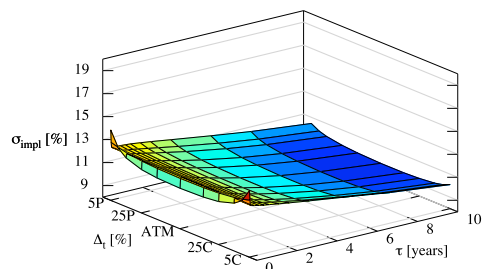
B.3.1. Calibrated Heston Volatility Surfaces

Volatility Surface of Calibrated Heston Model for EUR-USD, $t_0 = 23/09/2009$



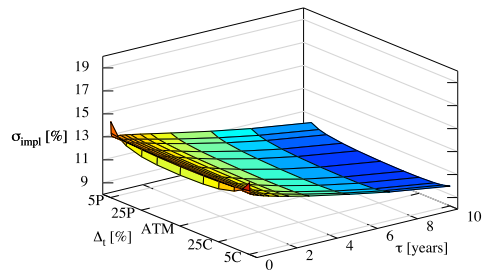
Implied volatility σ_{impl} denoted in % depending on the driftless delta $\Delta_{\text{dl},t}$ in % of the OTM option and maturity τ in years, c.f. Section 4.2.2.

Volatility Surface of Calibrated Heston Model for EUR-USD, $t_0 = 07/10/2009$



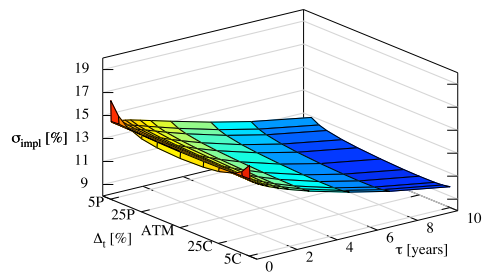
Implied volatility σ_{impl} denoted in % depending on the driftless delta $\Delta_{\text{dl},t}$ in % of the OTM option and maturity τ in years, c.f. Section 4.2.2.

Volatility Surface of Calibrated Heston Model for EUR-USD, $t_0 = 21/10/2009$



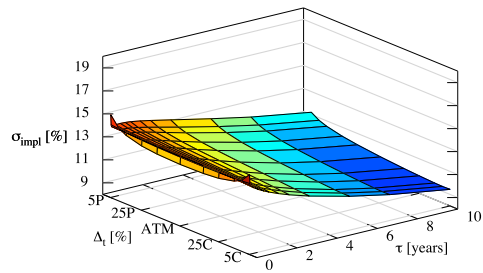
Implied volatility σ_{impl} denoted in % depending on the driftless delta $\Delta_{\text{dl},t}$ in % of the OTM option and maturity τ in years, c.f. Section 4.2.2.

Volatility Surface of Calibrated Heston Model for EUR-USD, $t_0 = 04/11/2009$



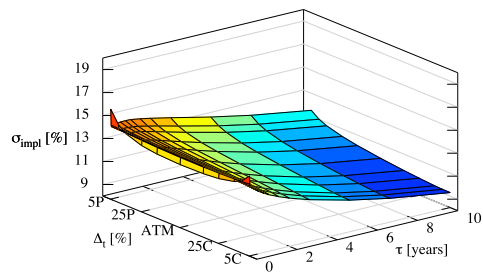
Implied volatility σ_{impl} denoted in % depending on the driftless delta $\Delta_{\text{dl},t}$ in % of the OTM option and maturity τ in years, c.f. Section 4.2.2.

Volatility Surface of Calibrated Heston Model for EUR-USD, $t_0 = 18/11/2009$



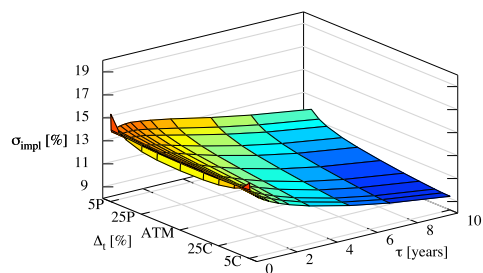
Implied volatility σ_{impl} denoted in % depending on the driftless delta $\Delta_{\text{dl},t}$ in % of the OTM option and maturity τ in years, c.f. Section 4.2.2.

Volatility Surface of Calibrated Heston Model for EUR-USD, $t_0 = 02/12/2009$



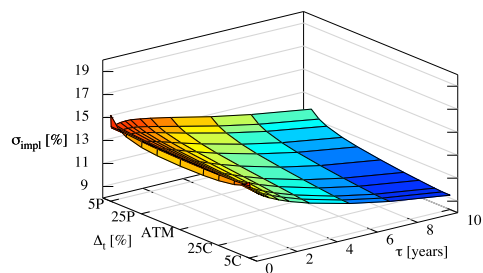
Implied volatility σ_{impl} denoted in % depending on the driftless delta $\Delta_{\text{dl},t}$ in % of the OTM option and maturity τ in years, c.f. Section 4.2.2.

Volatility Surface of Calibrated Heston Model for EUR-USD, $t_0 = 16/12/2009$



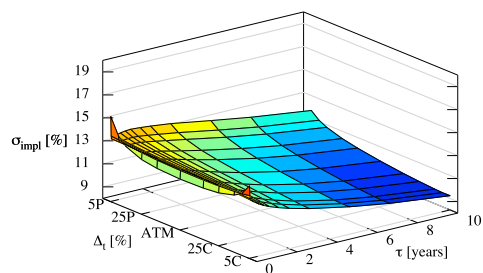
Implied volatility σ_{impl} denoted in % depending on the driftless delta $\Delta_{\text{dl},t}$ in % of the OTM option and maturity τ in years, c.f. Section 4.2.2.

Volatility Surface of Calibrated Heston Model for EUR-USD, $t_0 = 30/12/2009$



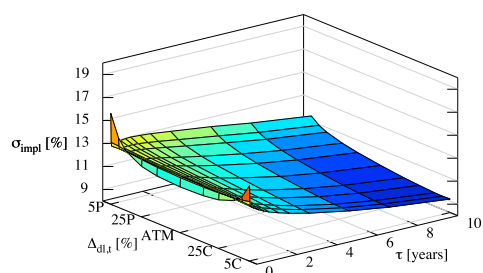
Implied volatility σ_{impl} denoted in % depending on the driftless delta $\Delta_{\text{dl},t}$ in % of the OTM option and maturity τ in years, c.f. Section 4.2.2.

Volatility Surface of Calibrated Heston Model for EUR-USD, $t_0 = 06/01/2010$



Implied volatility σ_{impl} denoted in % depending on the driftless delta $\Delta_{\text{dl},t}$ in % of the OTM option and maturity τ in years, c.f. Section 4.2.2.

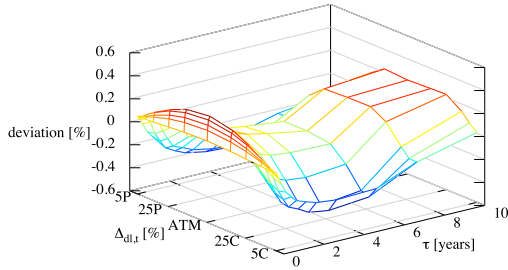
Volatility Surface of Calibrated Heston Model for EUR-USD, $t_0 = 20/01/2010$



Implied volatility σ_{impl} denoted in % depending on the driftless delta $\Delta_{\text{dl},t}$ in % of the OTM option and maturity τ in years, c.f. Section 4.2.2.

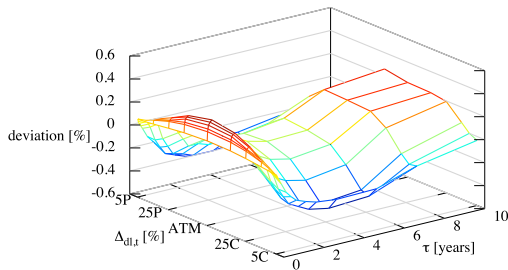
B.3.2. Deviations of the Heston Call Prices

Deviation of Heston to Market Call Prices: EUR-USD, $t_0 = 23/09/2009$



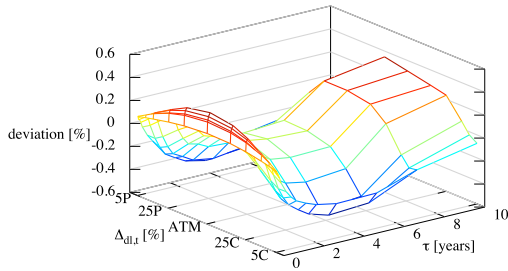
Deviation of Heston call prices to the market call prices relative to the stock price in percent, i.e. $\frac{C_{model} - C_{market}}{S_t}$ [%], depending on the driftless delta $\Delta_{dl,t}$ in % of the OTM option and maturity τ in years, c.f. Section 4.2.2.

Deviation of Heston to Market Call Prices: EUR-USD, $t_0 = 07/10/2009$



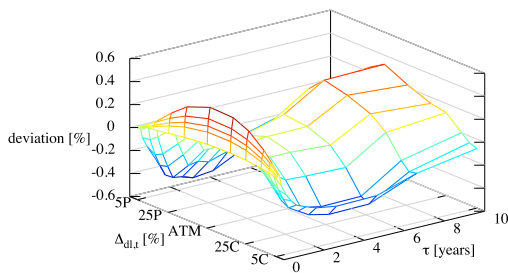
Deviation of Heston call prices to the market call prices relative to the stock price in percent, i.e. $\frac{C_{mdel} - C_{market}}{S_t}$ [%], depending on the driftless delta $\Delta_{dl,t}$ in % of the OTM option and maturity τ in years, c.f. Section 4.2.2.

Deviation of Heston to Market Call Prices: EUR-USD, $t_0 = 21/10/2009$



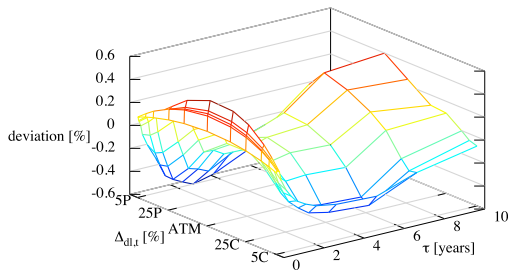
Deviation of Heston call prices to the market call prices relative to the stock price in percent, i.e. $\frac{C_{model} - C_{market}}{S_t} [\%]$, depending on the driftless delta $\Delta_{dl,t}$ in % of the OTM option and maturity τ in years, c.f. Section 4.2.2.

Deviation of Heston to Market Call Prices: EUR-USD, $t_0 = 04/11/2009$



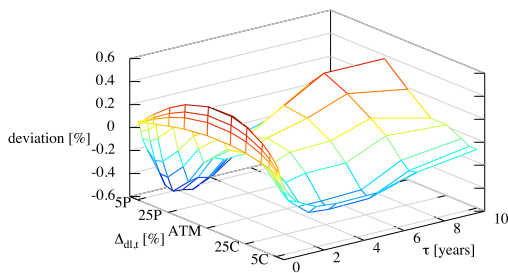
Deviation of Heston call prices to the market call prices relative to the stock price in percent, i.e. $\frac{C_{model} - C_{market}}{S_t} [\%]$, depending on the driftless delta $\Delta_{dl,t}$ in % of the OTM option and maturity τ in years, c.f. Section 4.2.2.

Deviation of Heston to Market Call Prices: EUR-USD, $t_0 = 18/11/2009$



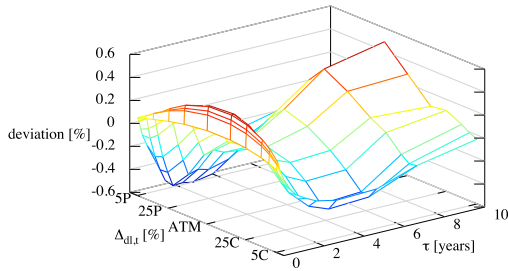
Deviation of Heston call prices to the market call prices relative to the stock price in percent, i.e. $\frac{C_{model} - C_{market}}{S_t} [\%]$, depending on the driftless delta $\Delta_{dl,t}$ in % of the OTM option and maturity τ in years, c.f. Section 4.2.2.

Deviation of Heston to Market Call Prices: EUR-USD, $t_0 = 02/12/2009$



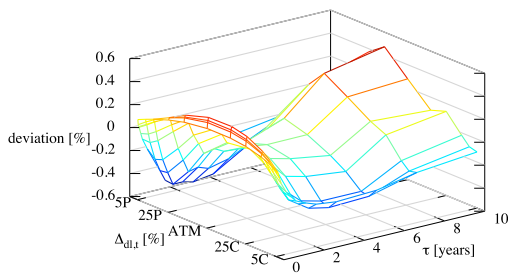
Deviation of Heston call prices to the market call prices relative to the stock price in percent, i.e. $\frac{C_{model} - C_{market}}{S_t} [\%]$, depending on the driftless delta $\Delta_{dl,t}$ in % of the OTM option and maturity τ in years, c.f. Section 4.2.2.

Deviation of Heston to Market Call Prices: EUR-USD, $t_0 = 16/12/2009$



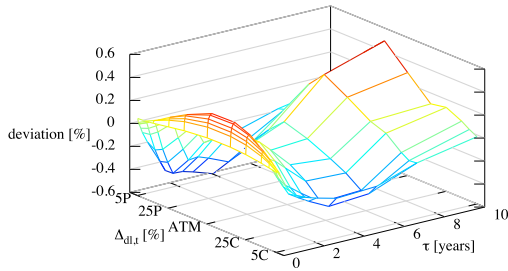
Deviation of Heston call prices to the market call prices relative to the stock price in percent, i.e. $\frac{C_{model} - C_{market}}{S_t}$ [%], depending on the driftless delta $\Delta_{dl,t}$ in % of the OTM option and maturity τ in years, c.f. Section 4.2.2.

Deviation of Heston to Market Call Prices: EUR-USD, $t_0 = 30/12/2009$



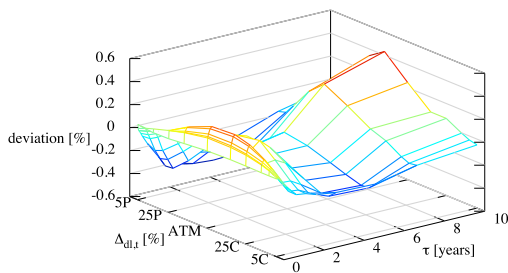
Deviation of Heston call prices to the market call prices relative to the stock price in percent, i.e. $\frac{C_{model} - C_{market}}{S_t}$ [%], depending on the driftless delta $\Delta_{dl,t}$ in % of the OTM option and maturity τ in years, c.f. Section 4.2.2.

Deviation of Heston to Market Call Prices: EUR-USD, $t_0 = 06/01/2010$



Deviation of Heston call prices to the market call prices relative to the stock price in percent, i.e. $\frac{C_{model} - C_{market}}{S_t} [\%]$, depending on the driftless delta $\Delta_{dl,t}$ in % of the OTM option and maturity τ in years, c.f. Section 4.2.2.

Deviation of Heston to Market Call Prices: EUR-USD, $t_0 = 20/01/2010$

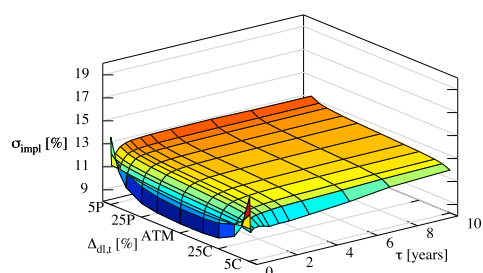


Deviation of Heston call prices to the market call prices relative to the stock price in percent, i.e. $\frac{C_{model} - C_{market}}{S_t} [\%]$, depending on the driftless delta $\Delta_{dl,t}$ in % of the OTM option and maturity τ in years, c.f. Section 4.2.2.

B.4. Grafical Results of the Heston-Nandi Model with ML Estimated Parameters

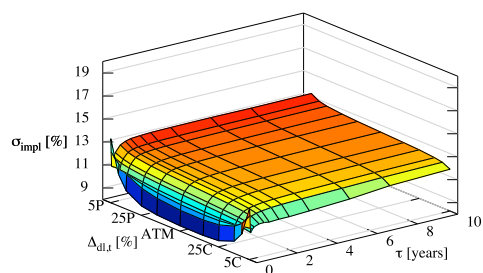
B.4.1. Heston-Nandi Volatility Surfaces with ML Estimated Parameters

Heston-Nandi Volatility Surfaces with ML Estimated Parameters for EUR-USD, $t_0 = 23/09/2009$



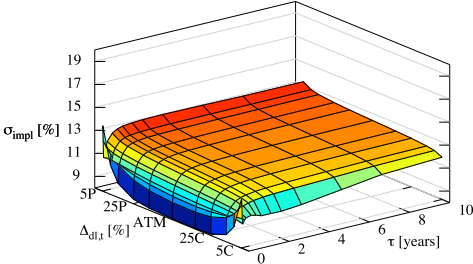
Implied volatility σ_{impl} denoted in % depending on the driftless delta $\Delta_{\text{dl},t}$ in % of the OTM option and maturity τ in years, c.f. Section 4.2.2.

Heston-Nandi Volatility Surfaces with ML Estimated Parameters for EUR-USD, $t_0 = 07/10/2009$



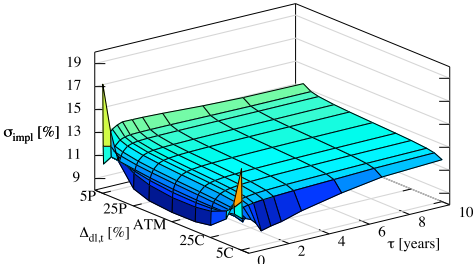
Implied volatility σ_{impl} denoted in % depending on the driftless delta $\Delta_{\text{dl},t}$ in % of the OTM option and maturity τ in years, c.f. Section 4.2.2.

Heston-Nandi Volatility Surfaces with ML Estimated Parameters for EUR-USD, $t_0 = 21/10/2009$



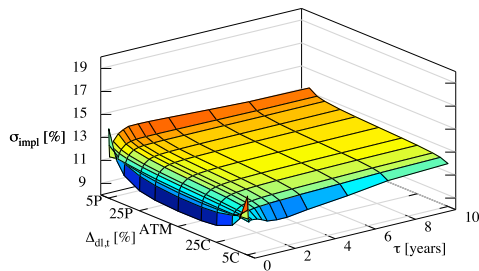
Implied volatility σ_{impl} denoted in % depending on the driftless delta $\Delta_{\text{dl},t}$ in % of the OTM option and maturity τ in years, c.f. Section 4.2.2.

Heston-Nandi Volatility Surfaces with ML Estimated Parameters for EUR-USD, $t_0 = 04/11/2009$



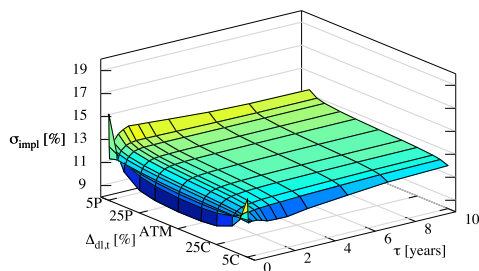
Implied volatility σ_{impl} denoted in % depending on the driftless delta $\Delta_{\text{dl},t}$ in % of the OTM option and maturity τ in years, c.f. Section 4.2.2.

Heston-Nandi Volatility Surfaces with ML Estimated Parameters for EUR-USD, $t_0 = 18/11/2009$



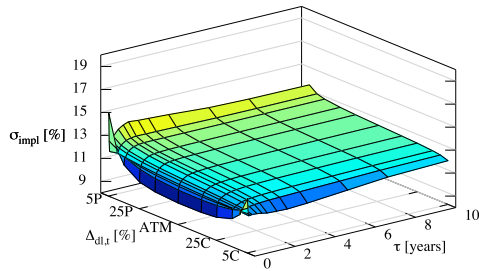
Implied volatility σ_{impl} denoted in % depending on the driftless delta $\Delta_{\text{dl},t}$ in % of the OTM option and maturity τ in years, c.f. Section 4.2.2.

Heston-Nandi Volatility Surfaces with ML Estimated Parameters for EUR-USD, $t_0 = 02/12/2009$



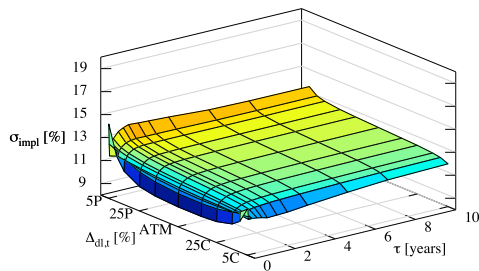
Implied volatility σ_{impl} denoted in % depending on the driftless delta $\Delta_{\text{dl},t}$ in % of the OTM option and maturity τ in years, c.f. Section 4.2.2.

Heston-Nandi Volatility Surfaces with ML Estimated Parameters for EUR-USD, $t_0 = 16/12/2009$



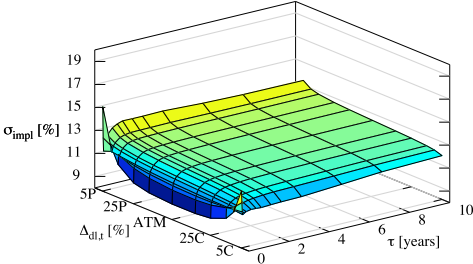
Implied volatility σ_{impl} denoted in % depending on the driftless delta $\Delta_{\text{dl},t}$ in % of the OTM option and maturity τ in years, c.f. Section 4.2.2.

Heston-Nandi Volatility Surfaces with ML Estimated Parameters for EUR-USD, $t_0 = 30/12/2009$



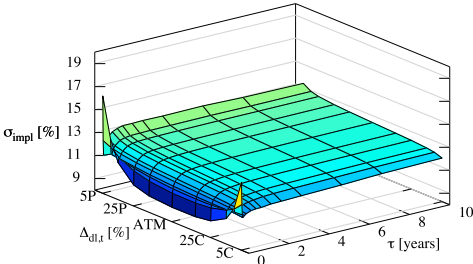
Implied volatility σ_{impl} denoted in % depending on the driftless delta $\Delta_{\text{dl},t}$ in % of the OTM option and maturity τ in years, c.f. Section 4.2.2.

Heston-Nandi Volatility Surfaces with ML Estimated Parameters for EUR-USD, $t_0 = 06/01/2010$



Implied volatility σ_{impl} denoted in % depending on the driftless delta $\Delta_{\text{dl},t}$ in % of the OTM option and maturity τ in years, c.f. Section 4.2.2.

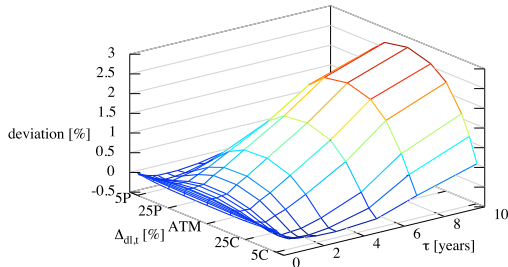
Heston-Nandi Volatility Surfaces with ML Estimated Parameters for EUR-USD, $t_0 = 20/01/2010$



Implied volatility σ_{impl} denoted in % depending on the driftless delta $\Delta_{\text{dl},t}$ in % of the OTM option and maturity τ in years, c.f. Section 4.2.2.

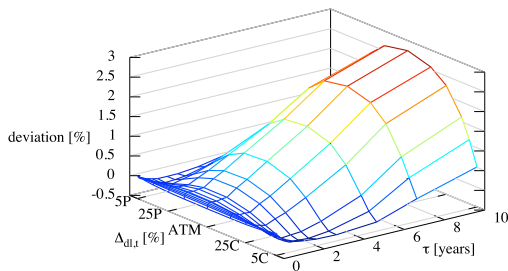
B.4.2. Deviations of the Heston-Nandi Call Prices with ML Estimated Parameters

Deviation of Heston-Nandi Call Prices with ML Estimated Parameters to Market Call Prices: EUR-USD, $t_0 = 23/09/2009$



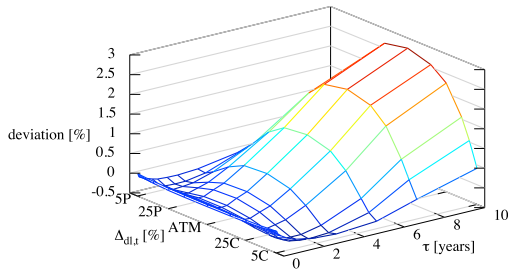
Deviation of Heston-Nandi Call Prices with ML Estimated Parameters call prices to the market call prices relative to the stock price in percent, i.e. $\frac{C_{model} - C_{market}}{S_t} [\%]$, depending on the driftless delta $\Delta_{dl,t}$ in % of the OTM option and maturity τ in years, c.f. Section 4.2.2.

Deviation of Heston-Nandi Call Prices with ML Estimated Parameters to Market Call Prices: EUR-USD, $t_0 = 07/10/2009$



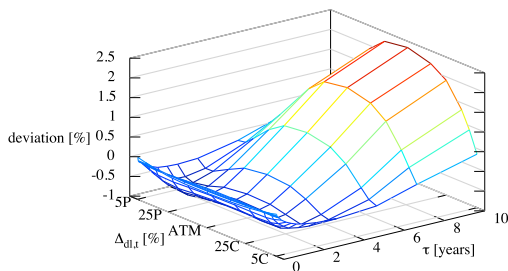
Deviation of Heston-Nandi Call Prices with ML Estimated Parameters call prices to the market call prices relative to the stock price in percent, i.e. $\frac{C_{mdel} - C_{market}}{S_t} [\%]$, depending on the driftless delta $\Delta_{dl,t}$ in % of the OTM option and maturity τ in years, c.f. Section 4.2.2.

Deviation of Heston-Nandi Call Prices with ML Estimated Parameters to Market Call Prices: EUR-USD, $t_0 = 21/10/2009$



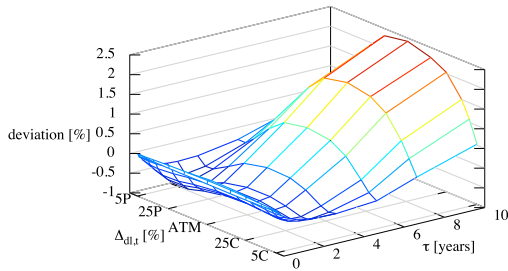
Deviation of Heston-Nandi Call Prices with ML Estimated Parameters call prices to the market call prices relative to the stock price in percent, i.e. $\frac{C_{model} - C_{market}}{S_t} [\%]$, depending on the driftless delta $\Delta_{dl,t}$ in % of the OTM option and maturity τ in years, c.f. Section 4.2.2.

Deviation of Heston-Nandi Call Prices with ML Estimated Parameters to Market Call Prices: EUR-USD, $t_0 = 04/11/2009$



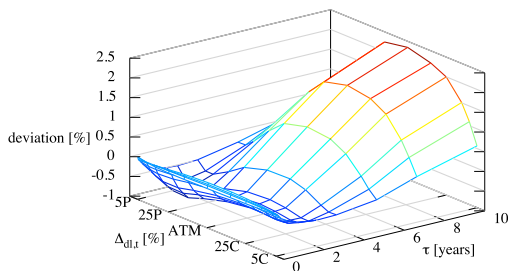
Deviation of Heston-Nandi Call Prices with ML Estimated Parameters call prices to the market call prices relative to the stock price in percent, i.e. $\frac{C_{model} - C_{market}}{S_t} [\%]$, depending on the driftless delta $\Delta_{dl,t}$ in % of the OTM option and maturity τ in years, c.f. Section 4.2.2.

Deviation of Heston-Nandi Call Prices with ML Estimated Parameters to Market Call Prices: EUR-USD, $t_0 = 18/11/2009$



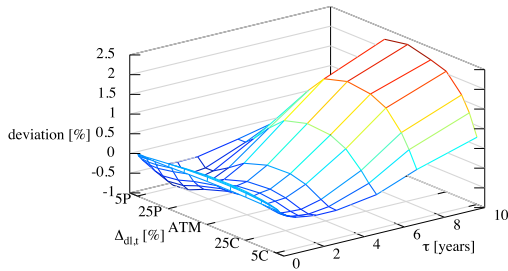
Deviation of Heston-Nandi Call Prices with ML Estimated Parameters call prices to the market call prices relative to the stock price in percent, i.e. $\frac{C_{model}-C_{market}}{S_t} [\%]$, depending on the driftless delta $\Delta_{dl,t}$ in % of the OTM option and maturity τ in years, c.f. Section 4.2.2.

Deviation of Heston-Nandi Call Prices with ML Estimated Parameters to Market Call Prices: EUR-USD, $t_0 = 02/12/2009$



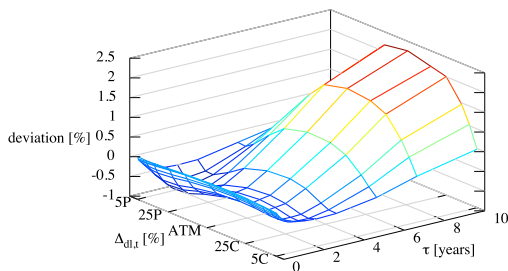
Deviation of Heston-Nandi Call Prices with ML Estimated Parameters call prices to the market call prices relative to the stock price in percent, i.e. $\frac{C_{model}-C_{market}}{S_t} [\%]$, depending on the driftless delta $\Delta_{dl,t}$ in % of the OTM option and maturity τ in years, c.f. Section 4.2.2.

Deviation of Heston-Nandi Call Prices with ML Estimated Parameters to Market Call Prices: EUR-USD, $t_0 = 16/12/2009$



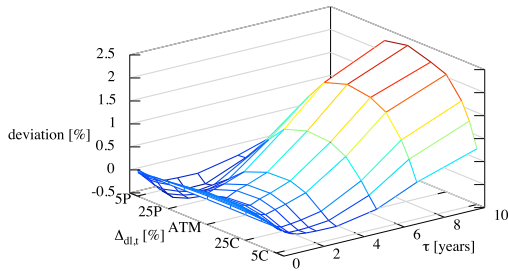
Deviation of Heston-Nandi Call Prices with ML Estimated Parameters call prices to the market call prices relative to the stock price in percent, i.e. $\frac{C_{model}-C_{market}}{S_t} [\%]$, depending on the driftless delta $\Delta_{dl,t}$ in % of the OTM option and maturity τ in years, c.f. Section 4.2.2.

Deviation of Heston-Nandi Call Prices with ML Estimated Parameters to Market Call Prices: EUR-USD, $t_0 = 30/12/2009$



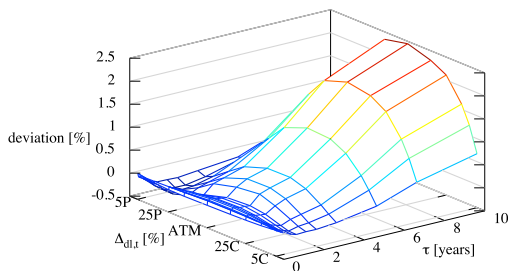
Deviation of Heston-Nandi Call Prices with ML Estimated Parameters call prices to the market call prices relative to the stock price in percent, i.e. $\frac{C_{model}-C_{market}}{S_t} [\%]$, depending on the driftless delta $\Delta_{dl,t}$ in % of the OTM option and maturity τ in years, c.f. Section 4.2.2.

Deviation of Heston-Nandi Call Prices with ML Estimated Parameters to Market Call Prices: EUR-USD, $t_0 = 06/01/2010$



Deviation of Heston-Nandi Call Prices with ML Estimated Parameters call prices to the market call prices relative to the stock price in percent, i.e. $\frac{C_{model}-C_{market}}{S_t} [\%]$, depending on the driftless delta $\Delta_{dl,t}$ in % of the OTM option and maturity τ in years, c.f. Section 4.2.2.

Deviation of Heston-Nandi Call Prices with ML Estimated Parameters to Market Call Prices: EUR-USD, $t_0 = 20/01/2010$

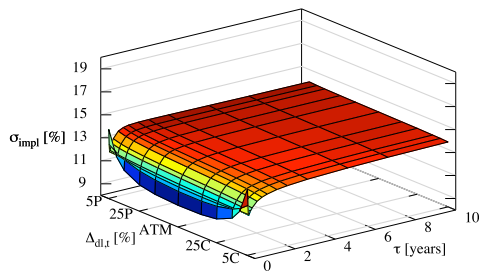


Deviation of Heston-Nandi Call Prices with ML Estimated Parameters call prices to the market call prices relative to the stock price in percent, i.e. $\frac{C_{model}-C_{market}}{S_t} [\%]$, depending on the driftless delta $\Delta_{dl,t}$ in % of the OTM option and maturity τ in years, c.f. Section 4.2.2.

B.5. Grafical Results of the Heston-Nandi Model with Calibrated Volatility Index Parameters

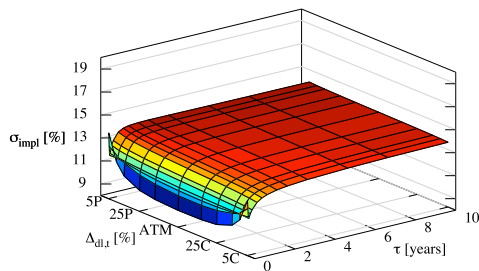
B.5.1. Heston-Nandi Volatility Surfaces with Calibrated Volatility Index Parameters

Heston-Nandi Volatility Surfaces with Calibrated Volatility Index Parameters for EUR-USD, $t_0 = 23/09/2009$



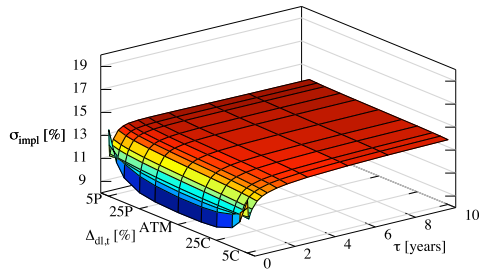
Implied volatility σ_{impl} denoted in % depending on the driftless delta $\Delta_{\text{dl},t}$ in % of the OTM option and maturity τ in years, c.f. Section 4.2.2.

Heston-Nandi Volatility Surfaces with Calibrated Volatility Index Parameters for EUR-USD, $t_0 = 07/10/2009$



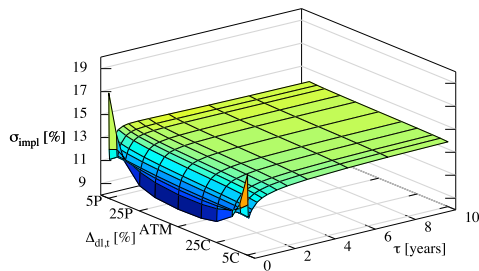
Implied volatility σ_{impl} denoted in % depending on the driftless delta $\Delta_{\text{dl},t}$ in % of the OTM option and maturity τ in years, c.f. Section 4.2.2.

Heston-Nandi Volatility Surfaces with Calibrated Volatility Index Parameters for EUR-USD, $t_0 = 21/10/2009$



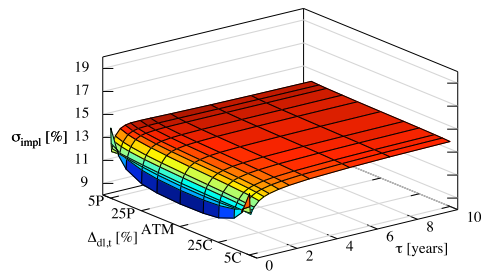
Implied volatility σ_{impl} denoted in % depending on the driftless delta $\Delta_{\text{dl},t}$ in % of the OTM option and maturity τ in years, c.f. Section 4.2.2.

Heston-Nandi Volatility Surfaces with Calibrated Volatility Index Parameters for EUR-USD, $t_0 = 04/11/2009$



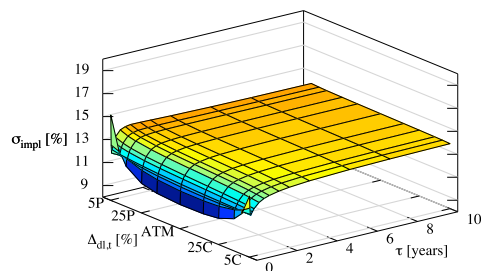
Implied volatility σ_{impl} denoted in % depending on the driftless delta $\Delta_{\text{dl},t}$ in % of the OTM option and maturity τ in years, c.f. Section 4.2.2.

Heston-Nandi Volatility Surfaces with Calibrated Volatility Index Parameters for EUR-USD, $t_0 = 18/11/2009$



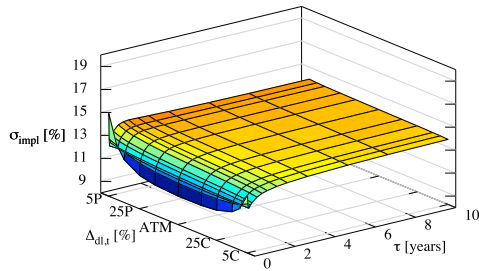
Implied volatility σ_{impl} denoted in % depending on the driftless delta $\Delta_{\text{dl},t}$ in % of the OTM option and maturity τ in years, c.f. Section 4.2.2.

Heston-Nandi Volatility Surfaces with Calibrated Volatility Index Parameters for EUR-USD, $t_0 = 02/12/2009$



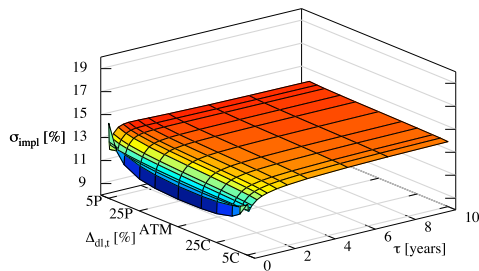
Implied volatility σ_{impl} denoted in % depending on the driftless delta $\Delta_{\text{dl},t}$ in % of the OTM option and maturity τ in years, c.f. Section 4.2.2.

Heston-Nandi Volatility Surfaces with Calibrated Volatility Index Parameters for EUR-USD, $t_0 = 16/12/2009$



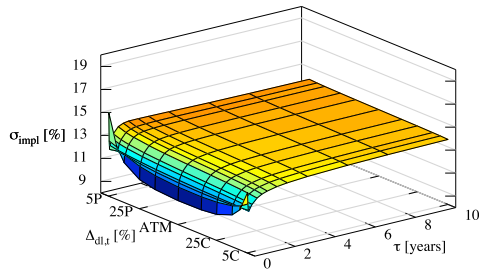
Implied volatility σ_{impl} denoted in % depending on the driftless delta $\Delta_{\text{dl},t}$ in % of the OTM option and maturity τ in years, c.f. Section 4.2.2.

Heston-Nandi Volatility Surfaces with Calibrated Volatility Index Parameters for EUR-USD, $t_0 = 30/12/2009$



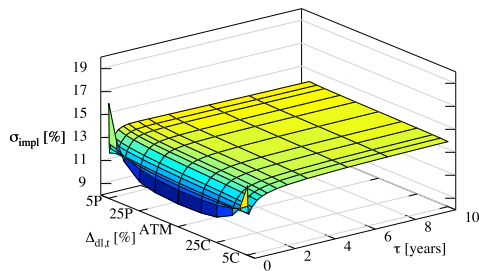
Implied volatility σ_{impl} denoted in % depending on the driftless delta $\Delta_{\text{dl},t}$ in % of the OTM option and maturity τ in years, c.f. Section 4.2.2.

Heston-Nandi Volatility Surfaces with Calibrated Volatility Index Parameters for EUR-USD, $t_0 = 06/01/2010$



Implied volatility σ_{impl} denoted in % depending on the driftless delta $\Delta_{\text{dl},t}$ in % of the OTM option and maturity τ in years, c.f. Section 4.2.2.

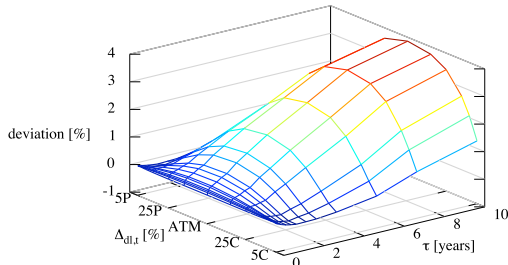
Heston-Nandi Volatility Surfaces with Calibrated Volatility Index Parameters for EUR-USD, $t_0 = 20/01/2010$



Implied volatility σ_{impl} denoted in % depending on the driftless delta $\Delta_{\text{dl},t}$ in % of the OTM option and maturity τ in years, c.f. Section 4.2.2.

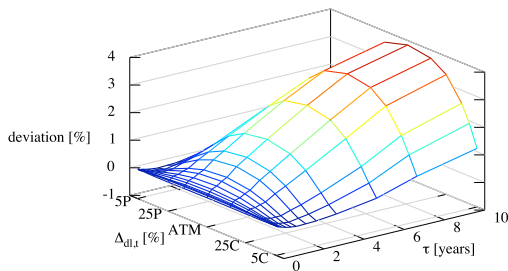
B.5.2. Deviations of the Heston-Nandi Call Prices with Calibrated Volatility Index Parameters

Deviation of Heston-Nandi Call Prices with Calibrated Volatility Index Parameters to Market Call Prices: EUR-USD, $t_0 = 23/09/2009$



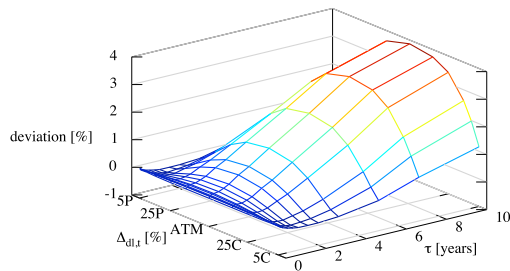
Deviation of Heston-Nandi Call Prices with Calibrated Volatility Index Parameters call prices to the market call prices relative to the stock price in percent, i.e. $\frac{C_{model} - C_{market}}{S_t} [\%]$, depending on the driftless delta $\Delta_{dl,t}$ in % of the OTM option and maturity τ in years, c.f. Section 4.2.2.

Deviation of Heston-Nandi Call Prices with Calibrated Volatility Index Parameters to Market Call Prices: EUR-USD, $t_0 = 07/10/2009$



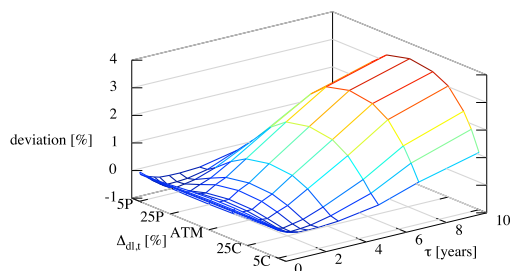
Deviation of Heston-Nandi Call Prices with Calibrated Volatility Index Parameters call prices to the market call prices relative to the stock price in percent, i.e. $\frac{C_{mdel} - C_{market}}{S_t} [\%]$, depending on the driftless delta $\Delta_{dl,t}$ in % of the OTM option and maturity τ in years, c.f. Section 4.2.2.

Deviation of Heston-Nandi Call Prices with Calibrated Volatility Index Parameters to Market Call Prices: EUR-USD, $t_0 = 21/10/2009$



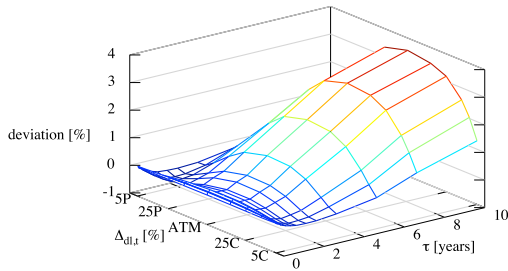
Deviation of Heston-Nandi Call Prices with Calibrated Volatility Index Parameters call prices to the market call prices relative to the stock price in percent, i.e. $\frac{C_{model}-C_{market}}{S_t} [\%]$, depending on the driftless delta $\Delta_{dl,t}$ in % of the OTM option and maturity τ in years, c.f. Section 4.2.2.

Deviation of Heston-Nandi Call Prices with Calibrated Volatility Index Parameters to Market Call Prices: EUR-USD, $t_0 = 04/11/2009$



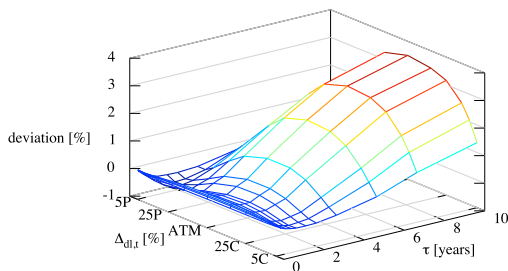
Deviation of Heston-Nandi Call Prices with Calibrated Volatility Index Parameters call prices to the market call prices relative to the stock price in percent, i.e. $\frac{C_{model}-C_{market}}{S_t} [\%]$, depending on the driftless delta $\Delta_{dl,t}$ in % of the OTM option and maturity τ in years, c.f. Section 4.2.2.

Deviation of Heston-Nandi Call Prices with Calibrated Volatility Index Parameters to Market Call Prices: EUR-USD, $t_0 = 18/11/2009$



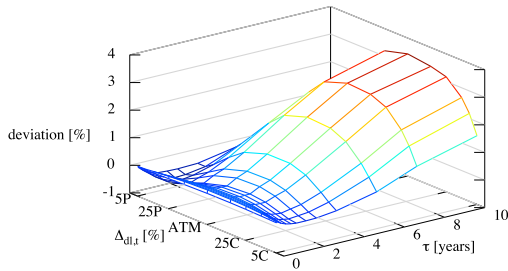
Deviation of Heston-Nandi Call Prices with Calibrated Volatility Index Parameters call prices to the market call prices relative to the stock price in percent, i.e. $\frac{C_{model}-C_{market}}{S_t} [\%]$, depending on the driftless delta $\Delta_{dl,t}$ in % of the OTM option and maturity τ in years, c.f. Section 4.2.2.

Deviation of Heston-Nandi Call Prices with Calibrated Volatility Index Parameters to Market Call Prices: EUR-USD, $t_0 = 02/12/2009$



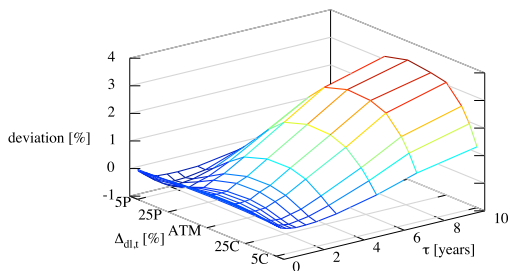
Deviation of Heston-Nandi Call Prices with Calibrated Volatility Index Parameters call prices to the market call prices relative to the stock price in percent, i.e. $\frac{C_{model}-C_{market}}{S_t} [\%]$, depending on the driftless delta $\Delta_{dl,t}$ in % of the OTM option and maturity τ in years, c.f. Section 4.2.2.

Deviation of Heston-Nandi Call Prices with Calibrated Volatility Index Parameters to Market Call Prices: EUR-USD, $t_0 = 16/12/2009$



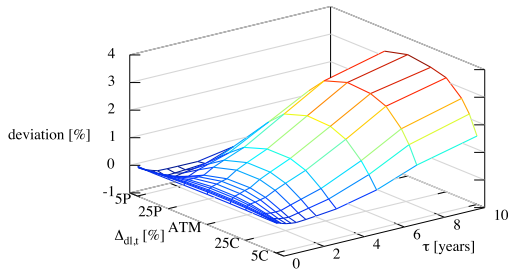
Deviation of Heston-Nandi Call Prices with Calibrated Volatility Index Parameters call prices to the market call prices relative to the stock price in percent, i.e. $\frac{C_{model}-C_{market}}{S_t} [\%]$, depending on the driftless delta $\Delta_{dl,t}$ in % of the OTM option and maturity τ in years, c.f. Section 4.2.2.

Deviation of Heston-Nandi Call Prices with Calibrated Volatility Index Parameters to Market Call Prices: EUR-USD, $t_0 = 30/12/2009$



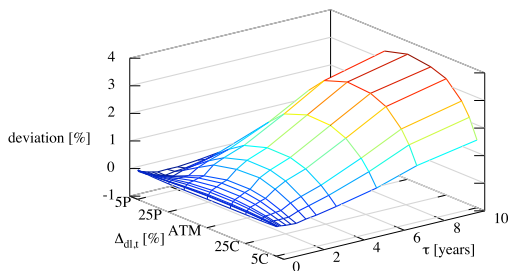
Deviation of Heston-Nandi Call Prices with Calibrated Volatility Index Parameters call prices to the market call prices relative to the stock price in percent, i.e. $\frac{C_{model}-C_{market}}{S_t} [\%]$, depending on the driftless delta $\Delta_{dl,t}$ in % of the OTM option and maturity τ in years, c.f. Section 4.2.2.

Deviation of Heston-Nandi Call Prices with Calibrated Volatility Index Parameters to Market Call Prices: EUR-USD, $t_0 = 06/01/2010$



Deviation of Heston-Nandi Call Prices with Calibrated Volatility Index Parameters call prices to the market call prices relative to the stock price in percent, i.e. $\frac{C_{model}-C_{market}}{S_t} [\%]$, depending on the driftless delta $\Delta_{dl,t}$ in % of the OTM option and maturity τ in years, c.f. Section 4.2.2.

Deviation of Heston-Nandi Call Prices with Calibrated Volatility Index Parameters to Market Call Prices: EUR-USD, $t_0 = 20/01/2010$



Deviation of Heston-Nandi Call Prices with Calibrated Volatility Index Parameters call prices to the market call prices relative to the stock price in percent, i.e. $\frac{C_{model}-C_{market}}{S_t} [\%]$, depending on the driftless delta $\Delta_{dl,t}$ in % of the OTM option and maturity τ in years, c.f. Section 4.2.2.

List of Figures

2.1.	Growth of the Forex Market and the Underlying Contracts	4
2.2.	Payoff Curves of a Forward at Maturity T	7
2.3.	Payoff Curves of a European Option at Maturity T	9
3.1.	Simulated Price Process with BSM Price Process	18
3.2.	fig:VolaCallRelation	26
4.1.	Market Volatility Surface: EUR-USD $t_0 = 23/09/2009$	36
4.2.	Market Volatility Smile of Individual Maturities: EUR-USD, $t_0 = 23/09/2009$	37
4.3.	Volatility Surface in the BSM Model, $t_0 = 23/09/2009$	38
4.4.	Deviation of BSM to Market Call Prices: EUR-USD, $t_0 = 18/09/2009$	39
4.5.	Return Time Series of $\frac{USD}{EUR}$ during 04/01/1999 – 20/01/2010	48
4.6.	Return Histogram of Returns from $\frac{USD}{EUR}$ during 04/01/1999 – 20/01/2010	49
5.1.	Simulated Price Process with Underlying Heston Volatility Process	52
5.2.	Volatility Surface of Calibrated Heston Model for EUR-USD, $t_0 = 23/09/2009$	60
5.3.	Deviation of Heston to Market Call Prices: EUR-USD, $t_0 = 18/09/2009$	61
6.1.	Simulated Price Process with Underlying GARCH Variance h_t	63
6.2.	Heston-Nandi Volatility Surface with ML Estimated Parameters for EUR-USD, $t_0 = 23/09/2009$	74
6.3.	Deviation of Heston to Market Call Prices: EUR-USD, $t_0 = 18/09/2009$	75
6.4.	Volatility Surface of Calibrated GARCH Parameters to a Volatility Index, $t_0 = 23/09/2009$	76
6.5.	Deviation of Heston-Nandi with Calibrated Volatility Index Parameters to Market Call Prices: EUR-USD, $t_0 = 18/09/2009$	77
6.6.	Volatility Surface of Calibrated Heston-Nandi Model for EUR-USD, $t_0 = 23/09/2009$	78
7.1.	Progression of the Calibrated BSM Implied Volatilities	83
7.2.	Progression of the Calibrated Heston Parameters	87
7.3.	Comparison of the Implied Volatility Index to the Fitted NGARCH Process, during 04/01/1999 – 20/01/2010	90
8.1.	MSE Values of the Examined Models	94
8.2.	Return Histogram of MC Simulation Generated by Calibrated Heston Parameters	97

8.3. Return Histogram of MC Simulation Generated by NGARCH Parameters from MLE	98
8.4. Return Histogram of MC Simulation Generated by NGARCH Parameters from Volatility Index Fit	99

List of Tables

2.1. Overview of the Forex Market: The Leading Forex Markets, Currency Traders and Currency Pairs	5
4.1. Driftless Delta Quotation Example: Comparing C- Δ_t -Quotes to Money-ness M_{t_0} and Strikes K with Different Maturities τ	35
7.1. Calibrated BSM Implied Volatilities	83
7.2. Calibrated Heston Parameters	86
7.3. Estimated Heston-Nandi Parameters by MLE	88
7.4. Values of the NGARCH Variance Process h_t at Specific Dates	89
7.5. Calibrated NGARCH Parameters to a Volatility Index	90
7.6. Values of the NGARCH Variance Process h_t at Specific Dates	91
7.7. Calibrated Heston-Nandi Parameters at $t_0 = 23/09/2009$	92
8.1. MSE Values of the Examined Models	95
9.1. Example of Pricing Cliquets with Stochastic Volatility Models	101

Bibliography

- [BIS07] BIS, Bank for International Settlements (2007). Triennial Central Bank Survey of Foreign Exchange and Derivatives Market Activity in April 2007. <http://www.bis.org/publ/rpfx07t.pdf>.
- [Bloomberg10] Bloomberg (2010). <http://www.bloomberg.com>.
- [Bollerslev86] Bollerslev, Tim (1986). Generalized Autoregressive Conditional Heteroskedasticity. *Journal of Econometrics* volume 31 pp. 307–327.
- [Chriss96] Chriss, Neil A. (1996). *Black-Scholes and Beyond - Option Pricing Models*. McGraw-Hill, 1st edition. ISBN 0786310251.
- [CMS Forex09] CMS Forex (2009). Forex Overview. <http://www.cmsfx.com/en/forex-education/online-forex-course/chapter-1-forex-basics/>.
- [Cont04] Cont, Rama and Tankov, Peter (2004). *Financial Modelling With Jump Processes*. Chapman & Hall/CRC, 1st edition. ISBN 1-58488-413-4.
- [DB07] DB, Deutsche Bank (2007). DBIQ Index Guide. https://index.db.com/dbiqweb2/data/guides/FX_Impact_Guide_v1.pdf.
- [Desmettre07] Desmettre, Sascha (2007). *Four Generations of Asset Pricing Models and Volatility Dynamics*. Master's thesis, Technische Universität Kaiserslautern.
- [Duan95] Duan, Jin-Chuan (1995). The GARCH Option Pricing Model. *Mathematical Finance* volume 5(1) pp. 13–32.
- [EconomyWatcher] EconomyWatch (2009 September). FX: Forex, Foreign Exchange. <http://www.economywatch.com/forex/>.
- [Engle82] Engle, Robert F. (1982). Autoregressive Conditional Heteroscedasticity with Estimates of the Variance of United Kingdom Inflation. *Econometrica* volume 50(4) pp. 987–1008.
- [Engle91] Engle, Robert F. and Ng, Victor K. (1991). Measuring And Testing The Impact of News on Volatility. NBER Working Papers Series volume W(3681).

- [Euromoney08] Euromoney (2008). Forex Poll 2008. <http://www.euromoney.com/Article/1922137/FX-poll-2008-Global-FX-market-continues-dramatic-growth.html>.
- [Fahrmeir05] Fahrmeir, Ludwig; Raßer, Günter and Kneib, Thomas (2005). Stochastische Prozesse.
- [Foster94] Foster, Dean P. and Nelson, Daniel B. (1994). Asymptotic Filtering Theory for Univariate Arch Models. *Econometrica* volume 62(1) pp. 1–41.
- [Gatheral06] Gatheral, Jim (2006). *The Volatility Surface*. Wiley & Sons, 1st edition. ISBN 0-471-79251-9.
- [Grimmett01] Grimmett, Geoffrey and Stirzaker, David (2001). *Probability and Random Processes*. Oxford University Press, 3rd edition. ISBN 0-19-857222-0.
- [Haug98] Haug, Espen G. (1998). *The Complete Guide to Option Pricing Formulas*. McGraw-Hill, 1st edition. ISBN 0-7863-1240-8.
- [Held06] Held, Leonhard (2006). *Statistik III*.
- [Henry-Labordère08] Henry-Labordère, Pierre (2008). *Analysis, Geometry, and Modeling in Finance: Advanced Methods in Option Pricing*. Chapman & Hall/CRC, 1st edition. ISBN 1-4200-8699-7.
- [Heston93] Heston, Steven L. (1993). A Closed-Form Solution for Options with Stochastic Volatility with Applications to Bond and Currency Options. *The Review of Financial Studies* .
- [Heston00] Heston, Steven L. and Nandi, Saikat (2000). A Closed-Form GARCH Option Valuation Model. *The Review of Financial Studies* volume Fall 2000(13) pp. 585–625.
- [Hull02] Hull, John C. (2002). *Options, Futures, and Other Derivatives*. Prentice Hall, 5th edition. ISBN 0-13-046592-5.
- [IFSL07] IFSL, International Financial Services London (2007). Foreign Exchange 2007. http://www.ifsl.org.uk/upload/CBS_Foreign_Exchange_2007.pdf.
- [IVolatility.com09] IVolatility.com (2009). Implied Volatility Surface by Delta. <http://www.ivolatility.com/doc/deltasurfacemethodology.pdf>.
- [Kishimoto08] Kishimoto, Manabu (2008). On the Black-Scholes Equation: Various Derivations.
- [Kitco07] Kitco (2007). The World’s Biggest Market. <http://www.kitco.com/ind/Downs/feb022007.html>.

- [Neftci04] Neftci, Salih N. (2004). Principles of Financial Engineering. Elsevier Academic Press, 1st edition. ISBN 0-12-515394-5.
- [Nelson91] Nelson, Daniel B. (1991). Conditional Heteroskedasticity in Asset Returns: A New Approach. *Econometrica* volume 59(2) pp. 347–370.
- [Nögel03] Nögel, Ulrich and Mikhailov, Sergei (2003). Heston’s Stochastic Volatility Model Implementation, Calibration and Some Extensions. *Wilmott Magazin* .
- [Overhaus07] Overhaus, Marcus; Bermúdez, Ana; Buehler, Hans; Ferraris, Andrew; Jordinson, Christopher and Lamnouar, Aziz (2007). *Equity Hybrid Derivatives*. John Wiley & Sons, Inc., 1st edition. ISBN 0-471-77058-2.
- [RBA07] RBA, Reserve Bank of Australia (2007). Reserve Bank Bulletin. http://www.rba.gov.au/PublicationsAndResearch/Bulletin/bu_jan08/aus_fx_derivatives_mrkts.html.
- [Rebonato99] Rebonato, Riccardo (1999). *Volatility and Correlation: In the Pricing of Equity, FX and Interest-Rate Options*. John Wiley & Sons, Ltd, 1st edition. ISBN 0-471-89998-4.
- [Reuterser] Reuters (2009 September). Financial Glossary - FX Swap. http://glossary.reuters.com/index.php?title=FX_Swap.
- [Rouah07] Rouah, Fabrice Douglas and Vainberg, Gregory (2007). *Option Pricing Models & Volatility*. John Wiley & Sons, Inc., 1st edition. ISBN 0-471-79464-6.
- [Schmitt96] Schmitt, Christian (1996). Option Pricing Using EGARCH Models. *ZEW Discussion Papers* volume 20(96) pp. 1311–1336.
- [Staunton02] Staunton, Mike (2002). *Deriving Black-Scholes From Lognormal Asset Returns*. *Wilmott* .
- [Teräsvirta06] Teräsvirta, Timo (2006). An Introduction to Univariate GARCH Models. *Working Papers in Economics and Finance* volume 646.
- [Wikipediaera] Wikipedia (2009 September). Foreign Exchange Market. http://en.wikipedia.org/wiki/Foreign_exchange_market.
- [Wikipediaerb] Wikipedia (2009 September). Moneyiness. <http://en.wikipedia.org/wiki/Moneyiness>.
- [Wikipediaerc] Wikipedia (2009 September). Numéraire. <http://en.wikipedia.org/wiki/Numraire>.
- [Wikipediary] Wikipedia (2010 January). Simulated Annealing. http://en.wikipedia.org/wiki/Simulated_annealing.

- [Wilmott07a] Wilmott, Paul (2007). Frequently Asked Questions in Quantitative Finance. John Wiley & Sons, Ltd, 2nd edition. ISBN 0-470-05826-8.
- [Wilmott07b] Wilmott, Paul (2007). Paul Wilmott Introduces Quantitative Finance. John Wiley & Sons, Ltd, 2nd edition. ISBN 0-470-31958-5.
- [Wilmott10] Wilmott, Electronic Media Limited (2010). http://www.wilmott.com/messageview.cfm?catid=3&threadid=58805&FTVAR_MSGDBTABLE=&STARTPAGE=1.
- [Wystup07] Wystup, Uwe (2007). FX Options and Structured Products. John Wiley & Sons, Ltd, 1st edition. ISBN 0-470-01145-9.

Eidesstattliche Erklärung

Hiermit versichere ich, die vorliegende Arbeit selbstständig und unter ausschließlicher Verwendung der angegebenen Literatur und Hilfsmittel erstellt zu haben.

Die Arbeit wurde bisher in gleicher oder ähnlicher Form keiner anderen Prüfungsbehörde vorgelegt und auch nicht veröffentlicht.

München, February 26, 2010 _____